Abilities and limitations in the use of Regional Climate Models

Morten Andreas Ødegaard Køltzow

Dissertation for the degree of Ph. D.

Department of Geosciences
University of Oslo

October 2012

Series of dissertations submitted to the
Faculty of Mathematics and Natural Sciences, University of Oslo
No. 1236

ISSN 1501-7710

Cover: Inger Sandved Anfinsen.
Printed in Norway: AIT Oslo AS.

Produced in co-operation with Akademika publishing.
The thesis is produced by Unipub merely in connection with the
thesis defence. Kindly direct all inquiries regarding the thesis to the copyright
holder or the unit which grants the doctorate.

Preface

The work presented in this thesis is carried out at met.no through a series of different projects supported by grants from the Norwegian Research Council and EU. When the finish line (finally) emerged and the original funding was long gone, met.no gave me additional time to wrap up everything.

I am deeply grateful to my supervisor, Professor Trond Iversen for guidance, interest and an invaluable source of ideas and discussions through the years, and for really pushing me forward the last months before finishing the thesis.

Special thanks also to Dr. Jan Erik Haugen. Without him, I had spent many more hours, days, weeks and probably months on struggling with numerical models on super computers.

I also want to thank all my different leaders at met.no for encouragement on finishing the thesis and actually giving me the time of doing it. Likewise thanks to all colleagues for a good social place to work, good discussions, inspiring work and for the question “How is the progress on your thesis?”

Finally, I want to thank my nearest family, and especially Astrid, who found the fine balance between not asking too many questions on the progress of the thesis and encouragement, support and reminding me that also other thing than work are important.

Content:

Papers:

Køltzow, M. (2007) The effect of a new snow and sea ice albedo scheme on regional climate model simulations. *J. Geophys. Res*., 112, D07110, doi:10.1029/2006JD007693.

Køltzow, M.; Iversen, T.; Haugen, J.E. (2008) Extended Big-Brother experiments: the role of lateral boundary data quality and size of integration domain in regional climate modeling. *Tellus*, 60A, 398-410.

Køltzow M.A., Iversen T., Haugen J.E. (2011) The Importance of Lateral Boundaries, Surface Forcing and Choice of Domain Size for Dynamical Downscaling of Global Climate Simulations. *Atmosphere*; 2(2):67-95.

1. Introduction.

The work presented in this thesis deals with regional climate models (RCMs) and numerous aspects of their quality and uncertainty due to their set up. Even though the thesis deals with RCMs for climate projections purposes, several of the issues discussed are also relevant for limited area models in day to day weather forecasting.

Climate is generally defined as the long-term average of daily weather and the frequency at which different weather appears. Because of the internal dynamics of the climate system a long period is necessary to capture the existence of different weather regimes. Furthermore, the earth's climate evolves in time under the influence of external forcings (i.e. volcanic eruptions, solar variations, human-induced changes in atmospheric composition). At the moment the earth experience an increase in the atmospheric green house gases due to human-induced pollution and thereby possibly changes in climate.

Regarding a possible change in global mean temperature between late 20^{th} and 21^{th} century, the best estimate for a low emission scenario of green house gases is an increase of 1.8°C (likely range 1.1°C to 2.9°C), while the best estimate for a high emission scenario is an increase of 4.0°C (likely range 2.4°C to 6.4°C) (IPCC, 2007). Similar regional estimates for Norway suggest an increase in temperature between 2.3°C and 4.6°C at the end of this century. The largest increase is expected during winter and in the northern parts of Norway. Also an increase between 5% and 30% in precipitation is expected for the same time period (Hansen-Bauer et al., 2009).

The findings mentioned are just a glimpse of different estimates of potential climate change in the future. It is important to recognize that all such estimates are associated with uncertainty. Presented for all (possible) scenarios of future climate change, a natural question to ask is "how are these climate change estimates constructed?" and "how certain are they?" These are simple questions that demands complex answers. The complex story on the construction of climate change estimates are documented in the IPCC reports (i.e. IPCC, 2007) and only a short version is given here, while parts of the certainty questions are discussed in the thesis.

The most common way to create climate projections is based on a climate model approach and scenarios for future emissions of green house gases. The emission scenarios are

used as input to General Circulation Models (GCMs) or Earth System Models (ESMs, if bio-geochemical processes are included on-line). In GCMs (and ESMs) the physical laws describing the climate are modelled mathematically. However, the full descriptions of the relevant physical processes are computational expensive. With respect to available computer resources (central processing units and storage capacity) GCMs can only be employed on a quite coarse horizontal and vertical resolution (i.e. the physical processes can only be described as an average over a certain area or grid box). In the 4th Assessment Report (IPCC, 2007), the horizontal resolution of the atmospheric components in the global models was typically on the order of 150-300km. This is a source of errors in (regional) climate simulations. Additionally the lack of regional details makes the GCM output inappropriate for many impact studies that require regional details.

Several methods or techniques have therefore been developed to add fine scale features to the GCM results needed in impact studies. These methods are called downscaling. The different techniques in use are; variable resolution GCMs, global time slices simulations with an atmosphere GCM and statistical and dynamical downscaling.

GCMs with stretched grids employ finer resolution for the area of interest than for the rest of the earth. The advantages of stretched-grid GCMs are that they do not require any lateral boundary conditions/forcing and are free of the associated computational problems (i.e. Fox-Rabinoviz et al., 2006).

In time slice experiments, the atmospheric component of a GCM is run without the full coupled ocean component of the model. The sea surface boundary conditions are based on observations in the historical run, while the same data are perturbed for the projection runs. Without the ocean component and simulations only of slices of time, higher resolution of the atmospheric model become affordable (see i.e. IPCC, 2007)

In statistical downscaling a relationship between large-scale variables as predictors (i.e. mean sea level pressure) and local variables as predictands (i.e. temperature and precipitation) is created and assumed constant under climate change. Statistical methods can in principle use both global and regional model results as input (see i.e. IPCC, 2007).

Dynamical downscaling is a widely applied approach for high resolution climate prediction. In dynamical downscaling a RCM is employed on a limited area of interest. A limited area for the RCM implies that higher horizontal and vertical resolution is affordable. In

the 3th Assessement Report from IPCC (2001), the horizontal resolutions of the atmosphere part of the GCM employed were 250-300km. This increased with a factor of 1.5-2 to the 4th Assessement Report (IPCC, 2007). In the latter report most regional climate models where employed with approximately 50km resolution although some climate simulations were performed on much finer resolution. In other words the RCMs clearly increase the resolution compared to GCMs. This increased resolution is a potential source for better description of the climate system by better resolving the dynamics of the system and better description of surface forcings (i.e. topography, land-sea and vegetation contrasts). However, there are issues regarding the nesting strategy of the RCMs and the choice of integration domains. These issues are discussed further in this thesis.

In many assessment studies there are a further need for even finer resolution than provided by RCMs. Removal of regional systematic errors (bias correction) in the RCM output may also be desirable. Several geostatistical approaches are therefore applied for further refinements of the RCM output (i.e. Engen-Skaugen et al, 2007, Hageman et al., 2011). A challenging task for these bias corrections are to couple observed present day climate with one or more realizations of present day climate from (regional) climate model(s).

As described above, the generation of climate change estimates based on a model approach constitutes of a sequence of methods/models employed on different scales. All steps in the cascade add uncertainty to the estimates of future climate change. Rowell (2006) describes four different sources of uncertainty; (1) The uncertainty due to emission rate scenarios, (2) the uncertainty due to GCM formulations, (3) the uncertainty due to the RCM formulations and set up, and (4) the uncertainty due to internal variability in the climate system. Rowell (2006) and Déqué et al. (2007) studied the relative importance of the different sources of uncertainty for seasonal means of temperature and precipitation. They found that the major source of uncertainty is connected with the choice of GCM. For temperature the uncertainty of the RCM formulation and setup is comparable to the uncertainty connected to internal variability but slightly smaller than that associated with the emission scenario. For precipitation the GCM still plays the major role, but now the RCM add more uncertainty than the emission scenarios. However, Déqué et al. (2007) emphasize that other sources of uncertainty may play an important role and that the discussion done is only valid for the current state of the art models. Räisänen (2001) compared the results from 15 GCMs and

concluded that model differences create larger uncertainty than that from internal variability of each model. A general discussion on the different aspects of uncertainty in climate modeling can be found in Foley (2010).

One way to quantify these different sources of uncertainty in regional climate projections is to employ ensemble techniques, i.e. perform a range of model calculations with different prescribed emission rates, different GCMs, different RCMs and simulations with different initial states. Such an approach will give a consensus estimate for future climate change (i.e. (weighted) ensemble mean) and an associated estimate of uncertainties and other possible outcomes.

The thesis is in the following organized as follows. In chapter 2, a short introduction to RCMs, how they differ from regional weather forecast models and methods for validation of RCMs is given. In chapter 3 issues concerning the use of RCMs are discussed, while chapter 4 summarizes the papers included in the thesis. These papers are in the following referred to as paper 1 (Køltzow, 2007), paper 2 (Køltzow et al., 2008) and paper 3 (Køltzow et al., 2011). Finally, some concluding remarks are drawn in chapter 5.

2. Regional models.

The main purpose of a regional model or a limited area model (LAM) is to provide added value when forced (i.e. at the lateral and surface boundaries) by a GCM (or some other coarse resolution data set) to the latter regarding more detailed description of small scale features of weather and climate.

In the following we describe the use of regional climate models (RCMs). However, a brief introduction to similarities and differences between RCMs and LAMs for Numerical Weather Prediction (NWP) is given in the next section. A RCM is in principal similar to a GCM, but only applied for a limited area with open lateral boundaries. While a GCM most commonly constitutes both atmosphere and ocean coupled together, the most common approach in RCMs is purely an atmospheric or ocean model. However, examples exist of global atmosphere (ocean) models only and of coupled RCMs (i.e. Döscher et al., 2002, Rinke et al., 2003). Since the RCM is applied for shorter time periods and at a limited spatial area compared to GCMs, better horizontal and vertical resolution is affordable and therefore more detailed simulations are possible.

With increased (horizontal) resolution there are three major sources for a better description of fine scale motions: (1) improved description of ground surface structures and contrasts, (2) more explicit description of nonlinear dependencies in the dynamics and (3) a better description of hydrodynamic instabilities (Denis et al., 2002).

Downscaling global projection data by employing RCMs with higher resolution has become common procedure in recent years (IPCC, 2001 and 2007). A review of the RCM concept can be found in Rummukainen (2010). Laprise et al. (2008) summarized the original views on the RCM concept, and their validity, in 4 tenets concerning the nesting strategy (i.e. not the quality of the RCM itself). Based on own experiments and based on others work they confirmed that (1) RCMs do generate small scale features (even without strong surface forcing) absent in the driving data and (2) that these small scales features for mid-latitudes have the appropriate amplitudes and climate statistics. However, for the full spin-up of small scale features a rather large domain are required and especially in the upper troposphere. Furthermore, they argued for the partial failure of (3) the development of fine scales features with correct geographical location for a specific time. An exception to this failure was possible

seen for very short time scales when the small scales were present in the initial conditions. The failure of tenet (3) has little impact for climate projection purposes since it do not alter the climate statistics, but large implications in weather prediction. Due to internal variability of the RCM they also argued for the failure of a fourth tenet (4): "RCM generated small scales are uniquely defined for a given set of lateral boundary conditions".

As described above, the main purpose of RCMs are to add realistic small scale features to their driving data. An extended view is that in addition to the positive impact on small scale features, the RCM could also have a positive impact on the large scale circulation and improving this as well. This is also discussed by Laprise et al. (2008) as a possible fifth tenet with alternative wordings: The large scales are (5a) unaffected, (5b) improved or (5c) degraded within the RCM domain. The wording of such a tenet is still up for debate (Laprise et al. 2008). For practical purposes (5a) is mostly true for small integration domains, while (5b) and (5c) means that the lateral boundaries should put less constrains on the large scale circulation in the interior of the RCM domain. The latter is probably not a desirable effect if the purpose is to downscale re-analysis for better small scale information. However, since GCMs do contain errors in their large scales tenet 5b might be a desirable feature especially since the large scales may be a prerequisite for regional features (Simmons, 2006, Diaconescu et al., 2007). In paper 2 and in Veljovic et al. (2010) the idea of also improving the large scales was supported. Veljovic et al. (2010) suggest that in addition to better resolution in RCMs, an improved physical description in the RCM compared to the GCM can contribute to improvement of the large scales of the driving data.

Several issues concerning the nesting process was called for further investigations by Laprise et al. (2008) and several of them are included in the discussion in chapter 3.

3. Differences and similarities between regional models for the purpose of weather forcasting and for the purpose of climate predictions.

So far in this thesis no attempt has been made to distinguish between LAMs for the purpose of numerical weather prediction and for the purpose of regional climate downscaling. There are many similarities, but also some important differences. Here we briefly outline some of the differences before discussing RCMs only in the rest of the thesis.

The problem of weather forecasting can mainly be described as an initial value problem, while the climate prediction problem can be described as a boundary value problem. In weather forecasting the objective is to give an estimate of the weather for a given place and time together with its uncertainty and probabilities for other outcomes. In climate projections the objective is to give estimates of the statistics of weather and the frequency for different weather events. However, global and regional numerical models are used for both cases.

In weather forecasts the most important sources of error is found in the initial state uncertainty and in the model formulation. Most regional NWP models therefore employ systems for assimilating observational data to estimate the initial state and reduce the initial state uncertainty. In addition, a proper assimilation system will ensure that fine scale structures are present from the integration start. Due to the (partial) failure of tenet 3 described in the previous section an ensemble approach should be included in designing a proper weather forecasting system to take into account the initial uncertainty. However, some LAMs are also used in a pure downscaling mode in the forecast context, but then with a smaller resolution jump between the regional model and the driving data compared to common use by RCMs.

In climate projections the results are sensitive to the natural and anthropogenic forcing (i.e. a change in the CO2 content of the atmosphere) and model formulation. Additional, both in weather forecasting and for climate simulations the set up and nesting of the regional model may be reflected in the quality of the simulations. To deal with internal variability in the

system also an ensemble approach is needed to calculate climate statistics for a time-dependent change in external forcing. Another possibility to overcome the internal variability problem is to perform averaging over a very long time period (even though this can be problematic under a changing climate).

Furthermore, the relevant processes differs on which time scales they operate, i.e. the need for information about deep ocean processes is not necessary for a 2-day weather forecast, but is of critical importance in climate projections. The different demands on the accuracy of the description of the physical processes may also be noticed. A small systematic drift is negligible for day-to-day forecasts as the model get a new initialization for each model run. However, such artificial systematic drifts will eventually ruin a climate prediction simulation.

While NWP models always need to be ready as fast as possible to be used by duty forecasters and others, RCM simulations do not experience a similar demand.

State of the art limited area NWP models are today employed with resolutions of 1-10km, which is finer than in most RCMs (i.e 10km and coarser). This difference reflects the length of the simulations needed and differences in the requirements for a limited NWP compared with a RCM.

4. Validation and verification methods of RCMs.

As described above the objective for limited area models for weather forecasting and climate predictions differs and therefore also the verification and validation methods employed. Here only validation of RCMs is discussed (for an introduction to weather forecast verification see Joliffe and Stephenson (2003)).

One step in the validation of atmospheric downscaling with RCMs is the performing of Perfect Boundary Experiments (PBEs) (e.g. Christensen et al., 1997; Rinke et al., 1999). When GCM-data are downscaled with a RCM, systematic and random errors imposed at the lateral boundary and at the ocean surface are unavoidable due to the imperfections inherent in any GCM. In PBEs the RCM is driven with analysed atmospheric fields at the lateral boundaries and similar for the ocean surface. Hence, a PBE is a demanding test of the quality of the RCM with regard to downscaling, as the results can be compared directly with observed climate data over the specific time-period.

However, as advocated by Denis et al. (2002), regular atmospheric climate observations often lack the spatial and temporal resolutions needed for adequate validation of the fine scale features calculated by the RCM. Fields from very-high resolution data assimilation are contaminated by inaccuracies of the assimilation method and errors in the model used for the purpose. Finally, PBEs does not differ between errors originating from the RCM itself and from the downscaling technique. Denis et al. (2002) therefore suggested a new type of PBE which are fully based on models. This is nick-named the Big Brother experiments (BBEs) and enables evaluation of nesting strategies for dynamical downscaling. First a reference climate from a simulation is established as a pure model product using the resolution intended for use when downscaling GCM data. This simulation is called the Big Brother (BB). The BB simulation can also be established by using a large integration domain (but not global) and if this is the case it is occasionally in the literature called poor-man BBE. In the method proposed by Denis et al., (2002) and used in later experiments (Denis et al., 2003; Antic et al., 2004; Herceg et al., 2006; Diaconescu et al., 2007, Leduc and Laprise, 2009, Leduc et al., 2011) data from the BB are then degraded towards the common resolution used in the

atmospheric components of the global climate models (GCM) by simply removing, or filtering off, the smaller scales. The resulting filtered fields are then used as lateral boundary data to drive an RCM (called the Little Brother, LB) which is integrated using the same resolution as the BB, in a subarea of the BB domain. The climate statistics of the LB is validated by comparing with the unfiltered BB data in the LB domain. Differences between the two statistics can then unambiguously be attributed to errors associated with the dynamical downscaling technique, and not to model errors or observational limitations

Independent of experimental set up it is necessary to compare the RCM output, the driving data and some observational data to assess the quality and added value by the RCM. A comparison, i.e. by eye, of maps of precipitation or near surface temperature from a GCM and a RCM will probably reveal small scale details in the RCM, apparently quite realistic, not present in the GCM. However, this is not sufficient evidence that the RCM really add value to its driving data. Such fine structures are often smoothed in the time averaged fields with reduced differences between the driving data and the RCM. Given this, a comparison of the area mean skill of the GCM and the RCM against observations will not necessarily prove added value by the RCM. One exception is regions with strong local forcing (see i.e. all three papers of this thesis). Furthermore, the added value is more likely to be associated with a better frequency distribution, and reflecting more intense and localized weather events (Laprise, 2008). It is therefore argued that it is a pressing need to expand on existing tools to identify and extract the added value of RCMs (Laprise et al., 2008). This is similar to the need to show added value by high resolution LAMs in NWP.

Along these lines Di Luca et al. (2010) elaborated on the concept of Potential Added Value (PAV). The PAV explore a necessary (but not sufficient) condition for RCMs to produce added value, namely, that small scales features (not present in the driving data) are present in the RCM results. They showed that for precipitation (and their specific integration domain) this is true, but PAV is much higher for short temporal scales, higher in the warm season (compared to the cold season) and enhanced in regions of complex topography. Their results also suggest that PAV varies between RCMs (model formulation and set up). The added value at smaller scales was further studied by Feser (2006) who applied an isotropic digital spatial filter to evaluate LAM results separately at different scales and found a significant added value for temperature on regional scales. Kanamitsu and Dehaan (2011)

have suggested a somewhat complementary approach by defining an Added Value Index (AVI) as the area in the probability density function where the regional model skill is greater than that of the driving data. This was done to show that RCMs contain added value which often may be masked out when only examine area mean skill.

5. RCMs and added value.

There are a range of different ways RCMs can be employed; (i) forced by re-analysis (i.e. PBE, hindcasts), (ii) forced by GCMs for today's climate (i.e. as a reference for a climate projection), (iii) forced by GCMs for future climate and (iv) for sensitivity studies (i.e. study the importance of different parameterization schemes).

Most producers of RCM simulations compare their historical simulations with observations (either point based or gridded) and/or re-analysis to validate the RCM abilities in climate simulations. However, the actually added value by the RCM compared to the driving data is not well explored yet, but some results are reported in recent years (i.e. Prommel, 2010, Winterfeldt and Weisse, 2009, Feser et al., 2011). Feser et al. (2011) summarize some of these studies and conclude that in the presence of local forcing the RCMs do add value.

The results by Feser et al. (2011) suggest that spectral nudging (see chapter 3) give the highest added value. However, many of the mentioned investigations make use of measures not adequate for climate modeling purposes and more suitable for weather forecasting verification or high resolution hindcasts (i.e. they use measures that penalize deviation in time). In a climate modeling view it is the climate statistics (i.e. mean value and frequency distribution) that are of importance.

Furthermore, most added value experiments employs re-analysis as driving data with the implication that the large scales of the driving data are "perfect" and thereby penalizing deviations from this in comparison with observations and favors nesting strategy methods that ensure a large scale similarity between the RCM and the driving data (i.e. spectral nudging, frequent re-initializations and/or small integration domains). This is reasonable for hindcast simulations but does it necessarily be best practice for the production of future climate projections with more or less imperfect driving data from a GCM? It should therefore be noticed that the above conclusions are valid for "perfect" large-scale forcing data (re-analysis) and are necessarily not valid for imperfect GCM climate predictions.

6. Issues concerning the use of nested limited area models for climate downscaling.

Many studies support the basic assumption of dynamical downscaling, that RCMs only fed by large scale data produce realistic fine scale features (i.e. Køltzow et al. 2008, Denis et al., 2002, Laprise et al., 2008). Some studies also support the extended idea of also improving the large scale fields, even if this is rarely reported (i.e. Mesinger et al., 2002, paper 2, Veljovic et al., 2010). In addition, there are studies that report on added value by the RCMs as described in the previous chapter. Despite this, there are several issues connected to the RCM nesting and set up that need further investigation.

Denis et al. (2002) discussed 9 such issues originally discussed by Warner et al. (1997) for NWP and Giorgi and Mearns (1999) for RCMs . These issues are briefly outlined (below) and discussed in view of scientific achievements the last decade. The main emphases are on the specific subjects which constitute the main part of this thesis. More details can be found in Denis et al. (2002), Laprise et al. (2008), Rummukainen (2010).

Issue 1. Numerical nesting: mathematical formulation and nesting.

There are several approaches on how to force the RCM with global data when doing dynamical downscaling. Which method you use may depend on your goals for the regional model output.

The traditional approach is to force the RCM with large scale variables at the lateral boundaries and prescribed sea surface variables from the global data. This approach is also common in NWP. The objective is clear; “Air masses should flow into and out of the regional model as if it still formed part of a global air-mass” (MacDonald, 1997). However, no well-posed treatment of the lateral boundaries when applying the primitive equations exists (that is a unique solution which depends continuously on the boundary conditions) and pragmatic approached has been developed. Some completely over-specify the fields and filter out the generated noise while others try to be “fairly well posed” (MacDonald, 1997).

Many models make use of the flow relaxation formulation by Davies (1976) (i.e. 6 out of 8 RCMs compared in the study by Rinke et al., 2006). Here the regional model variables are relaxed toward the driving data in a relaxation zone at the lateral boundaries. At the outermost boundary an over-specification is done, but the generated errors are damped in the relaxation zone to minimize the effect on the interior solution. The width of the zone and weighting function may differ between model set ups. See i.e. MacDonald (1997) for a review on lateral boundary conditions. The met.no HIRHAM version used in all three papers in this thesis, make use of the flow relaxation formulation (Davies, 1976) with some modification. A cosine relaxation function is applied through the relaxation zone and a cubic interpolation is applied in time.

Spectral nudging is another approach, which differ from the classical nesting at the lateral boundaries by also prescribing the forcing in the interior of the domain on the largest spatial scales. By doing this the large scale stays close to the driving data and only small scales are free to develop. However, it can be argued that this can create inconsistency and dampen potential feedbacks between scales.

Kida (1991) introduced the spectral nudging technique for regional climate simulations and demonstrated the potential of the method. The concept was further elaborated by von Storch et al. (2000) who demonstrated that the large scales stayed close to the driving data while fine scale structures were allowed to develop. They also warned about the use of the method when dynamical aspects are addressed or when a significant two-way coupling is expected to take place (i.e. the life cycle of a hurricane).

Later, several studies have been published on the topic. Migues-Macho et al. (2004) showed less sensitivity to domain size and location for precipitation amounts and patterns when the regional model employed spectral nudging on the large scales. Alexandru et al. (2009) performed a series of experiments during a single summer season varying the vertical profile and intensity of the spectral nudging (from no spectral large scale nudging to strong large scale nudging). The results indicate on the one hand, a reduction of internal variability (more constraints by the large scales of the driving data), less dependency on the domain size, and improvement of geopotential height time means (again an effect of more constraints by the re-analysis used as large scale driving data). On the other hand the spectral nudging also showed a tendency to reduce precipitation maxima. Colin et al. (2010) investigated the effect

of spectral nudging on precipitation extremes and did not find that this systematically degraded the representation of the climate model's extremes. Furthermore, a positive impact on a T2m bias was found.

The results from spectral nudging experiments are mostly positive (i.e. more desirable than undesirable effects), but also some indications of undesirable behaviour is found. In addition, the positive/negative impacts may vary between set-ups, and no general rule to the applied strength of the spectral nudging is established. Since both the traditional approach of lateral boundary forcing and the spectral nudging approach do have strengths and weaknesses, the objective of the simulations may decide which of the methods are most appropriate in that particular case.

In the following sections mainly the traditional nesting approach is discussed with the exceptions where the spectral nudging can contribute to reduce some of the problematic issues experienced.

Issue 2. Spatial resolution and difference between the driving data and the nested model.

Denis et al. (2002) raised the question of jump in resolution between the driving data and the RCM. They noticed that reported ratios are usually between 2 and 5, but sometimes as high as 10.

The importance of the resolution jump was investigated in the BBE context by Denis et al. (2003) with a regional model with 45km horizontal resolution. They found for a winter case that the generated fields show satisfactory quality for most variables when the driving data is degraded up to a factor of 12. For a similar summer study Dimitrijevic and Laprise (2005) stated that T30 was the minimum acceptable resolution of the driving data, but the results were improved employing T60 resolution. However, it is reasonable to believe that these numbers are subject to RCM set up, resolution, domain area size and location (discussed later under issue 7).

With the HIRHAM RCM (used in all three papers in this thesis) experiments with the horizontal resolution of the lateral and surface boundary data where done with 2.5°, 2.0°, and 1.5° (the RCM employed 0.5°). An improvement was found when 2.0° was used instead of

2.5°. A further increased resolution of the forcing data from 2.0° to 1.5° gave little improvement (Haugen, 2012).

In the albedo sensitivity studies in paper 1, the HIRHAM RCM had 0.5 horizontal resolution and was forced with ERA40 data on a grid with 2.0° for the atmospheric variables and 1.25° for the surface soil variables. In the BBE in paper 2, the regional model applied 0.5° horizontal resolution forced by data interpolated to a grid with 2.8° horizontal resolution. In the last paper of the thesis (paper 3) a jump from T106 (MPI GCM) and 3.75°x2.5° (HAD GCM) to the RCM with 0.5° horizontal resolution was made. No technical difficulties were noticed in any of these experiments.

Issue 3. Spin-up.

What is the time needed for the RCM to develop proper small scale structures? This depends heavily on which component of the climate system we look at. Soil and hydrology processes need typically months to years to spin up in many cases, while small scale structures in the atmosphere need hours, up to a few days (Denis et al. 2002, Laprise et al., 2008).

Lately Leduc & Laprise (2009) demonstrated that the spin-up distance (the distance the large scale flow needs to travel before developing small scale features) depends on the flow speed, which means that it increases at higher levels in the atmosphere and varies with season. This existence of a spin-up distance was recognized early in the use of RCMs and Jones et al. (1995) suggested that the area should be small enough to keep the large scale flow as in the driving data, but large enough to allow small scale features to develop properly for the area of interest.

Issue 4. Update frequency of the lateral boundary conditions (LBCs).

At which temporal frequency should the lateral boundaries be updated? For RCM simulations with 45km horizontal resolution Denis et al. (2003) found for a winter case an upper limit of update frequency of 12hr ensuring acceptable results, while little difference was found with a further improvements from 6hr to 3hr. Dimitrijevic and Laprise (2005) did a

similar experiment on a summer case and found also only minor differences between 6hr and 3hr updates.

However, the updates at the lateral boundaries must be frequent enough to capture the phase speed of the meteorological phenomena we want to simulate. Finer horizontal resolution is required to describe smaller and more rapidly evolving systems, which therefore needs more frequent updates at the lateral boundaries than spatially coarser models. An effect of this is that several operational NWP runs (i.e. at met.no) employ an update frequency of 1hr. In NWP experiments testing 1hr versus 3hr update frequency, only minor impacts on the overall quality are found. However, some high-impact weather situations are considerably improved when 1hr update frequency is used (Martinsen et al., 2010).

Issue 5. Physical parameterisations consistencies.

Non-resolved physical processes in climate models are described by parameterisations where a certain large scale forcing give a certain (deterministic) output of the small scale processes trough complex physical descriptions. The processes typically include radiation transfer, turbulent fluxes, cumulus convection, cloud microphysics, cloud cover determination and land surface processes and are done separately in each vertical grid cell column.

A different description of the physics between the RCM and the GCM at the lateral boundaries combined with the dynamics of the RCM may generate undesirable noise at the boundaries which can propagate to the interior of the domain. This problem can be omitted if the same parameterizations are used in both the RCM and the GCM. However, because of the differences in resolution this is not desirable as one in general wish to use parameterizations appropriate to the model resolution.

Issue 6. Horizontal and vertical interpolation errors.

Which inconsistencies and imbalances are introduced when interpolations are made between the driving data and the RCM in the nesting process? The answer is not obvious since differences between topographic fields due to different resolution imply extrapolation below the surface of the driving model.

Wu et al. (2005) used four different interpolation techniques to create an ensemble of RCM simulations based on global re-analysis and showed that even if the effect of interpolation is smaller than i.e. the choice of driving data, it is not negligible.

Issue 7. Domain size and location.

The impact of the integration domain on RCM results has been widely recognized and discussed for a long period (see i.e. Jones et al., 1995, Seth and Giorgi, 1998, Christensen et al., 1997) and further discussed by Denis et al. (2003). In this thesis we also argue that not only the size but also the placement of the integration domain should be included. When Norway is the area of interest for RCM simulations the whole of Norway should be included in the integration domain. However, should Norway be located in the middle of the domain or perhaps slightly to the west, east, north or south? Domain size (and location) has gained a lot of attention the last decade. In the literature there exist many papers on the subject relevant for climate modelling, but fewer papers concerning weather forecasting. However, it has gained attention also in operational weather forecasting communities even though not published peer-review as commonly as with RCMs. An example is that for a very high resolution ensemble experiment the simulated probabilities for high impact weather show sensitivity to domain size and location (Kristiansen et al., 2011). A quite pragmatic approach is to make the domain size as large as possible given available computer resources and, in the NWP context, the time limits for making the forecasts available for duty forecasters and others. However, such an approach to decide on integration domain size should be made with care as demonstrated in the next paragraphs.

Paper 2 and 3 of this thesis shows that the integration domain size plays a role and may alter the RCM results. Basically, this is because with larger domains less constraint by the lateral forcing is put on the interior solution. Thereby more internal variability is allowed and the large scale flow in the RCM may deviate from that of the driving data. This is demonstrated and discussed in paper 2 and 3 and their references.

Leduc et al. (2011) demonstrated that the effect of the domain size is differently under different seasons. In other words, the importance of the domain size depends on the circulation regime. The optimal choice of domain may also depend on the meteorological variable of interest (see paper 2). This relates to how the domain size and location influence the necessary spin-up time/distance for small scale features (discussed under issue 3).

With increasing domain size, internal processes of the RCM become more important relative to the lateral boundary forcing. This is important to bear in mind when designing RCM experiments. For climate simulations the domain size must be of a size big enough to allow for added value by the RCM. In process studies (i.e. sensitivity experiments with a parameterization scheme) with regional models, the integration domain must be large enough to ensure that the actual sensitivity is not damped due to the control of the lateral boundary.

The internal variability of the RCM (i.e. the differences between simulations only different in their initial conditions) are a subject for investigation in several recent papers. Lucas-Picher et al. (2008) demonstrated that there is an almost linear relationship between the internal variability and the residence time of air parcels in the integration domain. This implies less internal variability in winter (compared to summer) and at high elevations of the troposphere (compared to near ground elevations). Furthermore, Alexandru et al. (2007) demonstrated that the internal variability varies with synoptic events, domain size and with respect to variable. In addition to these settings Crétat and Pohl (2011) launched the idea that also the choice of the employed physical parameterization package in the RCM contributes substantially to create internal variability.

As described in this section and highlighted in paper 1 to 3 there are many considerations to take into account when deciding upon an integration domain for the purpose of downscaling climate predictions. The spectral nudging approach has been suggested to reduce the dependence on domain size and location. Such an approach will possibly also have some other effects on the results (positive or negative dependent on the objective of the simulations) as already discussed under issue 1. One of these effects are the damping of the internal variability of the RCM.

Issue 8. Quality of the driving data.

Even with a perfect formulation of the RCM and a perfect nesting strategy the quality of the driving data is crucial for the quality of the RCM output.

Wu et al. (2005) investigated the importance of the initial and lateral boundaries on monthly mean atmospheric states by downscaling ensembles of four different global re-analyses. The impact of the initial conditions decreased with simulation length, while the impact of the lateral boundaries showed no such tendency, and the differences between the

global data sets contribute significantly to the uncertainty in the ensemble simulations. They also stated that the impact is dependent on variable.

Diaconescu et al. (2007) did further studies on the impact of the lateral forcing by forcing a RCM with several data sets with increasing errors at the boundaries and found (for that particular set up) an almost perfectly linear dependence between the large scale errors in the RCM and in the driving data. Furthermore, for the small scales the RCM only corrected errors in the driving data in the vicinity of orographic forcing or land-sea contrasts. The results indicate that the large scales precondition the small scales and the quality of the driving data is therefore also of importance for the correct generation of small scale features when strong surface forcing is absent. That the large scales precondition the small scales is also suggested by Simmons (2006) and by Anthes et al. (1985).

This thesis highlights some important aspects associated with the relative importance of the lateral boundary conditions. Paper 1, is a clear example that changes in the internal description of the RCM can change the RCM output significantly. While paper 3 demonstrates that the driving data have a major impact on the results. In paper 2, this is studied in more detail and some indications are found that the RCM may also improve the large scales of the driving models. The latter is similar to what is suggested by Mesinger et al. (2002) and Veljovic et al. (2010). The ability to improve on large scales is also an important finding if the large scales (to some extent) precondition the small scales.

Issue 9. Climate drift or systematic errors.

This issue differs from the previous 8 issues in the way that it also concerns about the quality of the RCM itself and that the issue is also relevant for GCMs. Can the RCM be run for a long period without systematic errors or with out a climate drift. It is important to notice that in addition to model deficits, all of the previous issues discussed can contribute to systematic errors in the RCM results. Small domains or spectral nudging may reduce such problems in RCMs.

The examples and discussion of the 9 issues, originally discussed by Giorgi and Mearns (1999), above are mainly on atmosphere RCMs. For fully coupled RCMs, which have started to become available the last decade (i.e. Döscher et al., 2002, Rinke et al., 2003), the issues are still valid. However, the relative importance of the different issues may change. For

example will coupled RCMs possibly allow more realistic feedback mechanisms, which will influence the relative importance of lateral forcing versus internal processes of the RCM. The HIRHAM RCM used in paper 1-3 was set up on the same domain as in paper 1 and applied in a sensitivity experiment on the effect of sea ice thickness (Mauritsen et al., 2011). A significant change in near surface temperature and mean sea level pressure were found as response to changed prescription of sea ice thickness. Krinner et al. (2009) performed experiments with an atmosphere RCM with a prescribed sea ice thickness (one thickness for all sea ice) compared to a more realistic sea ice thickness distribution an found a clear sensitivity in the marginal Arctic Seas in today's climate, and interestingly a sensitivity in central Arctic for future climate. These examples illustrate that a coupled RCM (or at least a better description of sea ice thickness distribution in atmosphere RCMs) has the potential of improving RCM climate projections. A coupled RCM may also (but not necessarily) introduce increased sensitivity to model description. The albedo scheme developed in paper 1 was tested in one GCM and in two coupled RCMs. In the GCM (Dethloff et al., 2006) it was shown that a more realistic sea ice albedo triggered changes in the Arctic and North Atlantic Oscillation pattern with implications for the European climate. In one of the coupled RCMs Dorn et al. (2007) noticed that a changed sea ice albedo description introduced a sensitivity similar to the parameterization of lateral ice growth (a commonly used parameterization for tuning sea ice models), while in the other coupled RCM (Döscher et al., 2006) all sea ice melted away within a few years with the new albedo scheme. Castro et al. (2005) showed that the ground surface boundary conditions are important in generating large scale variability in RCMs, and that this importance increases as the integration domain increases. Thus, large scale atmospheric variability tends to be increasingly underestimated as the domain size increases when the lower boundaries are prescribed as over oceans in atmosphere RCMs, and this may change in a fully coupled RCM.

7. Summary of papers.

This thesis constitutes of the work presented in three papers. The three papers address one or more of the issues summarized and discussed in the previous section.

In this context the first paper (paper 1: Køltzow, 2007), concerns the relative importance of internal processes in a RCM compared with external forcing. The second (paper 2: Køltzow et al. 2008) and third papers (paper3: Køltzow et al. 2011) addresses several of the issues in more detail (i.e. the size of the integration domain, the quality of the driving data, and the objective of the nesting strategy).

Paper1:
Køltzow, M. (2007):
The effect of a new snow and sea ice albedo scheme on regional climate model simulations.
J. Geophys. Res., 112, D07110, doi:10.1029/2006JD007693.

In this paper several parameterization schemes for snow and sea ice albedo are compared. Based on the results of the comparison a new scheme is proposed and implemented in the HIRHAM RCM. Experiments with the old and the new schemes have then been performed and the results are evaluated. This paper can therefore be regarded as a paper on the description of physical processes in RCMs. The final comparison between the old and the proposed new scheme is, however, an illustration of how internal processes (i.e. physical description) in a RCM can alter the simulated climate downscaled from the lateral boundary data.

The paper starts with a comparison of several existing parameterization schemes for snow and sea ice albedo. The different schemes are forced with observational data. For snow on land the description of albedo is divided into forested and non-forested areas. The most critical period for correct description of snow albedo is in spring, when snow still is present and the snow albedo is in transition, and the amount of solar radiation at the surface increases. The evaluation of the land snow albedo schemes therefore focused on this period. For forested areas the original HIRHAM scheme was the better of the compared schemes and therefore kept in the model. However, for non-forested areas the original HIRHAM scheme

underestimated the albedo for temperatures close to 0°C. In this case, a polynomial albedo dependency of temperature gave a more realistic result.

None of the compared sea ice albedo schemes adequately described the annual cycle of sea ice albedo. A common deficiency was too high albedo in summer. In addition, the temperature dependent schemes had too low albedo in the transition period between spring and summer. A new scheme was constructed to include the effect of melt ponds. Forced with observed temperatures and snow depths this scheme is in better agreement with observed albedo and absorbed solar radiation from the SHEBA experiment.

The new albedo schemes for sea ice and snow in non-forested areas were implemented and tested in the HIRHAM RCM for a pan-Arctic domain. The effect of the new sea ice albedo scheme is present in the period between April and September. The effect on 2m air temperature is mainly restricted to local changes associated with changes in the sea ice albedo and, compared to ERA40 data, a significant improvement of the model performance is found. The sea ice albedo does not only have an effect on near surface temperature, but alters also the simulated mean sea level pressure (MSLP). A positive impact of the new sea ice albedo scheme on MSLP was found in spring and autumn, while a negative impact was found in summer. The changes in MSLP is however, insignificant at the 5%-level.

The changes of the snow albedo scheme for non-forested land areas showed less impact on the simulation than the effect of the sea ice albedo. In spring a change of net solar radiation at the top of the atmosphere by 5W/m2 was found for some regions. However, little effect on other variables like near surface temperature, pressure and cloud cover was detected. In summer, some changes of 1-2°C in near surface temperatures and up to 1hPa in MSLP are seen in some areas with late snow melt.

The findings in this study illustrates that a RCM is not entirely steered by the lateral forcing, but that surface forcing and model physics are crucial for the quality of the RCM ouput. Furthermore the different response of HIRHAM to the changes in snow albedo changes (close to the lateral boundary) compared to the response of the changes in sea ice albedo (interior of the domains) illustrates that the RCM is sensitive to the size and distribution of the internal forcing.

Paper 2:

Køltzow, M.; Iversen, T.; Haugen, J.E. (2008)

Extended Big-Brother experiments: the role of lateral boundary data quality and size of integration domain in regional climate modeling.

Tellus, 60A, 398-410

This paper investigates the added value of dynamical downscaling. The objective was to study the nesting strategy and the investigation is conducted by adopting and extending the Big-Brother approach of Denis et al. (2002) which attribute errors solely to the dynamical downscaling method. In particular the role of the lateral boundary data quality and the size of the integration domain are investigated.

The traditional BBE approach is described in section 2.3. In addition to the traditional BBE we add a second BB simulation in order to realistically mimic the actual situation where the coarse-resolution data have to be taken from a coarse-resolution model where the large scale fields do contains errors. This is a similar approach as Diaconescu et al. (2007). In total 8 simulations for the period 1970 to 1990 were performed. First, two BB simulations were performed, one “fine-scale BB” with high resolution (0.5 horizontal resolution and 31 vertical levels) and one “coarse-scale BB” with coarse resolution (2.8 horizontal resolution and 19 vertical levels). A filtered version (small scale features are removed) of the “fine-scale BB” and the “coarse-scale BB” are then used to force LB simulations on a small, medium, and a large size domain.

The filtered fine resolution data represent the upper bound in the potential quality of coarse resolution data, since they contain resolution errors without phase shift. Comparison between downscaled versions of the two BB data-sets gives therefore valuable insight into the abilities of downscaling to improve the climatology of the coarse resolution BB.

The results are analyzed with respect to climate averages, daily statistics and extreme values and the truth is taken as the fine scale BB.

Forced by high quality lateral forcing the LBs captured well the MSLP patterns in the small and medium domain. However, larger deviations were found in the large domain due to reduced influence by the lateral forcing. When driven by the coarse-resolution BB data, little evidence of improvement of the MSLP pattern in the LBs was found over Norway. However there are some indications that the MSLP patterns are slightly improved in the Barents Sea and in the Greenland region employing the largest integration domain.

In the climate averages the near surface temperature (T2m) is well captured independent of the lateral forcing and domain size. The main reason for this behavior is strong local and regional surface forcing (i.e. topography, land sea contrasts and prescribed sea surface temperatures).

The main features of the BB precipitation are re-generated independent of lateral forcing, but the size of the integration domain is important. The precipitation was underestimated in the smallest area due to spin-up effects, but also for the large domain there were deficiencies most probably due to deviations in the large scale pattern.

For wind the LB simulations driven by high quality data captured the wind pattern very well in all domains. However, a bias was present when the LBs were driven by the coarse resolution BB, but this bias was to some extent corrected with increasing size of the integration domain. While the errors in the LBs were quite homogeneous over the annual cycle when forced with high quality data, the errors varied more throughout the year when forced with coarse resolution BB.

In general, the extremes were regenerated in the LB simulations. In this respect high quality driving data gave a better reproduction than LBs driven by the coarse resolution BB. However, in the latter the extremes were improved compared with the extremes in the coarse resolution BB. Which of the small, medium and large domains that did the better job in the re-production of the extremes varied with respect to variable and driving data.

The findings of this study suggest that your confidence in the driving data and what the purpose of the regional study are, should be taken into considerations when deciding on the model setup of the RCM.

Paper 3:

Køltzow, M. A. Ø., T. Iversen, J. E. Haugen (2011)

The Importance of Lateral Boundaries, Surface Forcing and Choice of Domain Size for Dynamical Downscaling of Global Climate Simulations.

Atmosphere, 2(2):67-95

The aim of this study was to explore (i) the importance of the surface forcing (i.e. sea surface temperature and sea ice), (ii) the importance of the lateral boundary forcing, and (iii) the importance of the size of the integration domain for dynamical downscaling with the HIRHAM RCM. This was done through a set of experiments where the surface forcing, the lateral forcing and the integration domain have been systematically varied. The lateral boundary and surface forcings were taken either from global simulations with the Hadley Centre GCM or the Max-Planck-Institute GCM while the HIRHAM RCM were employed on two different integration domains.

The main purpose for all simulations was to simulate the Norwegian climate for the period 1961–1990. In principle, there should therefore only be insignificant differences between the results since they are supposed to be realizations of the same climate. The highest sensitivity of the RCM results was found during winter, and the results for December-January-February were the subject of the analysis.

The analysis shows that the RCM climate was sensitive to both the lateral boundary and surface forcing, as well as to the size of the integration domain. The findings on the RCM sensitivity with respect to climate averages are summarized in Table 1.

Dividing Norway into sub-regions showed different sensitivities to changes in the external forcing. Several of the different simulations gave a statistical different climate for different variables for the Norwegian regions at a significance level of 5% with northern Norway experienced the highest sensitivity.

It is also worth noting that the different variables showed different sensitivity to changed forcing. Large scale variables like MSLP were sensitive to lateral forcing and size of integration domain, but less sensitive to surface forcing. However, more locally forced variables, like T2m, were less sensitive outside the areas of changed surface forcing.

Table 1. Summary of findings for RCM sensitivity on climate averages due to different surface forcing, lateral forcing and the size of the integration domain.

	MSLP	Precipitation	T2m
Different Surface forcing	modest local sensitivity	modest local sensitivity	Clear local response / minor remote response
Different Lateral forcing	Clear response (most pronounced near the main storm tracks)	Clear sensitivity at the Norwegian coast	Minor sensitivity.
Different Integration domain (small / large)	Clear sensitivity (in value and distribution).	Clear sensitivity at the Norwegian coast.	Minor Sensitivity.

In many respects, the results generated in this paper support earlier findings described in the previous chapters of this thesis, but highlight the importance of the Norwegian geography.

8. Concluding remarks.

Numerous aspects of the quality, added value and uncertainty associated with the employment of RCMs have been discussed extensively for almost two decades. This thesis contribute to this discussion and the main focus has been (i) the ability of RCMs to simulate fine scale features lacking in the driving data, (ii) the importance of the size of the integration domain, (iii) the importance of the quality of the lateral boundary forcing and (iv) the relative importance of external forcing versus internal RCM processes on the RCM results. The findings contribute to the existing body of knowledge. A particular finding (paper 2) is that when a RCM is forced with low quality lateral boundary conditions it has the possibility to improve not only on the small scales, but also on the large scales. This should be further investigated with RCM simulations with imperfect driving data since most studies on the topic so far has employed "perfect large scale driving data" either by re-analysis or in the BBE context. Whether RCMs also should improve the large scales of the driving data is still subject for debate (i.e. Laprise et al., 2008, Veljovic, 2010).

In the context of experiments on the abilities and limitations of RCMs this thesis add novelty by exploration of these issues with another RCM (than most other similar studies), other domain sizes and placements, the length of the experiments, and with a special focus on Norway and adjacent areas.

This thesis, together with previous studies suggests that the set up of a RCM should be done with care. This might even be of higher importance for some regions than for other regions. The choices made concerning size of integration domain and lateral- and surface forcing in dynamical downscaling may contribute to uncertainties in future climate scenarios. However, despite that careful considerations are needed, the potential of added value of RCMs is widely recognised and proved. Further investigations are anyway needed to fully understand the relevant issues and to fully take advantage of the added value produced by RCMs.

There are no reasons why these issues should be less important when RCMs now start to make use of horizontal resolutions well below 10km (i.e. Lucas-Picher et al., 2012, Kendon et al., 2012)

9. References:

Alexandru A, De Elía R, Laprise L, Šeparović L, Biner S (2009) Sensitivity study of Regional Climate Model simulations to large-scale nudging parameters. *Mon. Wea. Rev.* 137(5):1666–1686

Alexandru, A.; de Elía, R.; Laprise, R. (2007) Internal variability in regional climate downscaling at the seasonal time scale. *Mon. Wea. Rev*. 135, 3221-3238.

Antic, S., Laprise, R., Denis, B. and de Elia, R. (2004) Testing the down-scaling ability of a one-way nested regional climate model in regions of complex topography. *Clim. Dyn.* 23, 473–493.

Anthes, R. A., Y. H. Kuo, D. P. Baumhefner, R. P. Errico, and T. W. Bettge, 1985: Predictability of mesoscale atmospheric motions. Adv. Geophys., 28B, 159–202.

Castro, C. L., Pielke Sr, R. A. and Leoncini, G. 2005. Dynamical downscaling: assessment of value retained and added using the Regional Atmospheric Modeling System (RAMS). J. Geophys. Res. 110, D05108, doi:DOI: 10.1029/2004JD004721.

Christensen, J.H.; Machenhauer, B.; Jones, R.G.; Schar, C.; Ruti, P.M.; Castro, M.; Visconti, G. (1997) Validation of present-day regional climate simulations over Europe: LAM simulations with observed boundary conditions. *Clim. Dyn*., 13, 489-506.

Colin, J., Déqué, M., Radu, R. and Somot, S. (2010) Sensitivity study of heavy precipitation in Limited Area Model climate simulations: influence of the size of the domain and the use of the spectral nudging technique. *Tellus A*, 62: 591–604. doi: 10.1111/j.1600-0870.2010.00467.x

Crétat, Julien, Benjamin Pohl, (2012) How Physical Parameterizations Can Modulate Internal Variability in a Regional Climate Model. *J. Atmos. Sci.*, 69, 714–724. doi: http://dx.doi.org/10.1175/JAS-D-11-0109.1

Davies, H.C. (1976) A lateral boundary formulation for multi-level prediction models. *Quart. J. Roy. Meteorol. Soc*., 102, 405-418.

Denis, B., Laprise, R. and Caya, D. (2003). Sensitivity of a regional Climate model to the spatial resolution and temporal updating frequency of lateral boundary conditions. *Clim. Dyn.* 20, 107–126.

Denis, B.; Laprise, R; Caya, D.; Cote, J. (2002) Downscaling ability of one-way nested regional climate models: The big-brother experiment. *Clim. Dyn*., 18, 627-646.

Déqué, M., D. P. Rowell, D. Luthi, F. Giorgi, J. H. Christensen, B. Rockel, D. Jacob, E. Kjellstrom, M. de Castro, and B. van den Hurk, (2007) An intercomparison of regional climate simulations for Europe: assessing uncertainties in model projections. *Climatic Change*, 81, 53-70.

Dethloff, K., A. Rinke, A. Benkel., M. Køltzow, E. Sokolova, S. Kumar Saha, D. Handorf, W. Dorn., B. Rockel , H. Von Starch, J. E. Haugen, L. P. Røed, E. Roeckner, J. H. Christensen and M. Stendel, 2006, A dynamical link between the Arctic and the global climate system, Geophys. Res. Lett., 33, L03703, doi:10.1029/2005GL025245.

Diaconescu, E.P.; Laprise, R.; Sushama, L. (2007) The impact of lateral boundary data errors on the simulated climate of a nested regional climate model. *Clim. Dyn*., 28, 333-350.

Di Luca, A., de Elia, R., Laprise, R., (2011) Potential for added value in precipitation simulated by high-resolution nested Regional Climate Models and observations. *Clim. Dyn.*, doi:10.1007/s00382-011-1068-3

Dimitrijevic, M. and Laprise, R. (2005)Validation of the nesting technique in a regional climate model and sensitivity tests to the resolution of lateral boundary conditions during summer. *Clim. Dyn*. 25, 55–580.

Dorn, W., K. Dethloff, A. Rinke, S. Frickenhaus, R. Gerdes, M. Karcher, and F. Kauker (2007), Sensitivities and uncertainties in a coupled regional atmosphere-ocean-ice model with respect to the simulation of Arctic sea ice, J. Geophys. Res., 112, D10118,

Döscher, R., Willen, U., Jones, C., Rutgersson, A., Meier, H. E. M. and co-authors. (2002) The development of the coupled regional ocean-atmosphere model RCAO. *Boreal Eviron. Res.* 7, 1221–1234.

Döscher, R., H. E. M. Meier and K. Wyser (2006), Sensitivities in the Rossby Centre Arctic models, In: Global Implications of Arctic Climate Processes and Feedbacks. Report of the Arctic Climate Workshop. Alfred Wegener Institute for Polar and Marine Research. Potsdam (Germany) 5-7. September 2005. Edited by A. Rinke and K. Dethloff. Ber. Polarforsch. Meeresforsch. 520. ISSN 1618-3193.

Engen-Skaugen, T., Jan Erik Haugen and Ole Einar Tveito (2007) Temperature scenarios for Norway: from regional to local scale *Clim. Dyn*. Volume 29, Number 5, 441-453, DOI: 10.1007/s00382-007-0241-1

Feser, F. (2006) Enhanced detectability of added value in limited area model results separated into different spatial scales. *Mon. Wea. Rev*., 134, 2180–2190.

Feser, Frauke, Burkhardt Rockel, Hans von Storch, Jörg Winterfeldt, Matthias Zahn, (2011) Regional Climate Models Add Value to Global Model Data: A Review and Selected Examples. *Bull. Amer. Meteor. Soc.*, 92, 1181–1192. doi: http://dx.doi.org/10.1175/2011BAMS3061.1

Foley, A (2010) Uncertainty in regional climate modelling: A review, *Progress in Physical Geography*, 34 (5), 647-670.

Fox-Rabinovitz, M., J. Côté, B. Dugas, M. Déqué, and J. L. McGregor (2006), Variable

resolution general circulation models: Stretched-grid model intercomparison project (SGMIP), *J. Geophys. Res*., 111, D16104, doi:10.1029/2005JD006520.

Giorgi, F., and L. Mearns, 1999: Introduction to special section: Regional climate modeling revisited. *J. Geophys. Res.*, 104, 6335–6352

Hagemann, S., C. Chen, J. O. Haerter, J. Heinke, D. Gerten, C. Piani, (2011) Impact of a Statistical Bias Correction on the Projected Hydrological Changes Obtained from Three GCMs and Two Hydrology Models. *J. Hydrometeor.*, 12, 556–578.

Hansen-Bauer, I., H. Drange, E.J. Forland, L.A. Roald, K.Y. Borsheim, H. Hisdal, D. Lawrence, A. Nesje, S. Sandven, A. Sorteberg, S. Sundby, K. Vasskog og B.Adlandsvik (2009) Klima I Norge 2100. Bakgrunnsmateriale til NOU Klimatilpassning, Norsk klimasenter, September 2009, Oslo (only available in norwegian).

Haugen, J. E. (2012) *personal communication*.

Herceg, D., Sobel, A. H., Sun, L. and Zebiak, S. E. (2006) The Big Brother Experiment and seasonal predictability in the NCEP regional spectral model. *Clim. Dyn*. 27, 69–82.

IPCC (2007) Contribution of Working Group I to the Fourth Assessment Report of the Intergovernmental Panel on Climate Change. In IPCC, Climate Change 2007: The Physical Science Basis; Solomon, S., Qin, D., Manning, M., Chen, Z., Marquis, M., Averyt, K.B., Tignor, M., Miller, H.L., Eds.; Cambridge University Press: Cambridge, UK and New York, NY, USA, 2007; p. 996.

IPCC (2001): The Scientific Basis; Houghton, J.T., Ding, Y., Griggs, D.J., Noguer, M., van der Linden, P.J., Dai, X., Maskell, K., Johnson, C.A., Eds.; Cambridge University Press: Cambridge, UK, 2001; p. 881.

Jolliffe IT, Stephenson DB. (2003) Forecast Verification: A Practitioner's Guide in

Atmospheric Science. Wiley: Chichester.

Jones, R. G., Murphy, J. M. and Noguer, M. (1995) Simulation of climate change over Europe using a nested regional-climate model. I: assessment of control climate, including sensitivity to location of lateral boundaries. *Quart. J. Roy. Meteorol. Soc*. 121, 1413–1449.

Kanamitsu, M., and L. DeHaan (2011), The Added Value Index: A new metric to quantify the added value of regional models, *J. Geophys. Res.*, 116, D11106, doi:10.1029/2011JD015597.

Kendon, E. J., N. M. Roberts, C. A. Senior, M. J. Roberts (2012) Realism of rainfall in a very high resolution regional climate model, *Journal of Climate*, doi: http://dx.doi.org/10.1175/JCLI-D-11-00562.1

Kida, H., T. Koide, H. Sasaki, and M. Chiba (1991) A new approach to coupling a limited area model with a GCM for regional climate simulation. *J. Meteor. Soc. Japan*, 69, 723–728.

Krinner, G. , Rinke, A. , Dethloff, K. and Gorodetskaya, I. (2009): Impact of prescribed Arctic sea ice thickness in simulations of the present and future climate , Climate dynamics, 35 (4), pp. 619-633 . doi: 10.1007/s00382-009-0587-7

J. Kristiansen, S. L. Sørland, T. Iversen, D. Bjørge, M. Ø. Køltzow (2011) High-resolution ensemble prediction of a polar low development. *Tellus A* **63**:3, 585-604..

Køltzow, M. (2007) The effect of a new snow and sea ice albedo scheme on regional climate model simulations. *J. Geophys. Res*., 112, D07110, doi:10.1029/2006JD007693.

Køltzow, M.; Iversen, T.; Haugen, J.E. (2008) Extended Big-Brother experiments: the role of lateral boundary data quality and size of integration domain in regional climate modeling. *Tellus*, 60A, 398-410.

Køltzow M.A., Iversen T., Haugen J.E. (2011) The Importance of Lateral Boundaries, Surface

Forcing and Choice of Domain Size for Dynamical Downscaling of Global Climate Simulations. *Atmosphere*; 2(2):67-95.

Laprise, R.; de Elía, R.; Caya, D.; Biner, S.; Lucas-Picher, P.H.; Diaconescu, E.P.; Leduc, M.; Alexandru, A.; Separovic, L. (2008) Challenging some tenets of regional climate modelling. *Meteorol. Atmos. Phys*., 100, 3-22.

Laprise, R. (2008) Regional climate modelling. Special issue on "Predicting weather, climate and extreme events", *J. Comp. Phys.* 227, 3641–3666.

Leduc, M.; Laprise, R. (2009) Regional climate model sensitivity to domain size. *Clim. Dyn.*, 32, 833-854.

Leduc M, Laprise R, Moretti-Poisson M Morin JP (2011) Regional climate model sensitivity to domain size in middle latitudes for summer. *Clim. Dyn*., Volume 37, Numbers 1-2, 343-356, DOI: 10.1007/s00382-011-1008-2

Lucas-Picher, P., D. Caya, S. Biner, and R. Laprise, (2008) Quantification of the lateral boundary forcing of a regional climate model using an aging tracer, *Mon. Wea. Rev.*, 136, 4980-4996, doi: 10.1175/2008MWR2448.1.

Lucas-Picher, P., M. Wulff-Nielsen, J. H. Christensen, G. Aðalgeirsdóttir, R. Mottram, and S. B. Simonsen (2012), Very high resolution regional climate model simulations over Greenland: Identifying added value, *J. Geophys. Res*., 117, D02108, doi:10.1029/2011JD016267.

McDonald, A. (1997) Lateral boundary conditions for operational regional forecast models; a review. Dublin, November, *HIRLAM Technical Report,* No. 32.

Martinsen, E. H. Haakestad, M. Køltzow, D. Bjørge (2010) unpublished note, met.no

Mauritzen, C., Andersson, M., Hansen, E., Berx, B., Beszczynska-Möller, A., Burud, I.,

Christensen, K.H., Debernard, J., de Steur, L., Dodd, P., Gerland, S., Godøy, Ø., Hansen, B., Hudson, S., Høydalsvik, F., Ingvaldsen, R., Isachsen, P.E., Kasajima, Y., Koszalka, I., Kovac, K.M., Køltzow, M., LaCasce, J., Lee, C.M., Lavergne, T., Lydersen, C., Nicolaus, M., Nilsen, F., Nøst, O.A., Orvik, K.A., Reigstad, M., Schyberg, H., Seuthe, L., Skagseth, Ø., Skarðhamar, J., Skogseth, R., Sperrevik, A., Svensen, C., Søiland, H., Teigen, S.H., Tverberg, V., Wexels Riser, C., 2011. Closing the loop – approaches to monitoring the state of the Arctic Mediterranean during the International Polar Year 2007-2008. Progress in Oceanography 90, 62–89.

Mesinger, F.; Brill, K.; Chuang, H.; DiMego, G.; Rogers, E. (2002) Limited Area Predictability: Can "Upscaling'" Also Take Place? Research Activities in Atmospheric and Oceanic Modelling; Ritchie, H., Ed.; World Meteorological Organization: Geneva, Switzerland.

Miguez-Macho, G., G. L. Stenchikov, and A. Robock, (2004) Spectral nudging to eliminate the effects of domain position and geometry in regional climate model simulations. *J. Geophys. Res*., 109, D13104, doi:10.1029/2003JD004495.

Prömmel, K., B. Geyer, J. M. Jones, and M. Widmann (2010) Evaluation of the skill and added value of a reanalysis-driven regional simulation for Alpine temperature. *Int. J. Climatol.*, 30, 760–773

Räisänen, J. (2001) CO2-induced climate change in CMIP2 experiments. Quantification of agreement and role of internal variability. *J. Climate* 14, 2088–2104.

Rowell DP (2006) A demonstration of the uncertainty in projections of the UK climate change resulting from regional model formulation. *Clim. Change* 79:243–257

Rowell DP (2006) A demonstration of the uncertainty in projections of the UK climate change resulting from regional model formulation. *Clim. Change* 79:243–257

Rinke, A., Gerdes, R., Dethloff, K., Kandlbinder, T., Karcher, M. and co-authors. (2003) A case study of the anomalous Arctic sea ice conditions during 1990: insights from coupled and uncoupled re- gional climate model simulations. *J. Geophys. Res.* 108(D9), 4275, doi:10.1029/2002JD003146.

Rummukainen, M. (2010), State-of-the-art with regional climate models. *WIREs Clim Change*, 1:82–96. doi: 10.1002/wcc.8

Seth A, Giorgi F (1998) The effects of domain choice on summer precipitation simulation and sensitivity in a regional climate model. *J. Clim.* 11: 2698-2712

Simmons, A., (2006) Observations, assimilation and the improvement of global weather prediction - some results from operational weather forecasting and ERA-40. In: Predictability of Weather and Climate. T. Palmer and R. Hagedorn (Eds.), Cambridge University Press, 428-458.

Veljovic, K., Rajkovic B., Fennesey, M. J., Altshuler, E. L. and Mesinger, F. (2010) Regional climate modeling: should one attempt improving on the large scales? Lateral boundary condition scheme: any impact? *Meteorol Z* 19(3): 237-246.

von Storch, H., Langenberg, H. and Feser, F. (2000) A spectral nudging technique for dynamical downscaling purposes. *Mon. Wea. Rev*. 128, 3664–3672.

Warner, Thomas T., Ralph A. Peterson, Russell E. Treadon, (1997) A Tutorial on Lateral Boundary Conditions as a Basic and Potentially Serious Limitation to Regional Numerical Weather Prediction. *Bull. Amer. Meteor. Soc.*, 78, 2599–2617. doi: http://dx.doi.org/10.1175/1520-0477(1997)078<2599:ATOLBC>2.0.CO;2

Winterfeldt, J. and R. Weisse, (2009) Assessment of Value Added for Surface Marine Wind Speed Obtained from Two Regional Climate Models. *Mon. Wea. Rev*., 137, 2955–2965. doi: http://dx.doi.org/10.1175/2009MWR2704.1

Wu, Wanli, Amanda H. Lynch, Aaron Rivers (2005) Estimating the uncertainty in a regional climate model related to initial and lateral boundary conditions. *J. Climate*, 18, 917–933 doi: http://dx.doi.org/10.1175/JCLI-3293.1

I

The effect of a new snow and sea ice albedo scheme on regional climate model simulations

Morten Køltzow[1]

Received 23 June 2006; revised 28 September 2006; accepted 27 December 2006; published 13 April 2007.

[1] The HIRHAM snow and sea ice albedo scheme and several other existing snow and sea ice albedo parameterizations forced with observed input parameters are compared with observed albedo. For snow on land in non-forested areas, the original linear temperature-dependent snow albedo is suggested to be replaced with a polynomial temperature-dependent scheme. For sea ice albedo none of the evaluated schemes manage to simulate the annual cycle successfully. A suggestion of a new sea ice albedo including the effects of melt ponds, snow on the sea ice and the surface temperature is presented. Simulations with original and new snow and sea ice albedo are performed in the regional atmospheric model HIRHAM and the results are compared. Compared with ERA40 the control simulation with original surface albedo reveals a warm bias during spring in the Arctic. Changing the surface albedo, the biggest differences are found in the same period. Model simulations with old and new surface albedo in HIRHAM clearly reveal that the new albedo scheme is superior to the currently implemented scheme in reproducing the ERA40 temperature climatology. In these experiments the new snow albedo scheme has less impact than the new sea ice albedo. This is probably because areas with changed snow albedo have smaller extent than areas with sea ice in the model setup and are more constraint by the lateral boundaries.

Citation: Køltzow, M. (2007), The effect of a new snow and sea ice albedo scheme on regional climate model simulations, *J. Geophys. Res.*, *112*, D07110, doi:10.1029/2006JD007693.

1. Introduction

[2] This study addresses the representation of the albedo of snow on ground and sea ice in climate models. Surface albedo is defined as the fraction of incident radiation that is reflected by a surface. This implies that surface albedo is a key climate parameter. At high latitudes there are pronounced annual cycles in surface albedo due to changes in snow and sea ice features during the year [*Winther et al.*, 2002; *Perovich et al.*, 2002a, 2002b; *Lindsay and Rothrock*, 1994]. Furthermore, the positive sea-ice albedo feedback mechanism increases the climate sensitivity and might accelerate the effect of anthropogenic warming [*Lindsay and Zhang*, 2005]. There are also numerous papers that point out the importance of surface albedo in snow covered areas on the climate [e.g., *Thomas and Rowntree*, 1992; *Barnett et al.*, 1989].

[3] The albedo of snow depends on the grain-shape and size, the solar zenith angle, impurities in the snow, surface roughness and thickness of the snow layer [*Grenfell et al.*, 1994; *Curry et al.*, 1996]. The information required for describing snow and sea ice albedo based on the above mentioned characteristics are usually missing in present climate models. For land covered areas, usually a climatological background albedo is used, which is modified according to changes in the surface characteristics (i.e., snow cover and changes in vegetation). Simple schemes use only a constant albedo when snow and sea ice appear in the model, while schemes of medium complexity take into account snow age or temperature dependence. These dependencies account for the amount of water in the snow and snow metamorphism during the melting. Complex snow albedo schemes in addition include features like snow on vegetation and radiation wavelength dependency.

[4] Several studies have previously addressed the parameterization of snow albedo in climate and Numerical Weather Prediction (NWP) models. *Roesch et al.* [1999] compared simulated albedo in ECHAM4 with observations. Snow albedo was underestimated in cold periods, which partly could be attributed to the albedo description and partly to the description of snow cover. Furthermore, the influence of a spectral temperature-dependent snow albedo scheme (divided in near-infrared (NIR) and visible (VIS) wavelengths) in ECHAM4 was investigated by *Roesch et al.* [2002]. Only a small impact of the albedo was found, but the largest deviation from observations was found between 50°N and 70°N, which is an area of huge variability in snow cover. *Viterbo and Betts* [1999] removed a cold bias in the ECMWF model during spring for Eurasia by reducing boreal snow albedo from varying between 0.6 and 0.8 to 0.2, and thereby showed that snow albedo can have a considerable impact on the model results.

[5] Validation studies by forcing albedo schemes with observations are performed by *Loth and Graf* [1998]. A

[1]Norwegian Meteorological Institute, Oslo, Norway.

0148-0227/07/2006JD007693

scheme based on snow-age captured variations in snow albedo when forced with observations from Cole de Porte in the French Alps. *Pedersen and Winther* [2005] compared 7 different GCM snow albedo schemes with observations. They found that the snow albedo schemes had large scatter in their behavior.

[6] The sea ice albedo depends on the ice thickness, the melt pond fraction, brine volume and air bubbles in the sea ice, and the ice growth rate and melting conditions [*Perovich and Grenfell*, 1981; *Curry et al.*, 1996; *Perovich et al.*, 2002b]. The surface albedo varies with solar radiation wavelength.

[7] For sea ice albedo, complex schemes may use information on snow, melt pond fraction, and cloud fraction and radiation wavelength variations. In many models, however, information of one or several of these parameters is not available and only simple descriptions of sea ice albedo are possible (e.g., constant sea ice albedo or a surface temperature dependency).

[8] A comparison and validation study for sea ice albedo schemes of different complexity were performed by *Curry et al.* [2001]. Forced with observations all schemes performed well in some periods, but failed to succeed through the whole annual cycle. In summer the scheme were not able to capture the sea ice albedo evolution properly. An interesting finding of single-column model tests was that more advanced schemes allows for larger feedbacks.

[9] Snow and sea ice albedo are used as tuning parameters in some climate models. *Weatherly and Zhang* [2001] tuned the model albedo values to remove a cold bias in polar surface temperatures while *Mellor and Kantha* [1989] did the same to simulate the sea ice thickness properly. It is believed that such a treatment not allows for a reasonable description of the sea ice albedo feedback mechanism in climate models.

[10] At the Norwegian Meteorological Institute (met.no) the regional atmosphere climate model HIRHAM [*Christensen et al.*, 1996] is applied for regional climate assessments. HIRHAM is an example of a model which use a temperature-dependent parameterization for both snow and sea ice albedo. For Arctic simulations with HIRHAM a warm bias for 2 m air temperature is found during spring. Since surface albedo in general, and in the Arctic in particular is of importance we want to investigate the parameterization of snow and sea ice albedo in the regional climate model (RCM) HIRHAM; we investigate (1) the properties, and (2) the impact of various snow/sea-ice parameterizations on the simulated climate. Both the model sensitivity and the change in performance compared to observations are discussed.

[11] We apply an atmospheric RCM in this study. With such a model high horizontal resolution is possible, which may be crucial to simulate the Arctic climate properly [*Walsh et al.*, 2002]. Experiments can be set up as Perfect Boundary Experiments (PBE) and are suitable for testing the physical parameterization in the model. However, a major part of the sea ice albedo feedback will not be included since sea ice concentration and thickness are prescribed parameters in the model. Furthermore, to investigate remote implications of changing surface albedo, a Global Circulation Model (GCM) is needed. A GCM, however, demands huge computer resources and lacks the same high resolution RCMs can offer. A proper way to investigate the effects of physical schemes should therefore be to do both RCMs and GCMs. The effects of the newly developed snow and sea ice albedo scheme (presented in section 5) on sea ice thickness and areas outside the Arctic in a GCM are described in *Dethloff et al.* [2006].

[12] The present study validates albedo schemes by comparison with observations, and studies their impact on simulated climate in HIRHAM. First a description of the observational data used is given in section 2, and then different snow and sea ice albedo schemes are presented in section 3. An off-line comparison of the described schemes with observations is given in section 4, while a suggestion for a new albedo parameterization in HIRHAM is presented in section 5. The HIRHAM model and experimental setup is described in section 6, while the effects of the new scheme are given in section 7. Results will be discussed concerning model sensitivity to albedo parameterization and to what extent an improved albedo scheme improves the performance of the climate model. In section 8 we summarize and draw conclusions.

2. Observational Data

2.1. Snow

[13] To evaluate the snow albedo schemes we use Advanced Very High Resolution Radiometer (AVHRR) data from NOAA satellites. All data are collected from Scandinavia during cloud free periods with snow at the surface. From the AVHRR channel 1 we get the bi-directional reflectance in a visible wavelength interval (0.58–0.68 μm) and from channel 2 we get it in a near-infrared interval (0.72–1.10 μm). These channel values are normalized to solar nadir conditions by dividing with cosines of the solar zenith angle. These channel values are then used as estimates of albedo at visible wavelengths (α_{VIS}) and near-infrared wavelengths (α_{NIR}), respectively. The AVHRR channel 4 temperatures are used to estimate the surface temperature. However, a correction for atmospheric influence is not done. Since most of the investigated schemes only use a broadband albedo (albedo over all wavelengths), this is constructed following *Collins et al.* [2002]: $\alpha_{broadband} = 0.53\,\alpha_{VIS} + 0.47\,\alpha_{NIR}$. This equation is only valid for mean atmospheric conditions. The ratio of incoming visible and near-infrared radiation depends on the total water vapor column, which is not taken into account. The AVHRR data are then combined with the United States Geological Survey (USGS) (http://edcdaac.usgs.gov/glcc/glcc.html) data set for land type to discriminate between forested and non-forested areas. Each value of surface albedo and surface temperatures refers to an area of 1.5 km $\times$ 1.5 km.

2.2. Sea Ice

[14] During the SHEBA project (http://sheba.apl.washington.edu/), meteorological and sea ice parameters were collected in the Arctic sea from September 1997 to September 1998. This data set is suitable for evaluating different albedo schemes as shown in *Curry et al.* [2001]. In this study we use two data sets from the SHEBA project. The first are data from the Atmospheric Surface Flux group tower described in *Persson et al.* [2002]. These are data from one location with high temporal resolution, which rarely

Table 1. Description of Snow Albedo Schemes Used in Comparison With Observations

Scheme Number	Model/Reference	Area	Description
(1)	HIRHAM [*Christensen et al.*, 1996]	Non-forested areas	Linear function of surface temperature between −10°C and 0°C.
	ECHAM4 [*Roeckner et al.*, 1996]		For $T = 0$°C ; $\alpha_{min} = 0.4$
	REMO [*Mikolajewicz*, 2003]		For $T < -10$°C; $\alpha_{max} = 0.8$
(2)	HIRHAM [*Christensen et al.*, 1996]	Forested areas	Linear function of surface temperature between −10°C and 0°C.
	ECHAM4 [*Roeckner et al.*, 1996]		For $T = 0$°C ; $\alpha_{min} = 0.3$
	REMO [*Mikolajewicz*, 2003]		For $T < -10$°C ; $\alpha_{max} = 0.4$
(3)	ECHAM5 [*Roeckner et al*, 2003]	Non-forested areas	Linear function of surface temperature between −5°C and 0°C
			For $T = 0$°C ; $\alpha_{min} = 0.4$
			For $T < -5$°C ; $\alpha_{max} = 0.8$
(4)	ECHAM5 [*Roeckner et al.*, 2003]	Forested areas	Linear function of surface temperature between −5°C and 0°C
			For $T = 0$°C; $\alpha_{min} = 0.3$
			For $T < -5$°C; $\alpha_{max} = 0.4$
(5)	*Roesch* [2000]	Non-forested areas	Polynomial temperature dependency between −10°C and 0°C. $\alpha = 0.5 + a_1 T_S + a_2 T_S^2 + a_3 T_S^3 + a_4 T_S^4$ ($a_1 = -0.0758627$, $a_2 = -5.5360168\ 10^{-3}$, $a_3 = -5.2966269\ 10^{-5}$, $a_4 = 4.2372742\ 10^{-6}$)
			For $T = 0$°C; $\alpha_{min} = 0.5$
			For $T < -10$°C; $\alpha_{max} = 0.8$
(6VIS) (6NIR)	*Roesch et al.* [2002]	Non-forested areas	Spectral albedo divided in visible and near-infrared wavelengths, which is a linear function of surface temperature between −10°C and 0°C.
			For $T = 0$°C; $\alpha_{VIS,min} = 0.57$, $\alpha_{NIR,min} = 0.39$
			For $T < -10$°C; $\alpha_{VIS,max} = 0.95$, $\alpha_{NIR,max} = 0.65$
(7VIS) (7NIR)	NCAR, *Collins et al.* [2002]		Spectral albedo divided in visible and near-infrared wavelengths, which is a linear function of surface temperature between −1°C and 0°C.
			For $T = 0$°C; $\alpha_{VIS,min} = 0.88$, $\alpha_{NIR,min} = 0.55$
			For $T < -1$°C; $\alpha_{VIS,max} = 0.98$, $\alpha_{NIR,max} = 0.70$
(8)	*Viterbo and Betts* [1999]	Forested areas	Constant snow albedo = 0.2

include melt ponds during summer. The main advantages of this data set are the high temporal resolution, and that the measured albedo can directly be connected with other measured variables. The second data set is an average albedo over a 200-m long line [*Perovich et al.*, 2002a] a few hundred meters away from the tower. This albedo line is a better estimate of area average albedo, but do not have the straight forward connection with measurements taken at the surface tower. The observation period was only from June to September 1998.

3. Parameterization of Snow and Sea Ice Albedo

3.1. Parameterization of Snow Albedo

[15] A common approach to diagnosing snow albedo in climate models is to apply a snow temperature dependency. We limit this study to do the same. This is mainly due to the fact that the observational data set of snow albedo (described above) only contains surface temperature as a potential forcing variable, but also because the availability of forcing variables in HIRHAM (and other climate models) are limited. Table 1 presents different snow albedo schemes for forested and non-forested areas. Number in brackets in the text refers to where in Table 1 the albedo scheme is described.

3.2. The Parameterization of Sea Ice Albedo

[16] Several different types of sea ice albedo schemes were selected and forced with SHEBA observations. Descriptions of the different schemes are given in Table 2. In the following, the number in brackets refers to where in Table 2 the sea ice albedo scheme is described.

4. Results of Offline Comparison of Snow and Sea Ice Albedo

4.1. Results of Offline Comparison of Snow Albedo Schemes

[17] Systematic differences between AVHRR estimated albedo and the different albedo parameterization schemes forced with AVHRR estimated surface temperature are presented in Tables 3 and 4 for non-forested and forested areas, respectively.

[18] For non-forested areas the original HIRHAM [1] albedo has no systematic overall deviation compared to observations. A positive bias is found in the other schemes. The original HIRHAM scheme has however, a large underestimation of the snow albedo for surface temperatures close to 0°C, which is compensated for by an overestimation for cold temperatures. The same deficiency was found by *Loth and Graf* [1998]. Except for the NCAR [7] scheme all the other schemes show a better agreement with the AVHRR

Table 2. Description of Sea Ice Albedo Schemes Used in Comparison With Observations

Scheme Number	Model/Reference	Description
(9)	HIRHAM [*Christensen et al.*, 1996]	Linear function of surface temperature between −1.5°C and 0°C. Fixed above at $\alpha_{min} = 0.55$ and below at $\alpha_{max} = 0.75$
(10)	REMO [*Mikolajewicz*, 2003]	Linear function of surface temperature between −3.0°C and 0°C. Fixed above at $\alpha_{min} = 0.55$ and below at $\alpha_{max} = 0.85$
(11VIS) (11NIR)	NCAR CCSM *Collins et al.* [2002]	Distinguish between snow and ice surface, and between albedo at VIS and NIR wavelength. For each group linear function of temperature between −1°C and 0°C; Fixed above at $\alpha_{min}^{SNOW/VIS} = 0.88$ $\alpha_{min}^{SNOW/NIR} = 0.55$ $\alpha_{min}^{ICE/VIS} = 0.705$ $\alpha_{min}^{ICE/NIR} = 0.285$ Fixed below at $\alpha_{max}^{SNOW/VIS} = 0.98$ $\alpha_{max}^{SNOW/NIR} = 0.70$ $\alpha_{max}^{ICE/VIS} = 0.78$ $\alpha_{max}^{ICE/NIR} = 0.36$ A total surface albedo was found by; $\alpha_{VIS/NIR} = \alpha_{VIS/NIR}^{ICE}(1 - f_s) + f_s \alpha_{VIS/NIR}^{SNOW}$
(12)	*Mellor and Kantha* [1989]	$\alpha_{DRYSNOW} = 0.82$ $\alpha_{MELTINGSNOW} = 0.73$ $\alpha_{ICE} = 0.64$
(13)	*Melia* [2002]	Distinguish between snow, non-melting and melting sea ice. For non-melting ice the albedo is set to the constant value 0.71 and for melting ice 0.50. The treatment of snow albedo is more advanced and includes snow aging processes following *Douville et al.* [1995]. The snow albedo is allowed to vary between 0.50 and 0.85. After a snow fall the albedo is increased according to (8) $\alpha_t = \alpha_{t-1} - (\alpha_{t-1} - \alpha_{max}) \frac{P_s}{P_{s,new}}$ where α_t is the albedo at a given time t, Ps is the liquid precipitation rate (m/s) and Ps,new = 0.002 m/s. When no new snow falls, the albedo decreases with time. For melting and rainy, and dry cold conditions the decaying formulas are: $\alpha_t = \alpha_{t-1} - \frac{\tau^1}{\tau^d}$ when $T < 0$ C; $\alpha_t = \alpha_{t-1} - \frac{1}{\tau^d}(\alpha_{t-1} - \alpha_{min})$ when $T \geq 0$ C where τ^1, τ^e, τ^d are 0.008, 0.24 and 86400, respectively.

estimated albedo in the different temperature intervals. It is important to calculate the surface albedo properly under periods with high solar radiation. For snow covered areas this is typically in spring when surface temperatures are approaching 0°C with frequent melting. From a model perspective snow albedo should have small systematic errors under such conditions. Based on this, the polynomial approach by *Roesch* [2000] [5] seems like the most suitable albedo scheme for non-forested areas.

[19] For forested areas, 4 different albedo schemes are compared. However, the spectral approach by *Roesch et al.* [2002] [6] do not differ between near-infrared and visible wavelengths and only differ from the original HIRHAM [2] scheme conceptually. While HIRHAM [2] and ECHAM5 [4] have small overall systematic errors the use of the constant value of *Viterbo and Betts* [1999] [8] underestimates the snow albedo with 0.17. However, several observational studies support the low value of Viterbo and Betts [8]. *Ni and Woodcook* [2000] state that when forest cover is higher than 70%, presence of snow has little effect on surface albedo. However, for the AVHRR data the surface albedo increases when snow is presenting forested areas. In temperature intervals close to melting the original HIRHAM [1] scheme has lower errors than the other schemes.

[20] Based on the above comparison it is tempting to use the original HIRHAM [2] scheme for snow covered forested areas and the polynomial temperature-dependent albedo from *Roesch* [2000] [5] for non-forested areas. The effect of using these parameterizations in HIRHAM will be presented in section 7.

Table 3. Systematic Errors (Bias = Model-AVHRR) for Different Albedo Schemes and Separated Into Temperature Intervals in Non-Forested Areas[a]

Temperature Range , °C	*N*	Scheme (1)	Scheme (3)	Scheme (5)	Scheme (6VIS)	Scheme (6NIR)	Scheme (6)	Scheme (7VIS)	Scheme (7NIR)	Scheme (7)
−30, 0	6039	0.0	0.06	0.07	0.12	−0.05	0.04	0.27	0.08	0.18
−2, 0	1200	−0.16	−0.12	−0.03	−0.07	−0.10	−0.09	0.28	0.15	0.22
−4, −2	549	−0.14	−0.02	0.02	−0.04	−0.13	−0.08	0.26	0.10	0.18
−6, −4	496	−0.08	0.10	0.07	0.03	−0.11	−0.04	0.25	0.06	0.16
−8, −6	755	−0.01	0.12	0.10	0.11	−0.07	0.02	0.25	0.06	0.16
−10, −8	820	0.08	0.12	0.12	0.20	−0.02	0.09	0.27	0.06	0.17
−30, −10	2208	0.12	0.12	0.12	0.25	0.00	0.13	0.28	0.05	0.17

[a] Scheme number refers to description of scheme in Table 1. *N* is number of observations. All schemes are forced with estimated surface temperature from AVHRR.

Table 4. As in Table 3, but for Forested Areas and the Schemes (2), (4), (8)

Temperature Range, °C	*N*	Scheme (2)	Scheme (4)	Scheme (8)
−30, 0	9775	−0.01	0.03	−0.17
−2, 0	1558	−0.02	0.07	−0.13
−4, −2	1449	0.01	0.08	−0.12
−6, −4	1529	0.01	0.06	−0.14
−8, −6	1516	0.02	0.05	−0.15
−10, −8	1055	0.02	0.03	−0.17
−30, −10	2630	−0.06	−0.06	−0.26

4.2. Results of Offline Comparison of Sea Ice Albedo Schemes

[21] Table 5 shows monthly mean observed and simulated albedo. Since, the line-albedo is the best estimate of the area albedo with melt ponds [*Perovich et al.*, 2002a], the comparison of simulated values is done with the line albedo when this is available and with the tower albedo during winter/spring. This should give a good representation of the annual sea ice albedo cycle, since the sea ice surface is very homogenous during winter and very heterogeneous after the onset of the melt period and during the summer.

[22] During winter all schemes are in reasonable agreement with observations except for the HIRHAM [9] albedo which underestimates the sea ice albedo. When the snow starts to melt in June, the albedo in the temperature-dependent schemes (HIRHAM [9] and REMO [10]) rapidly decrease, leading to a negative albedo bias. Schemes which differ between snow on sea ice and snow-free sea ice (NCAR [11], Mellor and Kantha [12], Melia [13]), overestimate the albedo. In July, when melt ponds have formed, all schemes overestimate the albedo. The overestimations vary from 0.02 to 0.15, with the NCAR [11] scheme to fit the observed values best. A Kolmogorov-Smirnov test is performed on the data set and all schemes do significantly differ from the observations.

[23] In August, the observed surface albedo continue to decrease while the parameterized albedo keep their July values. In Figure 1, time series of the difference between observed absorption of solar radiation and modeled absorption with the different schemes are shown. This figure underlines some of the mentioned findings. During winter, the impact of different albedo schemes is small except for the HIRHAM [9] scheme which leads to a 10–20 W/m^2 overestimated absorption of solar radiation in the sea ice in late winter. The peak in the error by the HIRHAM [9] and the REMO [10] scheme at the onset of the melting season (around day 150) is a common deficiency for temperature-dependent schemes. A temperature-dependent scheme decreases the albedo immediately when the temperature approaches the melting point. From the figure it is also clear that too little radiation is absorbed during summer for all schemes. Table 5 and Figure 1 show that the NCAR scheme is most appropriate for a correct simulation of the annual albedo cycle.

[24] In Table 6, the deviation between simulated and observed absorbed radiation is presented as monthly means. In average over all months, the systematic error for the different models varies between an overestimation of 3.8 W/m^2 for HIRHAM [9] to an underestimation of −12.2 W/m^2 for the *Mellor and Kantha* [1989] [12] scheme. All schemes reflect too much radiation in July and August. The NCAR [11] scheme is closest with biases of 7.3 W/m^2 (July) and 14.2 W/m^2 (August). However, based on these numbers it is difficult to claim that one scheme performs reasonable well over the Arctic sea ice. This is in agreement with the findings of *Curry et al.* [2001] in a similar evaluation of other sea ice albedo schemes.

5. A New Description of Snow and Sea Ice Albedo in Hirham

5.1. The New Snow and Sea Ice Albedo Scheme

[25] From the above discussion, it can be concluded that the HIRHAM scheme should improve if we replace the original snow albedo for non-forested areas with the polynomial temperature dependency of *Roesch* [2000] [5]. We refer to this parameterization as the new snow albedo scheme.

[26] Replacement of the albedo for sea ice albedo does not look equally promising. Therefore we suggest a completely new parameterization for sea ice albedo. Three versions of the new sea ice albedo scheme with different input requirements are presented. All three schemes are based on observations from the SHEBA project and a literature study of observed sea ice albedo [*Køltzow et al.*, 2003]. All 3 schemes include the effect of melt ponds during summer and the effect of snow on sea ice in winter/spring.

5.1.1. A New Sea Ice Albedo Scheme: Version 1

[27] Forcing for this scheme is surface temperature, and the scheme can therefore be used in a variety of models.

Table 5. Average Monthly Mean Albedo From Observations and Different Albedo Schemes[a]

	Total	February	March	April	May	June	July	August
TOWALB	0.77	0.83	0.85	0.85	0.85	0.83	0.66	0.58
LINALB	0.58	–	–	–	–	0.75	0.55	0.45
Scheme (9)	0.69	0.75	0.75	0.75	0.75	0.68	0.59	0.58
Scheme (10)	0.75	0.85	0.85	0.85	0.85	0.73	0.60	0.60
Scheme (11)	0.74	0.85	0.85	0.85	0.85	0.80	0.57	0.57
Scheme (12)	0.76	0.82	0.82	0.82	0.82	0.81	0.70	0.64
Scheme 13)	0.77	0.81	0.84	0.85	0.85	0.80	0.63	0.65

[a]TOWALB is albedo observed at the SHEBA tower (described by *Persson et al.*, 2002), LINALB is albedo observed at the SHEBA albedo line (described by *Perovich et al.*, 2002a, 2002b).

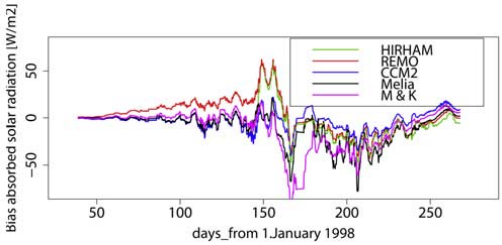

Figure 1. Time series of differences between observed and simulated absorbed solar radiation by using albedo parameterization from HIRHAM (red), REMO (green), NCAR (dark blue), Melia (light blue) and Mellor and Kantha (pink).

Snow and sea ice surfaces are not distinguished and the sea ice albedo is estimated by:

$$\begin{array}{ll} \alpha_{\text{seaice}} = 0.84 & T_S \le -2^\circ\text{C} \\ \alpha_{\text{seaice}} = 0.84 - 0.145(2 + T_S) & 0^\circ\text{C} > T_S > -2^\circ\text{C} \\ \alpha_{\text{seaice}} = 0.51 & T_S \ge 0^\circ\text{C} \end{array} \quad (1)$$

this relationship is based on examination of the SHEBA data set and maximum and minimum values given in Table 7. The high value for cold ice is supposed to include the effect of snow on sea ice in winter and spring. Melt pond albedo is parameterized following Table 7, while melt pond fraction is approximated by the surface temperature (°C);

$$\Delta\text{meltpond} = 0.11 \cdot (2 + T_S) \quad T_S \ge -2^\circ C \quad (2)$$

[28] No melt ponds develop for temperature below −2°C. This relationship is a crude estimate based on SHEBA data. This approximation is setting limitations to the parameterization. Firstly, this scheme will always predict melt ponds immediately when snow melting starts and therefore predict too low albedo in early summer. Secondly, this approximation limits the amount of melt pond fraction to 0.22 which is below several observations [*Tschudi et al.*, 2001]. The total albedo is given by:

$$\alpha_{surface} = (1 - \Delta\text{meltpond}) \cdot \alpha_{\text{seaice}} + \Delta\text{meltpond} \cdot \alpha_{\text{meltpond}} \quad (3)$$

5.1.2. A New Sea Ice Albedo Scheme: Version 2

[29] Forcing for this scheme is surface temperature and snow cover. The surface is divided into three types, snow, bare sea ice and melt ponds. The bare sea ice and snow covered sea ice is given an albedo based on the surface temperature (Table 7). In addition, melt pond fraction is calculated by equation (2), and melt pond albedo is taken from Table 7. The total area albedo is then

$$\alpha_{\text{area}} = \Delta\text{snow} \cdot \alpha_{\text{SNOW}} + \Delta\text{seaice} \cdot \alpha_{\text{SEAICE}} + \Delta\text{meltpond} \cdot \alpha_{\text{meltpond}} \quad (4)$$

where Δsnow, Δseaice, Δmeltpond is the fraction of snow covered surface, bare sea ice and melt ponds, respectively.

Table 7. Albedo Values for Different Surface Types in the Proposed New Sea Ice Albedo Scheme

$\alpha_{\text{DRYSNOW}} = 0.84$	*Grenfell and Perovich* [1984], *Grenfell et al.* [1994], *Curry et al.* [1996] and [*Curry et al.*, 2001]
$\alpha_{\text{MELTING\_SNOW}} = 0.77$	*Curry et al.*, 2001, *Lindsay and Rothrock* [1994] and *Perovich et al.* [2002a]
$\alpha_{\text{BARE\_ICE}} = 0.57$	[*Persson et al.*, 2002; *Eicken et al.*, 1994]
$\alpha_{\text{MELTING\_SEA\_ICE}} = 0.51$	*Curry et al.* [2001]
$\alpha_{\text{MELTPONDS}}$ (T_S) = 0.36−0.1 ($2 + T_S$) $T_S \ge -2°C$	*Tschudi et al.* [2001], *Perovich and Grenfell* [1981], *Langleben* [1969] and *Perovich et al.* [2002a]

5.1.3. A New Sea Ice Albedo Scheme: Version 3

[30] Forcing for this scheme is surface temperature, snow cover fraction and melt pond fraction. The surface is divided into three types, snow, bare sea ice, and melt ponds. The three different surface types are given an albedo based on the surface temperature (Table 7).

[31] As the sea ice albedo depends on ice thickness we use the above descriptions for sea ice thicker than 0.25 m. A linear decrease toward the ocean albedo is applied for thinner ice [*Perovich and Grenfell*, 1981].

5.2. Comparison of the New Sea Ice Albedo Scheme With Observations

[32] A first test of the new sea ice albedo schemes is to compare them with the SHEBA data set. However, melt pond data from the SHEBA data set is only available once every day. Because of too little input data we are not able to validate version 3 of the new sea ice albedo scheme.

[33] In Figure 2, the estimated and observed melt pond fractions are shown. The missing inertia in the model contributes to a swift response in the melt pond fraction, in addition, to the fact that the model calculates hourly values while observations are taken diurnally. Given that the observations in Figure 2 and Table 8 are not taken independently from the deduced model formulas the comparison is not a true validation, but serves to illustrate that the albedo scheme manage to reproduce melt pond frac-

Table 6. Monthly Mean of Differences Between Observed Absorption of Solar Radiation (W/m^2) and Simulated Values Using the Different Albedo Schemes[a]

	Total	February	March	April	May	June	July	August
Scheme (9)-OBS	3.8	1.4	6.1	11.9	15.7	22.9	−9.3	−22.3
Scheme (10)-OBS	−5.7	−1.2	−1.1	−2.2	−4.8	6.6	−12.6	−24.6
Scheme (11)-OBS	−6.0	−1.2	−1.2	−2.3	−5.1	−11.0	−7.3	−14.2
Scheme (12)-OBS	−12.2	−0.4	1.0	2.1	1.4	−11.9	−43.9	−34.0
Scheme (13)-OBS	−11.8	−0.3	−0.4	−1.5	−3.8	−10.4	−27.7	−38.8

[a]The albedo schemes are forced with observations to decide surface albedo, and then with observed incoming solar radiation to calculate absorbed energy. Positive values imply that the albedo schemes absorb more solar energy than measured. The observed absorption use the tower albedo from February to May and the line albedo from June to September (best estimate of observed surface albedo).

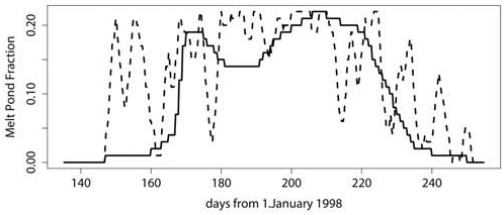

Figure 2. Observed (solid) and parameterized (dashed) melt pond fraction following equation (3).

tions. This is novel compared to earlier schemes. Unfortunately, independent data are not available. The gross features are the same for observed and the simulated melt pond fraction. As expected the simulated melt pond fraction increase immediately when the temperature reaches the melting point. In reality it takes time to accumulate meltwater. A more complex scheme should account for this inertia.

[34] Monthly mean albedo and systematic error for absorbed solar radiation are printed in Table 8. Versions 2 and 1 are very similar through the year, but version 1 has slightly higher biases than version 2. Both schemes are however, closer to observed albedo and has lower systematic error than existing schemes, regarding absorbed solar radiation (Table 6). In section 7 will the new snow albedo scheme be tested in HIRHAM, and version 1 for sea ice albedo, referred to as new sea ice albedo, in climate simulations with HIRHAM. *Dethloff et al.* [2006] tested the more advanced version 2 for sea ice albedo in a GCM and discussed global implications of sea ice albedo changes in the Arctic.

6. Hirham and Experimental Setup

[35] The regional climate model HIRHAM consists of the HIRLAM Eulerian grid point model [*Gustafsson*, 1993] and the ECHAM4 physical parameterization routine [*Roeckner et al.*, 1996]. In addition to this, some minor modifications are done and the whole model is described in detail by *Christensen et al.* [1996]. The dynamics include prognostic equations for surface pressure, horizontal wind components, specific humidity, cloud water, and temperature. Processes that are not resolved with the horizontal and vertical resolution are parameterized and include radiation transfer, turbulent fluxes, cumulus convection, large scale condensation and land surface processes. Over land surfaces, albedo is given by climatology and modified according to appearance of snow. The snow albedo scheme are described in section 3.1 (scheme number 1 (non-forested areas) and scheme number 2 (forested areas) in Table 1). Description of the sea ice albedo is given in section 3.2 (scheme number 9, Table 3).

[36] The treatment of heat conduction in sea ice and the diagnostic equation for snow fraction over land will in the following be described. Sea ice concentration is an input field in HIRHAM, while sea ice thickness in the Arctic is fixed to 2 m. Additional accumulation of snow on the sea ice is neglected. The sea ice skin temperature is calculated according to the linearized heat balance equation;

$$Q(T_{\mathrm{skin}}) = \frac{C_{\mathrm{p}}}{\mathrm{D}t}\left(T_{\mathrm{skin}} - T_{\mathrm{skin}}\{t - \mathrm{D}t\}\right) \tag{5}$$

where the capacity C_{p} corresponds to the fixed ice thickness, Q denotes the heat flux, T_{skin} the skin surface temperature and Δt is the time step.

[37] Fraction of snow cover on land (f_{snow}) is diagnosed as a function, of snow water equivalent (SWE), f_{snow} = SWE/(SWE + 0.01), which is a prognostic variable in the model given in meter. This implies that for approximately 20 cm of fresh snow the snow cover is approximately 95%.

[38] A control simulation (original snow and sea ice albedo), experiment 1 with new sea ice albedo (version 1 described in the previous section) and experiment 2 with new snow albedo for non-forested areas (from *Roesch* [2000], described as scheme number (5) in Table 1) are performed with HIRHAM. All simulations are 9 year long and the last 8 year (1991–1998) is used in the analyses. The model makes use of 0.5° horizontal resolution and 19 vertical levels. Lateral and surface boundary conditions are taken from the ERA40 data set, and the integration domain is shown in Figure 3. In the same figure fraction of forest is shown together with sea ice cover in May 1990.

7. Response to New Surface Albedo in Simulations With HIRHAM

7.1. Response to New Sea Ice Albedo in Simulations With HIRHAM

[39] Compared to the old sea ice albedo scheme, the new sea ice albedo scheme gives higher sea ice albedo in winter and spring and lower sea ice albedo in summer (June and July). In winter due to the effect of a snow cover which increases the albedo in the new formulation and the formation of melt ponds on the sea ice which decreases the albedo

Table 8. Monthly Mean Albedo and Radiation From Observations and Different Albedo Schemes[a]

	Total	Feb	Mar	Apr	May	Jun	Jul	Aug
Tower albedo	0.77	0.83	0.85	0.85	0.85	0.83	0.66	0.58
Line albedo	–	–	–	–	–	0.75	0.55	0.45
V2 albedo	0.70	0.84	0.84	0.84	0.84	0.74	0.51	0.49
V1 albedo	0.71	0.84	0.84	0.84	0.84	0.73	0.53	0.52
V2 ASW-OBS ASW	0.0	−0.9	−0.4	−0.7	−2.8	3.6	8.1	−6.7
V3 ASW-OBS ASW	−0.6	−0.9	−0.4	−0.7	−2.8	8.1	5.0	−12.3

[a] TOW ALB is albedo observed at the tower, LINALB is albedo observed at the albedo line. ASW is absorbed short wave radiation at the surface, while V1, V2 and V3 refer to versions of the new sea ice albedo scheme. The two last lines show monthly means of differences between observed absorption of solar radiation (W/m2) and simulated values using the different albedo schemes. The observed absorption use the tower albedo from February to May and the line albedo from June to September (best estimate of observed surface albedo).

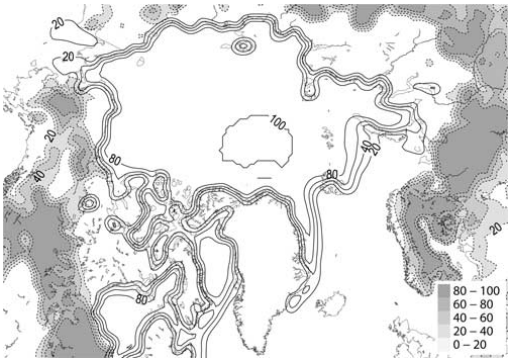

Figure 3. Integration domain for HIRHAM. Fraction of forest in grey, sea ice cover valid for may 1990 (solid lines).

in summer. This changes the fraction of absorbed solar radiation in the sea ice. In April and May, 4 W/m^2 less solar radiation is absorbed with the new scheme averaged over the integration domain. Furthermore, 2 W/m^2 more solar radiation is absorbed in the summer (JJA). For only sea ice covered areas these changes are up to 15 W/m^2 in monthly means. These findings are in agreement with the off-line evaluation of sea ice albedo schemes in sections 4 and 5.

[40] Figure 4 show differences in 2 m air temperature for March, April and May (MAM) between the control simulation and ERA40, and changes due to the new sea ice albedo scheme. In the control simulation a warm bias of up to 7°C is present in the Arctic. For large parts of the Arctic the new sea ice albedo scheme is 2–3°C colder than the old scheme. A statistical t-test is performed on the differences in temperature between the new sea ice albedo simulation and the control simulation. The areas where the probability that they differ is higher than 95% are marked in the figure, and enclose large parts of the Arctic Ocean, Labrador Sea and Hudson Bay. The new scheme is in better agreement with ERA40 temperatures, but still, HIRHAM with new sea ice albedo has a warm bias in Arctic (2–3°C). The contributions to the improved spring temperature in HIRHAM are similar in April and May month. In March, less solar radiation is present in the Arctic combined with a colder surface for which HIRHAM is less sensitive to differences in the albedo description. The new sea ice albedo tends to decrease mean sea level pressure (MSLP) bias compared to ERA40 during spring (Figure 5). This is seen for Northern Scandinavia and parts of Russia and Canada. However, a too high surface pressure seems to be present over the North Pole with the new sea ice albedo. None of these changes are statistical significant.

[41] In summer, the surface pressure response (Figure 6), although apparently large, is insignificant in the 5% level. In July and August considerably smaller differences are found for surface pressure.

[42] For the autumn (September, October and November) the 2-m air temperature with the new sea ice albedo is up to 1°C colder than the original scheme. This is mainly due to differences in September (Figure 7) where the new sea ice albedo gives a temperature 0.5–2.0°C colder than the old scheme and increasing the temperature gradient southwards. In October and November less solar radiation reaches sea ice covered parts of Arctic and only minor differences are found. However, compared to ERA40 the different albedo schemes are equally skillful during autumn regarding 2 m air temperature. The positive surface pressure bias in the eastern part of the Arctic is reduced by 1–2 hPa. As for surface air temperature the change in mean sea level pressure in autumn is mainly due to changes in September (Figure 8). The new sea ice albedo strengthens the low pressure system in the Barents Sea with up to 5 hPa, which is in better agreement with ERA40. However, none of the changes in autumn are statistical significant.

[43] Despite more solar radiation during summer (JJA) the change in sea ice albedo formulation has larger impact in spring (MAM). This is partly due to less sea ice in summer and partly due to the model formulation with prescribed sea ice thickness and cover. Early in June the surface temperatures of the sea ice reaches 0°C with both

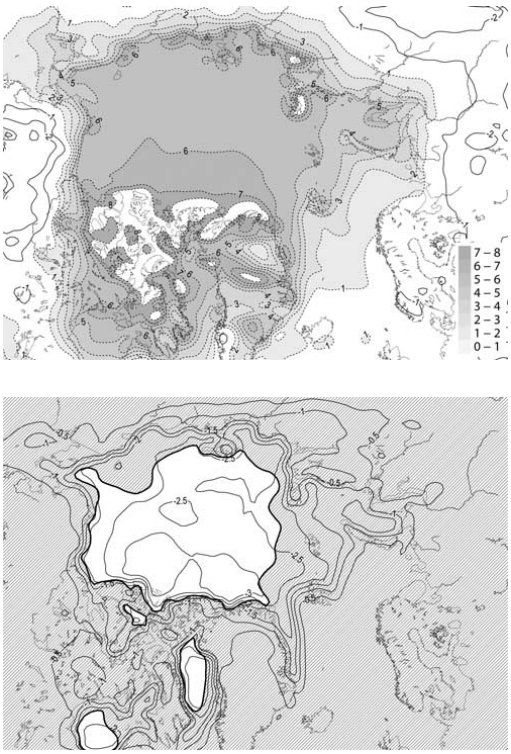

Figure 4. (a) 2 m air temperature [°C], control simulation minus ERA40, average over March, April and May. Differences plotted in 1°C intervals. (b) 2 m air temperature [°C], new sea ice albedo simulation minus control simulation, average over March, April and May. Differences plotted in 0.5°C intervals. The two simulations differ with more than 95% probability in areas with white background enclosed by the black lines.

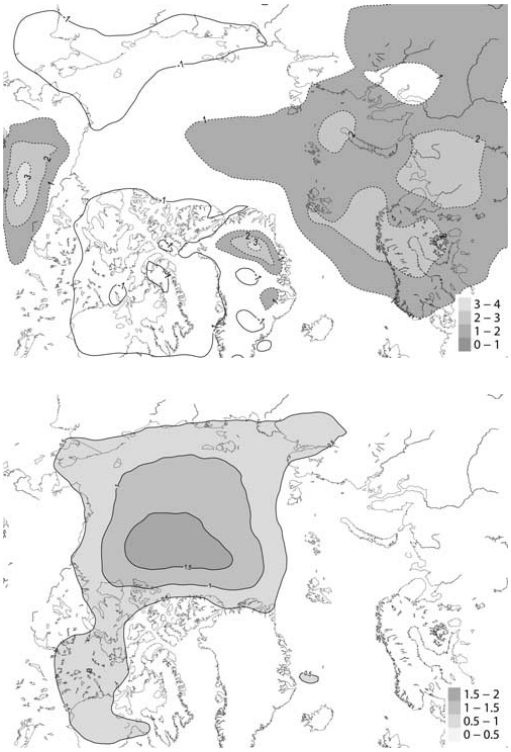

Figure 5. (a) Mean sea level pressure [hPa], control simulation minus ERA40, average over March, April and May. Differences plotted in 1-hPa intervals. (b) Mean sea level pressure [hPa], new sea ice albedo minus control simulation, average over March, April and May. Differences plotted in 0.5 hPa intervals.

sea ice albedo formulations. Little will therefore distinguish the two simulations during the rest of the melt period. In a coupled model system and in the real world, the situation would be different as the extra absorbed energy with the new albedo scheme will melt sea ice.

7.2. Response to New Snow Albedo in Simulations With Hirham

[44] The change of snow albedo scheme for non-forested areas shows less impact than for the new sea ice albedo. However, local responses are seen. Possible reasons for this is that the land surface in the integration domain is dominated by forested areas except for north of 65°N and some mountainous regions (Figure 3). These areas are smaller than sea ice covered areas and are more constrained by the lateral boundary fields.

[45] In MAM the new snow albedo gives higher surface albedo in snow covered areas close to the Arctic Ocean. In these areas a reduction of about 5 W/m^2 in net solar radiation at TOA is seen, but little impact on other parameters (T2M, MSLP, cloud cover). An impact in summer average (June, July and August) is found in some regions with late snowmelt. This is especially seen near the Kara Sea were the new snow albedo scheme is 1–2°C colder (Figure 9), and with 1 hPa higher surface pressure (not shown), and in better agreement with ERA40-data than the original scheme. Associated with these changes are an increase of 4–8% in cloud cover and a decrease of 10–15 W/m^2 of net solar radiation at TOA (not shown). However, none of these differences are statistical significant.

[46] In winter (December, January and February) little impact of changing snow and sea ice albedo is found due to the lack of solar radiation at high northern latitudes.

8. Summary and Conclusions

[47] Several existing snow and sea ice albedo schemes have been off-line validated against observed albedo. Compared with observations from the SHEBA experiment it was found a large scatter in the quality of different sea ice albedo schemes. However, no scheme were superior the other schemes as they failed to describe the entire annual cycle.

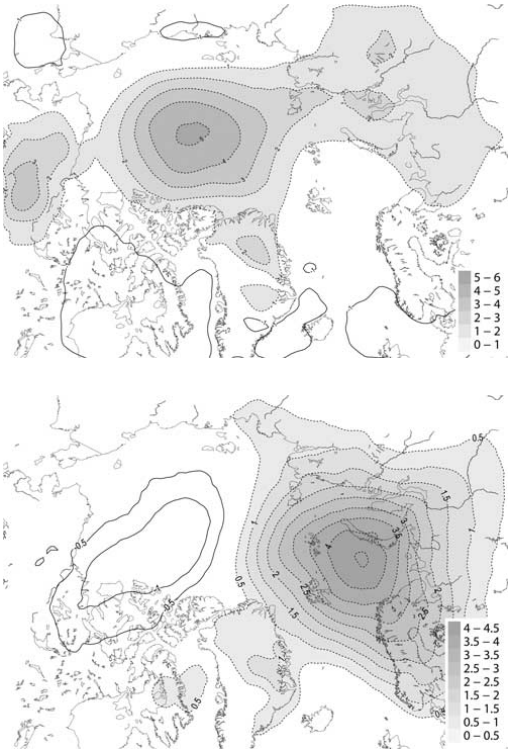

Figure 6. (a) Mean sea level pressure [hPa], control simulation minus ERA40, average over June. Differences plotted in 1 hPa intervals. (b) Mean sea level pressure [hPa], new sea ice albedo minus control simulation, average over June. Differences plotted in 0.5 hPa intervals.

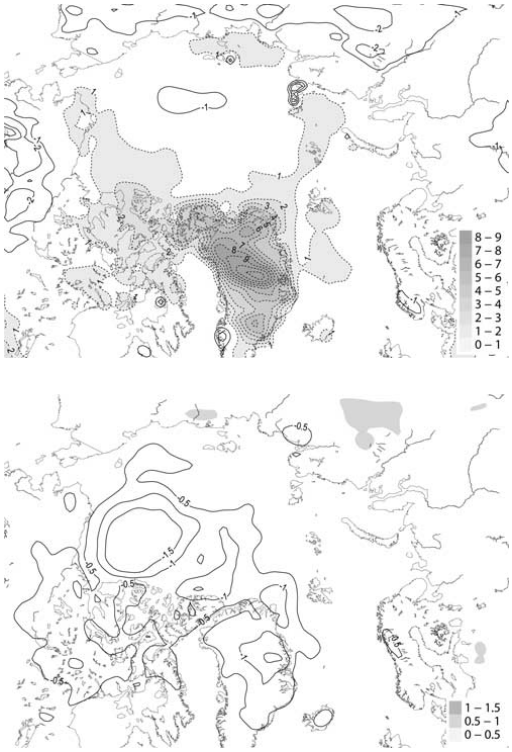

Figure 7. (a) 2 m air temperature [°C], control simulation minus ERA40, average over September. Differences plotted in 1°C intervals. (b) 2 m air temperature [°C], new sea ice albedo simulation minus control simulation, average over September. Differences plotted in 0.5°C intervals.

This is the same findings as *Curry et al.* [2001] in a similar comparison, but with other sea ice albedo schemes. A common deficiency was too high albedo in summer. In addition, the temperature-dependent schemes had too low albedo in the transition period between spring and summer. It was further shown that a sea ice albedo scheme should include the effects of snow and melt-ponds on the sea ice, and by doing this it was possible to improve the existing sea ice albedo scheme in HIRHAM and getting better agreement with observed albedo from the SHEBA campaign.

[48] For forested areas there were good agreement between estimated snow albedo from AVHRR and simulated snow albedo, except for the constant value of 0.2 suggested by *Viterbo and Betts* [1999]. For non-forested areas a large spread in simulated albedo was found. However, the most important period to correctly simulate the snow albedo is during melting in spring due to increased solar radiation. Having this in mind the polynomial temperature-dependent approach [*Roesch*, 2000] is probably the best of the compared snow albedo schemes and might improve the HIRHAM snow albedo.

[49] Effects of changing the description of snow and sea ice albedo in HIRHAM are seen in the period from April to September. From October to March the amount of solar radiation hitting snow and sea ice covered areas are small and only minor changes occur. The most pronounced change happens in surface air temperature over Arctic sea ice in spring due to changed sea ice albedo. The effect of new surface albedo on T2M is mainly restricted to local changes in surface albedo, which is in agreement with the findings of *Barnett et al.* [1989].

[50] Compared to ERA40 data a significant improvement of the model performance is found during spring. In mean sea level pressure a positive impact of new sea ice albedo is found in spring and autumn, while a decrease in quality is found in June. Except for the latter, the overall performance of HIRHAM is improved with new snow and sea ice albedo. This suggests that a RCM is not entirely steered by the lateral forcing, but that surface forcing and model physics are important for successful simulations. It is worth to notice that HIRHAM is much more sensitive to changes in sea ice albedo than snow albedo on land in the performed

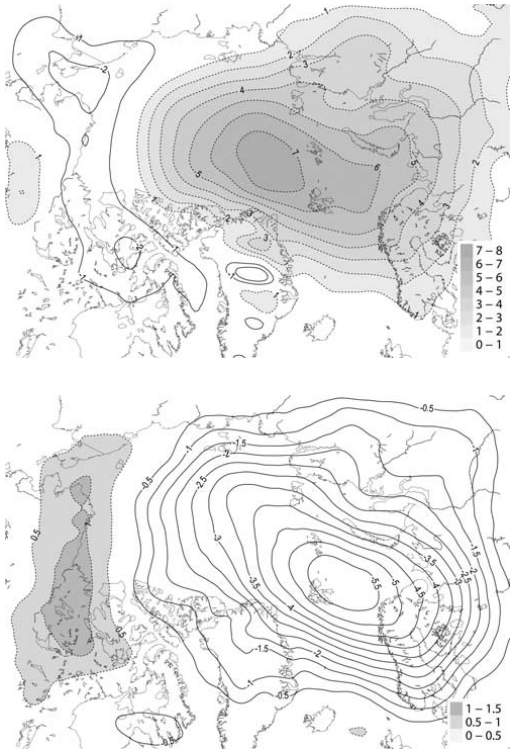

Figure 8. (a) Mean sea level pressure [hPa], control simulation minus ERA40, average over September. Differences plotted in 1 hPa intervals. (b) Mean sea level pressure [hPa], new sea ice albedo minus control simulation, average over September. Differences plotted in 0.5 hPa intervals.

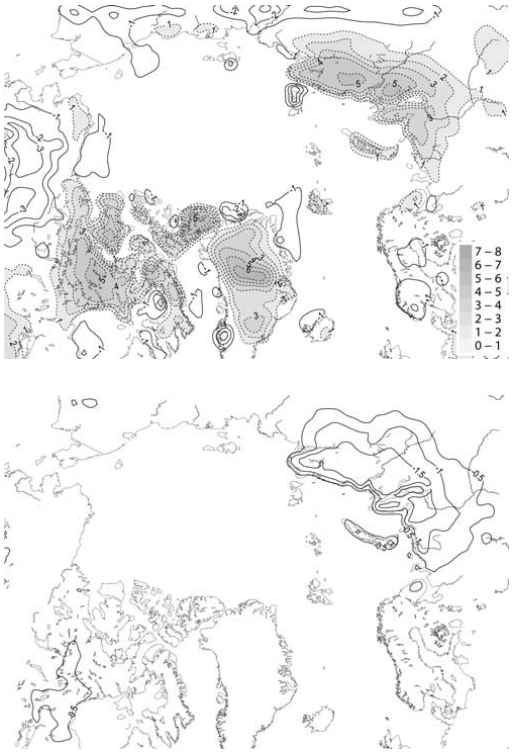

Figure 9. (a) 2 m air temperature [°C], control simulation minus ERA40, average over June, July and August. Differences plotted in 1°C intervals. (b) 2 m air temperature [°C], new snow albedo minus control simulation, average over June, July and August. Differences plotted in 0.5°C intervals.

simulations. This is due to (i) the integration domain and (ii) the sea-ice and land distribution within the model domain. In addition, it should be expected even higher sensitivity to changes in sea ice albedo in a coupled climate model because of the sea ice albedo feedback process.

[51] **Acknowledgments.** This work has been supported by the Research Council of Norway under the national project RegClim (grant no. 155976/720), and the EU project GLIMPSE (EVK2-2001-00337). Computer time on the SGI Origin 3800 at the Norwegian High Performance Computing Facility was granted by the Research Council of Norway. Grateful thank to Steinar Eastwood for providing AVHHR data, Dr. Jan Erik Haugen for help with the HIRHAM model and Prof. Trond Iversen for comments to the manuscript.

References

Barnett, T. P., L. Dumenil, U. Schlese, E. Roeckner, and M. Latif (1989), The effect of Eurasian snow cover on regional and global climate variations, *J. Atmos. Sci.*, *46*, 661–685.

Christensen, J. H., O. B. Christensen, P. Lopez, E. van Meijgaard, and M. Botzet (1996), The HIRHAM4, Regional Atmospheric Climate Model, Danish Meteorological Institute - Scientific Report - Copenhagen.

Collins, et al. (2002), Description of the NCAR Community Atmosphere model (CAM2). http://www.ccsm.ucar.edu/models/atm-cam/docs/description/index.html.

Curry, J. A., W. B. Rossow, D. Randall, and J. L. Schramm (1996), Overview of Arctic Cloud and Radiation Characteristics, *J. Clim.*, *9*, 1731–1764.

Curry, J. A., J. L. Schramm, D. K. Perovich, and J. O. Pinto (2001), Applications of SHEBA/FIRE data to evaluation of snow/ice albedo parameterizations, *J. Geophys. Res.*, *106*(D14), 15,345–15,355.

Dethloff, K., A. Rinke, A. Benkel, M. Køltzow, E. Sokolova, S. Kumar Saha, D. Handorf, W. Dorn, B. Rockel, H. von Storch, J.E. Haugen, L. P. Røed, E. Roeckner, J. H. Christensen, and M. Stendel (2006), A dynamical link between the Arctic and the global climate system, *Geophys. Res. Lett.*, *33*, L03703, doi:10.1029/2005GL025245.

Douville, H., J. F. Royer, and J. F. Mahfouf (1995), A new snow parameterization for the Meteo-France climate model, *Clim. Dyn.*, *12*, 21–35.

Eicken, H., T. Martin, and E. Reimnitz (1994), Sea ice conditions along the cruise track, In D. K. Futterer editor, The expedition Arctic'93. Leg ARK-IV/4 of RV Polarstern 1993, *Berichte zur Polarforschnung*, 149, 42–47.

Grenfell, T. C., and D. K. Perovich (1984), Spectral albedos of sea ice and incident solar irradiance in the southern Beaufort Sea, *J. Geophys. Res.*, *89*(C3), 3573–3580.

Grenfell, T. C., S. G. Warren, and P. C. Mullen (1994), Reflection of solar radiation by the Antarctic snow surface at ultraviolet, visible, and near-infrared wavelengths, *J. Geophys. Res.*, *99*(D9), 18669–18684.

Gustafsson, N. (1993), HIRLAM2 final report. HIRLAM Tech Rep 9, Swedish Meteorological and Hydrological Institute, Norrkoping, Sweden.

Køltzow, M., S. Eastwood, and J. E. Haugen (2003), Parameterization of snow and sea ice albedo in climate models, Research report no. 149, Norwegian Meteorological Institute.

Langleben, M. P. (1969), Albedo and degree of puddling of a melting cover of sea ice, *J. Glaciol.*, *8*, 54.

Lindsay, R. W., and D. A. Rothrock (1994), Arctic Sea Ice Albedo from AVHRR, *J. Clim.*, *7*, 1737–1749.

Lindsay, R. W., and J. Zhang (2005), The Thinning of Arctic Sea Ice, 1988–2003: Have We Passed a Tipping Point?, *J. Clim.*, *18*, 4879–4894.

Loth, B., and H.-F. Graf (1998), Modelling the snow cover in climate studies 2. The sensitivity to internal snow parameters and interface processes, *J. Geophys. Res.*, *103*(D10), 11329–11340.

Melia, S. (2002), A global couples sea-ice-ocean model, *Ocean Modell.*, *4*, 137–172.

Mellor, G. L., and L. Kantha (1989), An Ice-Ocean Coupled Model, *J. Geophys. Res.*, *94*(C8), 10937–10954.

Mikolajewicz, U. (2003), Private Communication with Uwe Mikolajewicz.

Ni, W., and C. E. Woodcook (2000), Effect of canopy structure and the presence of snow on the albedo of boreal conifer forests, *J. Geophys. Res.*, *105*(D9), 1187–11888.

Pedersen, C. A., and J.-G. Winther (2005), Intercomparison and Validation of Snow Albedo Parameterisation Schemes in Climate Models, *Clim. Dyn.*, *25*, 351–362, doi:10.1007/s00382-005-0037-0.

Perovich, D. K., and T. C. Grenfell (1981), Laboratory studies of the optical properties of young sea ice, *J. Glaciol.*, *27*, 96.

Perovich, D. K., T. C. Grenfell, B. Light, and P. V. Hobbs (2002a), Seasonal evolution of the arctic sea ice albedo, *J. Geophys. Res.*, *107*(C10), 8044, doi:10.1029/2000JC000438.

Perovich, D. K., W. B. Tucker III, and K. A. Ligett (2002b), Aerial observations of the evolution of ice surface conditions during summer, *J. Geophys. Res.*, *107*(C10), 8048, doi:10.1029/2000JC000449.

Persson, P. O. G., C. W. Fairall, E. L. Andreas, P. S. Guest, and D. K. Perovich (2002), Measurements near the Atmospheric Surface Flux Group tower at SHEBA: Near-surface conditions and surface energy budget, *J. Geophys. Res.*, *107*(C10), 8045, doi:10.1029/2000JC000705.

Roeckner, E., K. Arpe, L. Bengtsson, M. Cristoph, M. Claussen, L. Dumenil, M. Esch, M. Giorgetta, U. Schlese, and U. Schulzweida (1996), The atmospheric general circulation model ECHAM-4: Model description and simulation of present-day climate. MPI Rep 218, Max Planck Institute for Meteorology, Hamburg, Germany.

Roeckner, E., G. Bauml, L. Bonaventura, R. Brokopf, M. Esch, M. Giorgetta, S. Hagemann, I. Kirchner, L. Kornblueh, E. Manzini, A. Rhodin, U. Schlese, U. Schulzweida, and A. Tompkins (2003), The Atmospheric General Circulation Model ECHAM5: Part 1. Technical Report 349, Max Planck Institute for Meteorology.

Roesch, C. A. (2000), Assessment of the land surface scheme in climate models with focus on surface albedo and snow cover, Zurcher Klima-Schriften 78, ETH Geographisches Institut, Zurich.

Roesch, A., H. Gilgen, M. Wild, and A. Ohmura (1999), Assessment of GCM-simulated snow albedo using surface observations, *Clim. Dyn.*, *15*, 405–418.

Roesch, C. A., M. Wild, R. Pinker, and A. Ohmura (2002), Comparison of spectral albedos and their impact on the general circulation model

simulated surface climate, *J. Geophys. Res.*, *107*(D14), 4221, doi:10.1029/2001JD000809.
Thomas, G., and P. R. Rowntree (1992), The boreal forests and climate, *Quart. J. R. Met. Soc.*, *118*, 469–497.
Tschudi, M., J. A. Curry, and J. M. Maslanik (2001), Airborne observations of summertime surface features and their effect on surface albedo during FIRE/SHEBA, *J. Geophys. Res.*, *106*(D14), 15,335–15,344.
Viterbo, P., and A. K. Betts (1999), Impact on ECMWF forecasts of changes to the albedo of the boreal forests in the presence of snow, *J. Geophys. Res.*, *104*(D22), 27,803–27,810.
Walsh, J. E., V. M. Kattsov, W. L. Chapman, V. Govokova, and T. Pavlova (2002), Comparison of Arctic Climate Simulations by Uncoupled and Coupled Global Models, *J. Clim.*, *15*, 1429–1446.
Weatherly, J. W., and Y. Zhang (2001), The response of the Polar Regions to Increased CO2 in a Global Climate Model with Elastic-Viscous-Plastic Sea Ice, *J. Clim.*, *14*, 268–283.
Winther, J.-G., F. Godtliebsen, S. Gerland, and P. E. Isachsen (2002), Surface albedo in Ny-Ålesund, Svalbard: variability and trends during 1981–1997, *Global Planet. Change*, *32*, 127–139.

M. Køltzow, Norwegian Meteorological Institute, R&D, Niels Henrik Abelsvei 40, Oslo 0313, Norway. (famo@met.no)

II

Tellus (2008), 60A, 398–410
Printed in Singapore. All rights reserved

TELLUS

Extended Big-Brother experiments: the role of lateral boundary data quality and size of integration domain in regional climate modelling

By MORTEN KØLTZOW[1*], TROND IVERSEN[2] AND JAN ERIK HAUGEN[1], [1]*Norwegian Meteorological Institute, P.O. Box 43, Blindern, 0313 Oslo, Norway,*
[2]*Department of Geosciences, University of Oslo, Norway*

(Manuscript received 30 April 2007; in final form 10 December 2007)

ABSTRACT

Dynamical downscaling by atmospheric Regional Climate Models (RCMs) forced with low-resolution data should produce fine scale climate details with skill. This is investigated by adopting and extending the Big-Brother approach of Denis et al. (2002). A reference climate is established from a fine resolution RCM simulation in a large domain (the Big-Brother). These Big-Brother (BB) data are degraded by removing small scales, and then used for downscaling by the RCM (the Little Brother) with the same resolution as the BB in three domains of different size. Differences between the Little- and BB are attributed to errors caused by the downscaling. We have furthermore extended the original BB method and investigated the impact of the quality of the driving data. The RCM manage to reproduce the general large scale climate features of the BB when forced with high quality data, but show deficiencies when the driving data differ both in phase and scale from the BB. Forced with data with lower quality on a sufficiently large integration domain and in regions influenced by strong local forcing, the RCM significantly improve the climate statistics for local variables (2 m air-temperature, 10 m wind speed, precipitation). We even found that the improvement increased with domain size.

1. Introduction

Global projections for anthropogenic climate change are provided by coupled global climate models (GCMs) and scenarios for constituent emissions to the atmosphere. Typical horizontal resolution in GCMs for IPCC (2001) was 250–300 km in the atmosphere and 100–150 km in the oceans (Lambert and Boer, 2001). In the 4th Assessment Report of IPCC (2007), resolution has been increased a factor 1.5–2 by some GCMs, but this is still insufficient for most studies of impacts of climate change. The low resolution also constitutes a source of errors in the regional aspects of climate simulation results. Downscaling global projection data by employing regional climate models (RCMs) with higher resolution has therefore become common procedure in the recent years (see e.g. IPCC 2001 and 2007). There still is some discussion related to the proper set-up of dynamical downscaling, and to what extent the downscaling augments the value of the global calculations for the region.

This paper revisits these challenges by employing a further developed type of the 'Big-Brother Experiments' (BBE) introduced by Denis et al. (2002). We only consider pure atmospheric downscaling which makes use of nesting (e.g. Jones et al., 1995; Christensen et al., 1997; Noguer et al., 1998). The GCM data are imposed at the open lateral boundaries of the RCM and by the sea surface temperature and sea ice cover. We do not consider the method of spectral nudging (Kida et al., 1991; von Storch et al., 2000).With this method the large scale part of the GCM data are forced in the interior of the RCM integration domain. Another method for more fine scale simulations are GCMs with variable resolution and focus over the area of interest (e.g. Fox-Rabinovitz et al., 2001).

The rational behind dynamical downscaling is that RCMs should produce realistic fine-scale details over a region when fed by information from coarser-resolution GCM data at the boundaries, and that the results are better suited for impact assessment studies. In RCMs there should be at least three sources of motion systems on scales not resolved by GCMs: (1) improved description of ground surface structures and contrasts, (2) more explicit description of nonlinear dependencies in the dynamics and (3) improved resolution and more explicit description of hydrodynamic instabilities (Denis et al., 2002). There are two quality aspects which need to be addressed in this respect: (1) the ability to reproduce observed historical and present-day climate conditions and (2) the ability of the RCM to improve, or add value,

*Corresponding author.
e-mail: morten.koltzow@met.no
DOI: 10.1111/j.1600-0870.2008.00309.x

to the climate statistics of the GCM which provides data for downscaling.

There are also a number of issues concerning the use of the nesting technique and their outcome for regional climate modelling (Giorgi and Mearns, 1991, 1999; Denis et al., 2002). One issue is to force the RCM with GCM data in a proper way. This concerns not only the mathematical formulation, but also the difference in spatial resolution between the RCM and the GCM, the frequency of boundary data updates, and errors introduced by temporal and spatial interpolation of the GCM data. A second issue is inconsistent physical parametrizations in the GCM and RCM models. This was addressed by, for example, Rummukainen et al., (2001) who found that the relative humidity in the vicinity of the lateral boundaries in a RCM is dependent on differences in the way precipitation processes is handled in the GCM and in the RCM. Thirdly, there are aspects concerning the choice of integration domain for the RCM. Jones et al., (1995 and 1997) emphasize that the RCM circulation should be constrained by the fields of the driving model for features resolved by the latter and advocated the use of small RCM integration domains in order to secure this whilst others have proposed spectral nudging (Kida et al 1991). This opinion has been supported by others (e.g. von Storch et al., 2000), but not generally (e.g. Machenhauer et al., 1994; Christensen et al., 1997). In the Norwegian research project Regional Climate Development Under Global Warming (RegClim, 1997–2006) attention was not paid to this issue (Bjørge et al., 2000; Haugen and Iversen, 2008). Less controversial is the requirement that fine-scale features developed in the RCM should not be damped or destroyed by the open lateral boundary conditions (Jones et al., 1995). A fourth aspect concerns the application of atmosphere only RCMs. Castro et al., (2005) showed that the ground surface boundary conditions are important in generating large scale variability in RCMs, and that this importance increases as the integration domain increases. Thus, large scale atmospheric variability tends to be increasingly underestimated as the domain size increases when the lower boundary conditions are not allowed to respond to the atmosphere. In atmospheric RCMs the continental ground surface variables are adjustable whilst the ocean surface is fully prescribed from the GCM. Only a few RCMs include coupling to the ocean (e.g. Döscher et al., 2002; Rinke et al., 2003).

One step in the validation of the quality of atmospheric downscaling with RCMs is the performing of Perfect Boundary Experiments (PBEs) (e.g. Christensen et al., 1997; Rinke et al., 1999). When GCM-data are downscaled with a RCM, systematic and random errors imposed at the lateral boundary and at the ocean surface are unavoidable due to the imperfections inherent in any GCM. In PBEs the RCM is driven with analysed atmospheric fields at the lateral boundaries and similar for the ocean surface. Hence, a PBE is a demanding test of the quality of the RCM with regard to downscaling, as the results can be compared directly with observed climate data over the specific time-period. However, as advocated by Denis et al., (2002), regular atmospheric climate observations often lack the spatial and temporal resolutions needed for adequate validation of the fine scale features calculated by the RCM. Fields from very-high resolution data assimilation are contaminated by inaccuracies of the assimilation method and errors in the model used for the purpose. Finally, PBEs does not differ between errors originating from the RCM itself and from the downscaling technique.

Denis et al., (2002) therefore suggested a new type of PBEs which are fully based on models. This is nick-named the BBE and enables evaluation of nesting strategies for dynamical downscaling. First a reference climate from a RCM simulation is established as a pure model product using a large integration domain and the high resolution intended for use when downscaling GCM data. This simulation is called the Big Brother (BB). In the method proposed by Denis et al., (2002) and used in later experiments (Denis et al., 2003; Antic et al., 2004; Herceg et al., 2006; Diaconescu et al., 2007) data from BB are then degraded towards the common resolution used in the atmospheric components of the global climate models (GCM) by simply removing, or filtering of, the smaller scales. The resulting filtered fields are then used as lateral boundary data to drive an RCM (called the Little Brother, LB) which is integrated using the same resolution as the BB, in a subarea of the BB domain. The climate statistics of the LB is validated by comparing with the unfiltered BB data in the LB domain. Differences between the two statistics can unambiguously be attributed to errors associated with the dynamical downscaling technique, and not to model errors or observational limitations.

Denis et al., (2002, 2003) introduced the concept of the BBE, and performed it for a one month long simulation. They found that time mean and variability of fine scale features are successfully reproduced over regions with strong small-scale surface forcing. Over ocean and away from the surface, less reproducibility is achieved. Antic et al., (2004) extended the time period to yield 4 winter months on a domain covering the west coast of North America. These results are in agreement with predictability aspects of forced versus free flows (Anthes et al., 1985; Boer, 1994).

These results were also interpreted to be in favour of the idea that the RCMs should not be able to change the driving GCM data on the scales resolved by the latter (e.g. Jones et al., 1995, 1997). We advocate that this interpretation can be a false effect of the fact that the driving data for the LB are not taken from a coarse resolution model with associated errors, but from data which by construction are perfect on the coarser scales. In a BBE experimental set-up the large scale patterns of the LB should stay close to the BB data. We therefore take the original BBE a step further by comparing the original experiments with results for which the BB data have errors typical for coarse resolution models.

In Section 2, the RCM HIRHAM used in the study is described, before a more detailed description of the experiment

is given. Then the results are presented in Section 4, before a summary is given and conclusions are drawn in Section 5.

2. The regional climate model HIRHAM

Our version of the HIRHAM RCM was imported from Max Planck Institute for Meteorology (MPI) in 1997. A similar version was used at the Danish Climate Centre (Christensen et al., 1996, 1997, 1998). As described in Bjørge et al., (2000) the model has been used for dynamical downscaling of global climate scenarios on a rotated spherical grid with 0.5° (∼55 km) horizontal grid resolution and 19 levels in the vertical). The physical processes are adapted from the ECHAM4 ACGM (Roeckner et al., 1996).

A more recent version (Haugen and Haakenstad, 2006) of the HIRHAM RCM is used in this study. In this version, the dynamical core uses a two-time-level three-dimensional semi-Lagrangian semi-implicit time-integration scheme, adopted from the more recent version (no. 5) of the HIRLAM numerical weather prediction model (Undén et al., 2002.). The physical parametrization package of HIRHAM was modified to couple to this scheme. Furthermore, the lateral boundary relaxation scheme, the horizontal diffusion, and the surface albedo parametrization (Køltzow, 2007) was updated. The lateral boundary relaxation is based on Davies (1976) and is commonly in use in RCM's (e.g. used in 6 out of 8 RCM's in Rinke et al., 2006). The linear interpolation in time of the boundary data was replaced by a cubic interpolation. The changes were implemented in successive steps. In Haugen and Haakenstad (2006) the model output was validated by downscaling re-analyzed ERA40 data and compared to monthly CRU TS 2.1 gridded observations. Temperature and precipitation errors were slightly reduced for Europe in general, and the precipitation errors in particular in some mountainous areas were much reduced. In addition, the computational efficiency was improved.

3. The extension of the Big-Brother experiments

In this study the perfect prognosis approach called the poor man's Big-Brother Experiment (hereafter referred to as BB) is followed (Denis et al., 2002). Two BB simulations are done; the first uses of 0.5° × 0.5° horizontal grid and 31 levels on the big domain shown in Fig. 1. This simulation is referred to as the fine-resolution BB and is considered to represent the truth in the experiments. Small scales features in this fine-resolution BB are removed by interpolating to a 2.8° × 2.8° grid with 19 levels by a bi-linear interpolation in the horizontal and by interpolating from 31 to 19 vertical levels. As in Denis et al., (2002) this degraded data-set, hereafter referred to as *the filtered fine resolution BB data*, can be dynamically downscaled in a smaller domain, thus investigating to what extent the downscaling can regenerate the filtered small scale structures.

Compared to Denis et al., (2002) we extend the BB technique with a second BB simulation in order to more realistically mimic the actual situation where the coarse-resolution data have to be taken from a coarse-resolution model. To generate large-scale data, the model is run with coarser resolution (2.8° × 2.8° and 19 levels) directly in the same big domain, which is similar to the approach used by Diaconescu et al., (2007) independent of our present study. We refer to this simulation as the coarse-resolution BB.

The filtered fine resolution data must be regarded as representing the upper bound in the potential quality of coarse resolution data, since they contain resolution errors without phase shifts. Differences between results obtained from downscaling filtered fine resolution BB data and those from downscaling coarse resolution BB, represent a potential for improvement in dynamical downscaling.

Compared to output from GCM's, the BB data sets simulations are produced in a limited area with the same model tool as used for downscaling, thereby referred to as poor man's BB

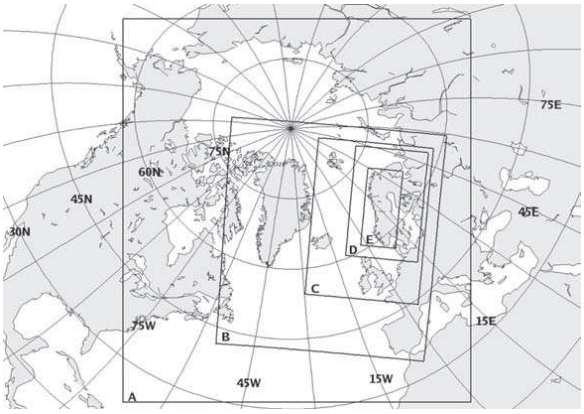

Fig. 1. The different integration domains used in the study. The large domain (marked A) is used in the fine- and coarse-resolution Big-Brother (BB) simulations. The smaller embedded areas are the large (marked B), medium (marked C) and small (marked D) Little Brother (LB) model domains. The common verification domain which is used in Figures 2–5 are the innermost area marked E.

experiments. Both BB runs are forced with the ECMWF ERA40 re-analysis data set at the lateral and surface boundary (Uppala et al., 2005). All simulations are for the period 1970–1990. The first year is considered as spin-up and not included in the analysis that thus contains 20 yr.

The dynamical downscaling of BB data uses the same model as used to generate the BB data, and is termed Little Brother simulations (hereafter referred to as LB). In this paper we apply three alternative LB runs based on three different integration domain sizes; small, medium and large. For each of the three LBs, data from both the filtered BB and the coarse-resolution BB data sets are downscaled. In the LB runs, data at the lateral boundaries are updated every 6 h, as supported by others (e.g. Dimitrijevic and Laprise, 2005; Antic et al., 2004). All the three integration domains are given in Fig. 1. Results from the different domains are intended to highlight the importance of the domain size.

It is expected that the filtered BB data set deviates from the coarse-resolution BB with respect to circulation patterns. Comparison between downscaled versions of the two data-sets is therefore expected to give valuable insight into the abilities of the downscaling to improve the climatology of the coarse-resolution BB. The original experiment by Denis et al., (2002) was not properly designed to address this problem, since the filtered data were perfect except for the finest scales. To generalize the BB experiments one step further towards practical realism, the downscaling should be run with several other models than the one used for producing the BB data. This is not attempted in this study.

4. Results

We focus our attention on the potential qualities of dynamical downscaling for Norway, even though some aspects of downscaling elsewhere are discussed. The 20-yr climatic averages of the fine-resolution BB, that is, our version of the 'truth', is compared with those of the three different LB's inside a common verification area for all model domains (see Fig. 1). Similarly, the quality of daily values of mean sea level pressure (MSLP), 2 m air temperature (T2m), precipitation (PREC), and wind speed at 10 m heights (V10) is discussed on the basis of bias error, root mean square error, and temporal correlations relative to the fine-resolution BB for all model grid points in Norway. Finally, the day-by-day variability is studied, including the reproduction of extreme values.

4.1. Reproduction of climate averages

Figure 2 show the temporal averages of MSLP for the years 1971–1990 in the fine- and coarse-resolution BB simulation, along with deviations of each LB version from the fine-resolution BB. The fine-resolution BB has low MSLP over the ocean west of Norway and higher over land with a gradient condensed along the western coastline. In the coarse-resolution BB the zone of strong MSLP gradient does not follow the coast to the same extent, and the extremes and gradients are weaker. All LB versions yield too high MSLP. When filtered fine resolution BB data are downscaled, the LB on small and medium domains give a 1–1.5 hPa bias with little geographical variation, whilst in the large domain the bias varies from 1.5 hPa in the north to 3.5 hPa in the south. With coarse-resolution BB for downscaling the bias is between 1 and 3 hPa with largest values to the west and south. The quality of the data for downscaling is shown to be particularly important, when the LB is applied to downscale filtered fine resolution BB data in the two smallest domains. For the largest domain, however, the MSLP bias is slightly worse when

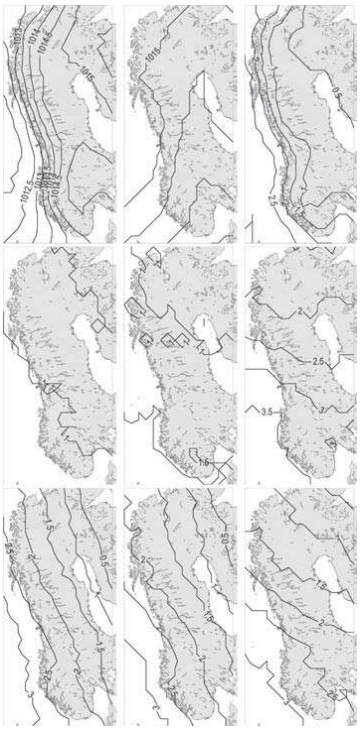

Fig. 2. Results for mean sea level pressure, with equidistance 0.5 hPa, averaged over the years 1971–1990. Upper left-hand side: fine-resolution BB; upper middle: coarse-resolution BB and upper right-hand side: the difference between the coarse- and fine-resolution BB. The middle row shows the downscaling errors (the difference between LB results and the fine-resolution BB) for the LB simulations driven by the filtered BB over the small (left-hand side), medium (middle) and large (right-hand side) LB integration domain. The bottom row shows the corresponding errors of the three LB simulations when driven by the coarse-resolution BB.

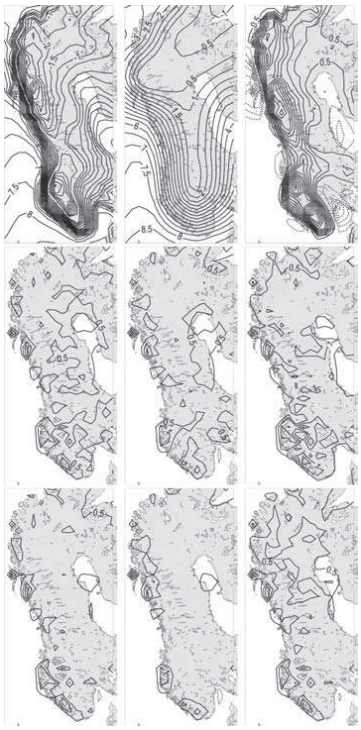

Fig. 3. Same as Fig. 2, but for air temperature 2 m above the ground surface with equidistance 0.5 °C.

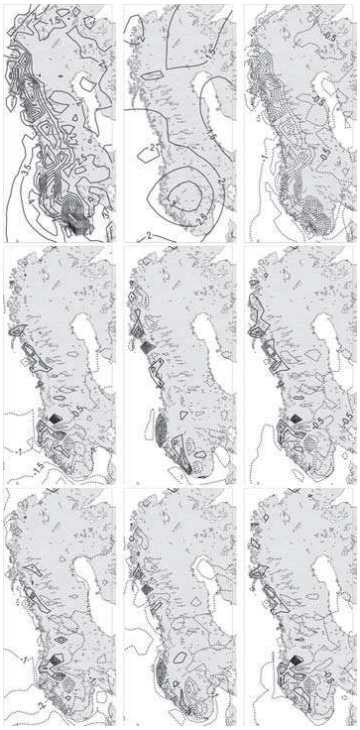

Fig. 4. Same as Fig. 2, but for 24 h accumulated precipitation with equidistance 0.5 mm (24 h)$^{-1}$.

downscaling filtered data, indicating that LB in that case is able to develop more of its own model-specific features in the interior. Comparing with the MSLP bias of the coarse-resolution BB, however, there is otherwise little evidence of improved MSLP-patterns in the results from downscaling of the coarse-resolution BB data. One exception is seen over the ocean North West of Norway (mostly outside the area covered by Figure 2), which will be discussed below under the comparison of areas outside Norway.

Figure 3 shows 20-yr climate averages for 2-m temperature (T2M), which is strongly influenced locally by the different resolution of the topography and other ground-surface features. Hence, over the ocean the coarse and the fine scale BB are similar since prescribed sea surface temperatures in both cases are taken from the ERA40 analysis. The Scandinavian mountains are too smooth and too low in the coarse resolution BB, which therefore is too warm in these areas. (The T2M from the coarse resolution BB is not height corrected by post-processing.) However, all LB computations show little bias error. In fact, the biggest deviations are found in the large-domain LB when filtered fine resolution BB data is downscaled. This case is ∼0.5° warmer than the other LB results. Some regions at the west coast of Norway have a 0.5° too warm climate in all LB simulations, originating from situations in autumn and winter together with an increased on-shore wind component compared to the fine scale BB (not shown).

Figure 4 show the 20-yr average climate statistics for precipitation. Also precipitation patterns are highly related to the topography, resulting in strong features over the westward facing coastlines in the fine resolution BB which are absent in the coarse resolution BB. All LB simulations show considerable agreement with the fine scale BB and there are almost no signals that can be related to the quality of the two data sets for downscaling. This is in agreement with, for example, Antic et al., (2004) who stated that complex topography enhances the downscaling ability of precipitation. Nevertheless, an important deviation is that precipitation is underestimated in LB with the small domain. This is a shortcoming of the closeness to the influx lateral boundary. Even though specific humidity and cloud water is included in the boundary forcing, the HIRHAM RCM needs a downwind distance time to establish dynamical balance

between fields like vertical motions and moisture. For the small domain there is insufficient (lagrangian) time to establish this balance in air downstream of the lateral boundary before it hits the mountains in our area of interest. Also, differences in land-sea mask between the coarse and fine grids close to the lateral boundary of the small domain, are prone to influence the evaporation from the sea surface. However, we have not quantified this error. Furthermore, also the precipitation in the large-domain LB is underestimated in some regions, leaving the LB on medium-sized domain with smallest precipitation bias. Downscaling the filtered fine resolution data yields the smallest bias, but the difference from downscaling the coarse resolution BB is only tiny. This indicates that the medium-sized domain is closest to the optimal trade-off between the requirement of necessary moisture spin-up and a proper control of the large scale flow pattern provided by the driving data. Too much precipitation at the West Coast of Norway is produced in the same areas where the T2M in the LB's show positive bias. Again these deviations are related to an increased on-shore wind component during autumn and winter (not shown).

Figure 5 shows the average climatology for wind speed at 10 m above ground surface. Also this parameter is strongly influenced by ground surface features such as topography and coast-lines. In the fine resolution BB, the pronounced average wind maxima occur over the oceans along the western coasts of Norway, which the coarse resolution BB fails to reproduce. This bias is to some extent corrected when downscaling the coarse resolution BB with LB applied in the two smallest domains. With the large domain, the LB results are less restricted by the lateral boundaries, and the biases are to a large extent corrected. Downscaling filtered fine-resolution BB data yields small biases independent of integration domain, but the improvement above downscaling coarse-resolution BB data in the largest domain is small.

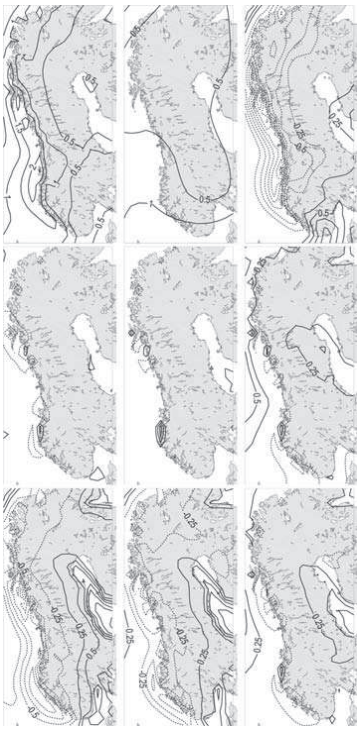

Fig. 5. Same as Fig. 2, but for wind speed at 10 m height with equidistance 0.5 m s^{-1}.

4.2. *Daily statistics for Norway*

In this section daily values are presented by monthly statistics in order to emphasize seasonal variations between BB and LB computations. In Fig. 6 20 yr statistics for MSLP error, that is, differences between fine resolution BB and all other model calculations, are given for all land grid points in Norway. The error measures are the bias, the error in variance of daily values as a measure of the day-to-day variability, the standard deviation (*SD*) of the error, are all shown along with the correlation with the fine resolution BB. The diagrams show that best verification results for MSLP are obtained for all statistical parameters when LB is applied with a small integration domain and filtered fine resolution BB data are downscaled. The annual cycles in statistics for errors in the coarse resolution BB are also present in the LB results obtained when coarse resolution BB data are downscaled, irrespective of domain size.

Errors are large in autumn and winter. In these seasons the reproduction of the average climatology of T2M and precipitation along the Norwegian West Coast was problematic (not shown), and the extra-tropical system of cyclones shows its highest activity. Stronger winds at the lateral boundaries increase the downwind distance that the RCM needs to develop smaller scaled features. At the same time, strong winds are associated with large gradients in pressure and temperature, and therefore an increased risk of phase errors in the simulations of synoptic and mesoscale features such as cyclones and fronts. For all measures the importance of the quality of the data used for downscaling is demonstrated. For MSLP, it is only for day to day variability, and to some extent for the correlation, obtained after downscaling with LB in a large domain, that it is possible to detect an added value of dynamical downscaling from the coarse resolution BB.

Figure 7 shows similar statistics for daily data for temperature 2 m above the ground. Downscaling decreases the temperature errors compared to those in the coarse resolution data throughout the year. This is mainly because the Scandinavian topography is considerably improved with better horizontal resolution. Annually averaged, the T2M is in good agreement with the fine scale BB, but this hides the fact there are underestimates in

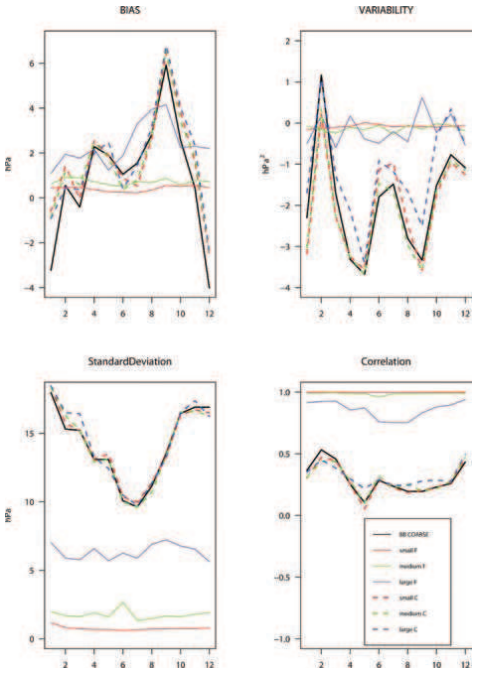

Fig. 6. Monthly mean error statistics, relative to fine resolution BB, of daily mean sea level pressure (hPa) over 20 yr and all land-based grid points in Norway. Shown are bias error (upper left-hand side), day-to-day variability (upper right-hand side), standard deviation (lower left-hand side), and correlation (lower right-hand side) for the six LB simulations and the fine resolution BB.

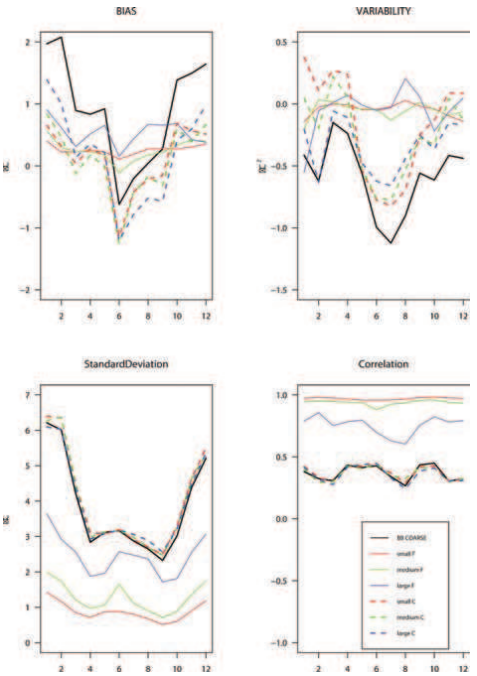

Fig. 7. Same statistics as in Fig. 6, but for 2 m air temperature T2M.

summer and autumn and overestimates during winter. The errors are considerably more evenly distributed through the year when the LB's downscale filtered fine resolution BB data. It is noticeable that during summer the smallest bias is calculated with LB in the medium-sized domain, whilst in winter the smallest bias is found with the smallest LB domain. This reflects that local forcing is relatively more important during the summer when information from the lateral boundary is slowly penetrating the integration domain. For *SD* and correlation no added value of dynamical downscaling of the coarse-resolution BB is found. For the day to day variability, however, a clear improvement in the downscaled data is apparent.

The monthly error statistics for daily precipitation is shown in Fig. 8. Again the best results are obtained when filtered fine resolution BB data are downscaled, but the smallest bias error is obtained when LB is applied with the medium sized domain. This domain is sufficiently small such that the synoptic circulation does not depart significantly from the data imposed at the boundaries (Jones et al., 1995), but is large enough to allow moisture to adjust downstream from the boundaries over the region of interest.

Even more important, however, is the added value in precipitation data obtained by downscaling the coarse resolution BB data. This is evident for bias error and the error of the day to day variability, and the best results are obtained with the largest LB domain. This contradicts the argument that smaller domains should be used to ensure that the LB stay close to the large scale flow in the coarse resolution model. For *SD* and correlation, downscaling of the coarse resolution BB worsen slightly or make no impact. The seasonal differences show less correlation and higher *SD* during summer and autumn when precipitation is strongly influenced by convection with a more stochastic nature. This confirms the findings of Dimitrijevic and Laprise (2005) based on simulations of 5 July months.

Figures 7 and 8 show that surface temperature and precipitation from downscaled scenarios are not crucially dependent on the quality of the data used for downscaling. This agrees with Noguer et al., (1998) who stated that parts of the distribution of the mentioned variables are controlled by internal processes in a RCM. However, seasonal deficiencies in the data used for

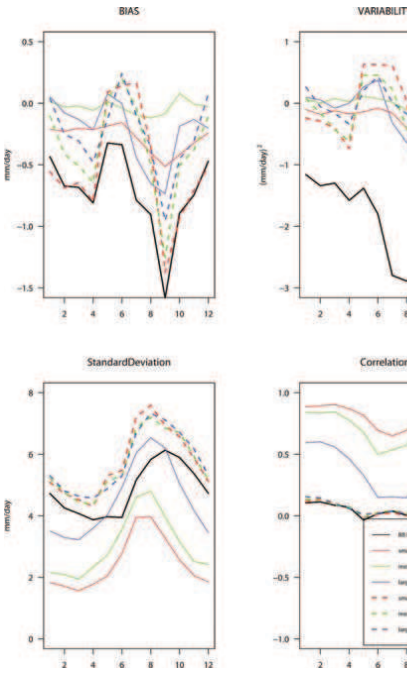

Fig. 8. Same statistics as in Fig. 6, but for valid for 24 h accumulated precipitation.

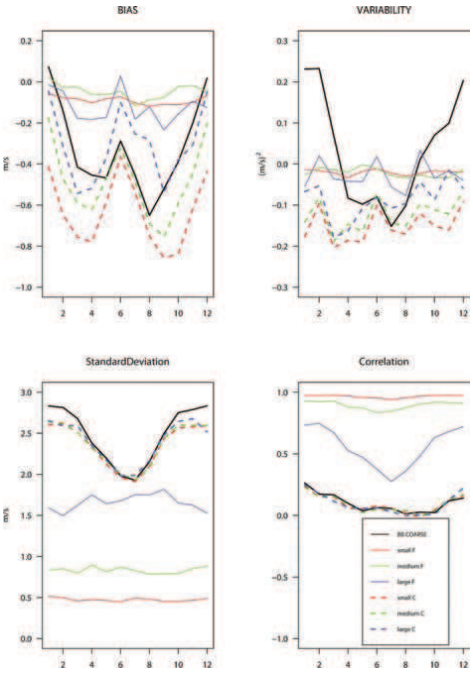

Fig. 9. Same statistics as in Fig. 6, but for 10 m wind speed.

downscaling are to some degree also seen in the downscaled data from the LB.

Figure 9 is similar to the three previous figures, but is valid for wind speed 10 m above the ground. The main features and differences in wind are seen over the ocean immediately west of Norway (see Fig. 5). The majority of these grid points are not included in the statistics of Fig. 9. Again the quality of the data used for downscaling is important. Downscaling of the coarse resolution BB adds value in summer, but only for the largest LB domain for bias error, and in winter for day to day variability for all LB domains.

From a deterministic point of view dynamical downscaling is not very efficient, since the *SD* is quite large for the different LB simulations. This was also one of the findings of de Elía et al., (2002). However, the method of dynamical downscaling shows skill in reproducing the climatology and the day to day variability. This is especially seen when the coarse resolution forcing is of high quality. However, also when the driving data deviates from the correct large scale circulation, dynamical downscaling is able to reproduce data in agreement with the fine resolution BB.

The analysis done in this section has also been performed in regions of Norway (Northern Norway, the West coast and the South East in-land). No differences in the ability of dynamical downscaling are found between the regions (not shown). This do not support earlier findings (Dimitrijevic and Laprise, 2005; Denis et al., 2003) which found that the skill in reproducing precipitation over the West Coast of North America is higher than the skill over the East Coast of North America, a region with weaker topographic forcing. This can be explained by the fact that in contrast to the wide North American continent, the southeast part of Norway is strongly influenced by improved topography in the fine resolution grid. The region with best agreement between the fine and the coarse scale BB varies. For MSLP and precipitation the southeast part of Norway is in best agreement while for wind speed, Northern Norway obtains the best agreement. For two meter temperature, only minor differences between regions are found.

4.3. *Extreme values for Norway*

From the 20-yr-long simulations we extract the 20 highest (MSLP, T2M, precipitation and wind) and lowest (MSLP and T2M) daily values from each model simulation. Spatial mean values and Mean Absolute Error (MAE), *SD* and Correlation of the extremes compared to the fine resolution BB are listed in

Table 1. Each cell in this table gives the average over Norway of the 20 highest and lowest extremes for MSLP, T2M, precipitation and wind speed at 10 m height in each grid square. Also the average over Norway of the mean absolute error, the standard deviation of the errors, and the Correlation with the fine resolution Big-Brother are given in each cell of the table.

	Fine resol. BB	Coarse resol. BB	Small LB forced with BBF	Medium LB forced with BBF	Large LB forced with BBF	Small LB forced with BBC	Medium LB forced with BBC	Large LB forced with BBC	
Max MSLP	1054.52	1049.78	1054.76	1055.05	1054.47	1049.30	1049.74	1052.16	Mean
		4.74	0.26	0.53	0.28	5.22	4.78	2.36	MAE
		1.98	0.19	0.27	0.35	1.40	1.28	1.04	*SD*
		0.33	0.99	0.99	0.97	0.71	0.79	0.85	Corr
Max T2m	293.54	289.81	293.52	293.33	293.71	290.23	290.58	291.08	Mean
		3.90	0.71	0.77	0.73	3.36	3.00	2.52	MAE
		3.04	1.33	1.30	1.28	2.45	2.09	1.86	*SD*
		0.73	0.96	0.96	0.96	0.84	0.91	0.94	Corr
Max Precip	33.89	19.05	33.06	34.34	34.19	37.08	35.60	35.28	Mean
		14.84	3.91	3.04	3.32	6.33	4.43	4.14	MAE
		8.36	5.56	3.99	4.50	8.57	5.32	5.89	*SD*
		0.42	0.83	0.91	0.89	0.71	0.84	0.83	Corr
Max wind	11.30	11.62	11.13	11.15	11.17	10.36	10.63	10.99	Mean
		2.34	0.64	0.64	0.65	1.30	1.08	0.78	MAE
		2.71	1.13	1.17	1.17	1.43	1.31	1.21	*SD*
		0.88	0.98	0.98	0.98	0.97	0.97	0.97	Corr
Min MSLP	970.72	970.17	971.39	971.78	972.79	973.07	973.74	972.06	Mean
		1.17	0.67	1.08	2.06	2.36	3.01	1.52	MAE
		1.32	0.25	0.59	0.87	1.04	1.22	1.19	*SD*
		0.85	0.99	0.90	0.88	0.87	0.86	0.89	Corr
Min T2m	252.00	254.92	252.37	253.56	252.22	253.60	252.02	253.26	Mean
		3.39	0.97	0.99	1.52	1.43	1.29	1.48	MAE
		4.10	1.54	1.30	1.58	1.84	1.32	1.57	*SD*
		0.94	0.99	0.99	0.99	0.99	0.99	0.99	Corr

Table 1. In each grid point in Norway, the average over the 20 most extreme values are calculated. The numbers given in Table 1 are averages of all the thus obtained grid point specific extremes in Norway. Table 1 also gives the MAE, the *SD* of the error, and the correlation with the fine-resolution BB data ('the truth'). The coarse resolution BB clearly underestimates the highest pressures, while the LB simulations stay close to their driving data. However, when the downscaling domain is sufficiently large, an improvement for events with high MSLP appears. For low surface pressures we do not see the same improvement.

The LB results which are produced by downscaling the filtered fine resolution BB data, reproduce the maximum temperatures well. The coarse resolution BB underestimates the highest temperatures considerably, and this also influences the results from the LB downscaling. However, the underestimation decreases when the LB domain increase in size. For the minimum T2M the coarse resolution BB overestimates, but for the LB downscaling the results' quality depend less critically on the data used for downscaling. Extremely low temperatures are often determined as a result of weak turbulent fluxes in the stable planetary boundary layer which is strongly influenced by long-wave radiative cooling during nights with anticyclonic subsidence and clear skies. Also extremely high temperatures are generated locally during anticyclonic subsidence and a stable boundary layer. The local component is further enhanced by the fact that evaporation from the ground is an important moderator (Schär and Jendritzky, 2004). However, whilst radiative cooling during night feeds positively back on the stabilization of the boundary layer, the strong solar radiation during heat-waves tends to destabilize the column. Extremely high temperatures therefore depend on dynamical processes which suppress destabilization, such as strong anticyclonic subsidence coupled with horizontal advection of deep tropospheric layers of potentially warm air. High temperatures are therefore more influenced by the lateral boundary conditions than low temperatures.

The maximum precipitation is considerably underestimated in the coarse resolution BB, but any downscaling with LB significantly improve this situation, even though there is a tendency of to overestimate when coarse resolution BB data are downscaled. Furthermore, relative high values of MAE and *SD* suggest that the localization is probably not the same in the downscaled data

as in the fine scale BB. The LB results obtained when using the medium or large domains are considerably better than those obtained when the small domain is used.

Little difference between the experiments is found for extreme winds, although surprisingly the strongest winds are produced with the coarse resolution BB. However, compared with the fine resolution BB the MAE, *SD* and correlation show considerable improvements by downscaling with the LB. The statistical parameters indicate that the coarse resolution BB compensate artificially for higher/lower wind speeds compared to the fine resolution BB. The high correlations for the LB which downscales the coarse resolution BB data, documents an increased ability to localize wind extremes. Also in this case, the best results are obtained with the largest LB domain.

4.4. Climate of the large LB domain

Figure 10a show the differences in climatological average of MSLP between the coarse- and the fine resolution BB. The highest resolution gives a deeper low pressure system in the North Atlantic Ocean, the Barents Sea, and parts of the westward facing European regions. Pressure is otherwise higher over major continental areas in Eurasia, Canada and Greenland. The difference over Greenland is probably a consequence of higher Greenland topography in the fine resolution version influencing the post-processing of MSLP.

The difference in climatology between the coarse resolution BB and its downscaled results with the large domain LB, is given in Fig. 10b. The patterns are to a large extent equal, but opposite in signs to those of Fig. 10a. Thus, downscaling partly repairs the MSLP errors over Greenland. Over the North Atlantic Ocean, however, the downscaling slightly increases the error in the MSLP present the coarse resolution BB, except over the Barents Sea where downscaling reduces MSLP and thus repairs the error in the coarse resolution BB. Over continental Eurasia (Finland/Russia) the LB increases the MSLP towards the fine resolution BB. It has earlier been stated that RCMs are not able to reduce circulation errors in coarse resolution driving

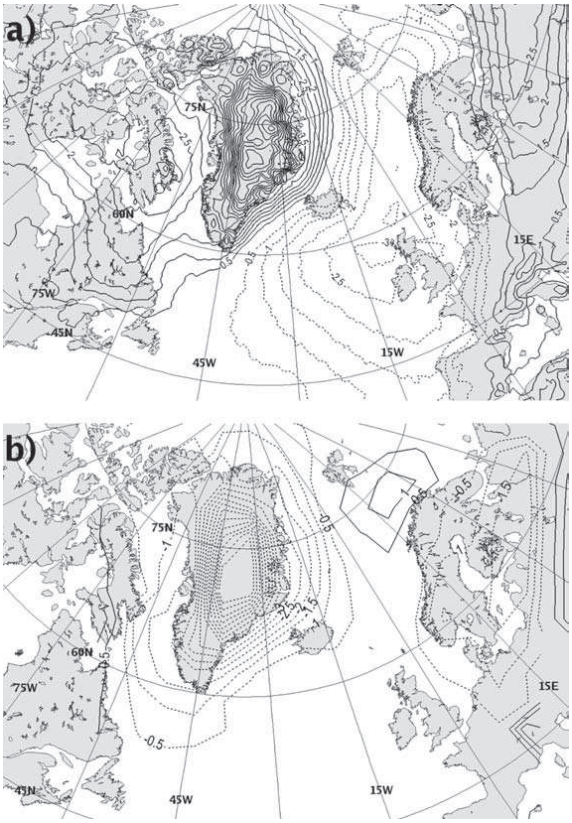

Fig. 10. (a) Fine scale Big-Brother MSLP (average 1971–1990) minus coarse resolution Big-Brother MSLP (1971–1990). Equidistance is 0.5 (b) Coarse resolution Big-Brother MSLP (1971–1990) minus MSLP (1971–1990) from downscaled coarse resolution Big-Brother with LB in the largest domain.

data (Noguer et al., 1998). However, this study indicates that at least in some regions and with a sufficiently large integration domain, it is possible to improve the climate of the large scale circulation.

Except for differences close to the lateral boundaries, the only major differences found in T2m, precipitation and wind speed are those already discussed for the Scandinavian area. Elsewhere they are remarkable similar (not shown).

5. Discussion and conclusions

In this study abilities and limitations of dynamical downscaling of global climate model data have been investigated by employing an extended version of the BB approach introduced by Denis et al., (2002). Compared to earlier studies, the simulation length (20 yr), the size of the integration domain, and the geographical scope are new. Furthermore, the investigation of the impact of the quality of the data being downscaled is an extension compared to the original method of Denis et al., (2002), and follows the same approach as Diaconescu et al., (2007).

Eight simulations were performed in total. Two 20-yr BB simulations are made, one with 0.5° horizontal resolution and 31 levels and another with 2.8° horizontal resolution and 19 levels. The first of these were established to mimic the truth, to which all the LB simulations (on a small, medium and large domain) were compared. The LBs were forced with both filtered data from the fine-resolution BB run ('the truth') and with data from the coarse BB simulation. The second constituted the data for dynamical downscaling. This is a step towards reality compared to the procedure of downscaling fine resolution BB data after removal of the fine-scale structures by filtering, which represent the highest possible quality of coarse resolution data.

When the LB is used to downscale high quality data they manage to reproduce the climatology and variability of the fine resolution BB very well. However, when the integration domain is large the LB circulation pattern may deviate from the fine resolution BB. This is especially seen in the MSLP fields. In a small domain the low-level circulations (i.e. the MSLP-pattern) is to a large extent steered by the lateral forcing and agree well with the fine resolution BB, but in this case the LB fails to regenerate some important features of precipitation because the closeness to the lateral boundary hampers upstream moisture adjustment. This illustrates that the optimal domain should be small enough to constrain the large scale circulation, but sufficiently large to allow small scale features to develop (Jones et al., 1995). On the other hand, this is not necessarily true when the quality of forcing data at the lateral boundaries is inferior. The regeneration of extreme values shows skill both in values and in localization.

The basic assumption behind dynamical downscaling is that RCMs should produce realistic fine scale features just by being fed by large scale and low resolution information at the boundaries. This study supports this assumption, although we find this positive impact in a region strongly dominated by local forcing by local topography and complex coastlines. This confirms suggestions by Anthes et al (1985) and Boer (1994), and does not contradict the results of de Elía and Laprise (2003) since they focused on unforced variability.

When the LB is used to downscale coarse resolution BB data which have lower quality than the filtered fine resolution data, it has problems in regenerating the correct large scale patterns, such as those characterized by the MSLP. This is in agreement with the findings of Diaconescu et al., (2007) with a rather small integration domain (4500 km × 4500 km) for the LB. However, our results indicate that with a sufficiently large domain, the LB is able to correct some of the deficiencies. For more local weather-related variables such as T2M, precipitation, and 10 m wind, skillful climate information is generated by the LB. We find that a large integration domain enhances the improvements, both in climate averages and for the day to day variations. Extremes in weather are potentially important when assessing consequences of climate change, and they are often related to features which are not properly resolved in GCMs. An important issue is therefore to what extent dynamical downscaling can reproduce extreme events when they are not explicitly present in the data applied for downscaling. Also in this respect we find that the LB has ability to regenerate extremes with quality which increases with increasing size of the integration domain.

In conclusion, we find that there is little doubt that downscaling may add value to coarse resolution data in areas dominated by local quasi-stationary forcing. We have also seen that, for a high-quality RCM, when the downscaling configuration allows improving the quality of the coarse resolution data, even better results may be obtained.

This conclusion should be used with some caution. For example, real dynamical downscaling of data from global climate scenarios represents even one step further in BB experimentation compared to our work. This step concerns that the coarse resolution GCM data in reality are produced with a considerably different model than the LB. Some aspects of our conclusions may depend on the simplification that the coarse resolution data are produced with the same model system as the LB except for resolution and integration domain. Deficiencies revealed in BBE may interact with other sources of error in a realistic downscaling set-up. Such aspects are recently discussed by Jacob et al., (2007), but without formally addressing the domain size.

Another caution relates to the fact that our 'truth' actually is a model product of the same type as used to produce the calculated data that are validated. Hence, the missing source of climate variability clearly present in a pure atmospheric RCM, is also missing both in our version of the 'truth' and in the coarse resolution BB data. Our experiments are therefore not designed to properly account for insufficient climate variability related to interactions with, for example, the oceans (Castro et al., 2005).

6. Acknowledgment

The work reported here is funded in part by the Norwegian Research Council, through grant no. 120656/720 to the Norwegian Meteorological Institute/RegClim. Computational costs are covered by a grant from the Research Council's Programme for Supercomputing.

References

Anthes, R. A., Kuo, Y. H., Baumhefner, D. P., Errico, R. M. and Bettge, T. W. 1985. Predictability of mesoscale motions. *Advances in Geophysics* Volume 28B, Academic Press, New York, USA 159–202.

Antic, S., Laprise, R., Denis, B. and de Elia, R. 2004. Testing the downscaling ability of a one-way nested regional climate model in regions of complex topography. *Clim. Dyn.* **23**, 473–493.

Bjørge, D., Haugen, J. E. and Nordeng, T. E. 2000. *Future climate in Norway*. DNMI Research Rep. No. 103, 41 pp. Norwegian Meteorological Institute, P. O. Box 43 Blindern, N-0313 Oslo, Norway, ISSN 0332-9879.

Boer, G. J. 1994. Predictability regimes in atmospheric flow. *Mon. Wea. Rev.* **122**, 2285–2295.

Castro, C. L., Pielke Sr, R. A. and Leoncini, G. 2005. Dynamical downscaling: assessment of value retained and added using the Regional Atmospheric Modeling System (RAMS). *J. Geophys. Res.* **110**, D05108, doi:10.1029/2004JD004721.

Christensen, J. H., Christensen, O. B., Lopez, P., van Meijgaard, E. and Botzet, M. 1996. *The HIRHAM4, Regional Atmospheric Climate Model*, Danish Meteorological Institute–Scientific Report–Copenhagen, Denmark.

Christensen, J. H., Machenhauer, B., Jones, R. G., Schar, C., Ruti, P. M., and co-authors. 1997. Validation of present-day regional climate simulations over Europe: LAM simulations with observed boundary conditions. *Clim. Dyn.* **13**, 489–506.

Christensen, O. B., Christensen, J. H., Machenhauer, B. and Botzet, M. 1998. Very high-resolution climate simulations over Scandinavia–present climate. *J. Climate* **11**, 3204–3229.

de Elía, R. and Laprise, R. 2003. Distribution-oriented verification of limited-area models in a perfect-model framework. *Mon. Wea. Rev.* 131, 2492–2509.

de Elía, R., Laprise, R. and Denis, B. 2002. Forecasting skill limits of nested, limitied-area models: a perfect-model approach. *Mon. Wea. Rev.* **130**, 2006–2023.

Davies, H. C. 1976. A lateral boundary formulation for multi-level prediction models. *Q. J. R. Meteorol. Soc.* **102**, 405-418.

Denis, B., Laprise, R., Caya, D. and Cote, J. 2002. Downscaling ability of one-way nested regional climate models: the Big-Brother Experiment. *Clim. Dyn.* **18**, 627–646.

Denis, B., Laprise, R. and Caya, D. 2003. Sensitivity of a regional Climate model to the spatial resolution and temporal updating frequency of lateral boundary conditions. *Clim. Dyn.* **20**, 107–126.

Dimitrijevic, M. and Laprise, R. 2005. Validation of the nesting technique in a regional climate model and sensitivity tests to the resolution of lateral boundary conditions during summer. *Clim. Dyn.* **25**, 55–580.

Diaconescu, E. P., Laprise, R. and Sushama, L. 2007. The impacts of lateral boundary data errors on the simulated climate of a nested regional climate model. *Clim. Dyn.* **28**, 333–350.

Döscher, R., Willen, U., Jones, C., Rutgersson, A., Meier, H. E. M. and co-authors. 2002. The development of the coupled regional ocean-atmosphere model RCAO. *Boreal Eviron. Res.* **7**, 1221–1234.

Fox-Rabinovitz, M. S., Takacs, L. L., Govindaraju, R. C. and Suarez, M. J. 2001. A variable-resolution stretched-grid general circulation model: regional climate simulation. *Mon. Wea. Rev.* **129**, 453–469.

Giorgi, F. and Mearns, L. O. 1991. Approaches to the simulation of regional climate change: a review. *Rev. Geophys.* **29**, 191–216.

Giorgi, F. and Mearns, L. O. 1999. Introduction to special section: regional climate modelling revisited. *J. Geophys. Res.* **104**(D6), 6335–6352.

Haugen, J. E. and Haakenstad, H. 2006. The development of HIRHAM version 2 with 50 km and 25 km resolution. RegClim Gen. Techn. Rep. No. 9. Norwegian Meteorological Institute, P. O. Box 43 Blindern, N-0313 Oslo, Norway.

Haugen, J. E. and Iversen, T. 2008. Response in extremes of daily precipitation and wind from a downscaled multi-model ensemble of anthropogenic global climate change scenarios. *Tellus **60A***, 10.1111/j.1600-0870.2008.00315.x.

Herceg, D., Sobel, A. H., Sun, L. and Zebiak, S. E. 2006. The Big Brother Experiment and seasonal predictability in the NCEP regional spectral model. *Clim. Dyn.* **27**, 69–82.

IPCC. 2001. *Climate Change 2001: The Scientific Basis* (eds J. T. Houghton, and co-editors), Cambridge University Press, UK. 881 pp.

IPCC. 2007. Climate change 2007: the physical science basis. *Contribution of Working Group I to the Fourth Assessment Report of the Intergovernmental Panel on Climate Change* (eds S. Solomon, D. Qin, M. Manning, Z. Chen, M. Marquis, and co-editors), Cambridge University Press, Cambridge, United Kingdom and New York, NY, USA, 996 pp.

Jacob, D., Barring, L., Christensen, O. B., Christensen, J. H., de Castro, M. and co-authors. 2007. An intercomparison of regional climate simulations for Europe: model performance in present-day climate. *Clim. Change* **81**, 31–52.

Jones, R. G., Murphy, J. M. and Noguer, M. 1995. Simulation of climate change over Europe using a nested regional-climate model. I: assessment of control climate, including sensitivity to location of lateral boundaries. *Quart. J. Roy. Meteorol. Soc.* **121**, 1413–1449.

Jones, R. G., Murphy, J. M., Noguer, M. and Keen, A. B. 1997. Simulation of climate change over Europe using a nested regional-climate model. II: comparison of driving and regional model responses to a doubling of carbon dioxide. *Quart. J. Roy. .Meteorol. Soc.* **123**, 265–292.

Kida, H., Koide, T., Sasaki, H. and Chiba, M. 1991. A new approach to coupling a limited area model with a GCM for regional climate simulation. *J. Met. Soc. Japan* **69**, 723–728.

Køltzow, M. 2007. The effect of a new snow and sea ice albedo scheme on regional climate model simulations. *J. Geophys. Res.,* **112**, D07110, doi:10.1029/2006JD007693.

Lambert, S. J. and Boer, G. J. 2001. CMIP1 evaluation and intercomparison of coupled climate models. *Clim. Dyn.* **17**, 83–106.

Machenhauer, B., Jacob, D. and Bozet, M. 1994. Using the MPI's nested limited area model for regional climate simulations. CAS/JSC WGNE Report No. 19. WMO/TD-No 592, pp. 758–760.

Noguer, M., Jones, R. and Murphy, J. 1998. Sources of systematic errors in the climatology of a regional climate model over Europe. *Clim. Dyn.* **14**, 691–712.

Rinke, A., Dethloff, K., Spekat, A., Enke W. and Christensen, J. H. 1999. High resolution climate simulations over the Arctic. *Polar Res.* **18**, 1–9.

Rinke, A., Gerdes, R., Dethloff, K., Kandlbinder, T., Karcher, M. and co-authors. 2003. A case study of the anomalous Arctic sea ice conditions during 1990: insights from coupled and uncoupled regional climate model simulations. *J. Geophys. Res.* **108**(D9), 4275, doi:10.1029/2002JD003146.

Rinke, A., Dethloff, K., Cassano, J. J., Christensen, J. H., Curry, J. A. and co-authors. 2006. Evaluation of an ensemble of Arctic regional climate models: spatiotemporal fields during the SHEBA year. *Clim. Dyn.* **27**, 459–472.

Roeckner, E., Arpe, K., Bengtsson, L., Christoph, M., Claussen, M. and co-authors. 1996. The atmospheric general circulation model ECHAM4: model description and simulation of present-day climate: MPI Rep No. 218.

Rummukainen, M., Räisänen, J., Bringfelt, B., Ullerstig, A., Omstedt, A. and co-authors. 2001. A regional climate model for northern Europe: model description and results from the downscaling of two GCM control simulations. *Clim. Dyn.* **17**, 339–359.

Schär, C. and Jendritzky, G. 2004. Hot news from summer 2003. *Nature* **432**, 559–560.

Undén, P., Rountu, L., Järvinen, H., Lynch, P., Calvo, J. and co-authors. 2002. *HIRLAM-5 Scientific Documentation*. HIRLAM-5 project, c/o Per Undén SMHI, S-60176 Norrkøping, Sweden.

Uppala, S. M., Kållberg, P. W., Simmons, A. J., Andrae, U., da Costa Bechtold, V. and co-authors. 2005. The ERA-40 re-analysis. *Quart. J. Roy. Meteorol. Soc.* **131**, 2961–3012. doi:10.1256/qj.04.176.

Von Storch, H., Langenberg, H. and Feser, F. 2000. A spectral nudging technique for dynamical downscaling purposes. *Mon. Wea. Rev.* **128**, 3664–3672.

III

Atmosphere **2011**, *2*, 67-95; doi:10.3390/atmos2020067

OPEN ACCESS

atmosphere

ISSN 2073-4433

www.mdpi.com/journal/atmosphere

Article

The Importance of Lateral Boundaries, Surface Forcing and Choice of Domain Size for Dynamical Downscaling of Global Climate Simulations

Morten A.Ø. Køltzow [1,*], Trond Iversen [1,2] and Jan Erik Haugen [1]

[1] Research & Development Department, Norwegian Meteorological Institute, P.O. Box 43 Blindern, 0313 Oslo, Norway; E-Mails: trond.iversen@met.no (T.I.); jan.erik.haugen@met.no (J.E.H.)

[2] Department of Geosciences, University of Oslo, P.O. Box 1047 Blindern, N-0316 Oslo, Norway

* Author to whom correspondence should be addressed; E-Mail: morten.koltzow@met.no.

Received: 5 March 2011; in revised form: 4 April 2011 / Accepted: 14 April 2011 / Published: 11 May 2011

Abstract: Dynamical downscaling by atmospheric Regional Climate Models (RCMs) forced with low-resolution data should produce climate details and add quality and value to the low-resolution data. The aim of this study was to explore the importance of (i) the oceanic surface forcing (sea-surface temperature (SST) and sea-ice), (ii) the lateral boundary condition data, and (iii) the size of the integration domain with respect to improved quality and value in dynamically downscaled data. Experiments addressing the three aspects were performed and the results were investigated for mean sea level pressure (mslp), 2 m air temperature (T2m) and daily precipitation. Although changes in SST gave a clear response locally, changes in the lateral boundary data and the size of the integration domain turned out to be more important with our geographical scope being Norway. The T2m turned out less sensitive to the changes in lateral forcing and the size of the integration domain than mslp and precipitation. The sensitivity for all three variables differed between Norwegian regions; northern parts of Norway were the most sensitive. Even though the sensitivities found in this study might be different in other regions and for other RCMs, these results call for careful consideration when choosing integration domain and driving lateral boundary data when performing dynamical downscaling.

Keywords: dynamical downscaling; lateral- and surface forcing; domain size

---

1. Introduction

State-of-science climate predictions are based on scenarios for future natural and societal developments which influence the external forcing of processes in the climate system. These processes are modelled mathematically by the use of General Circulation Models (GCMs) or Earth System Models (ESMs) if bio-geochemical processes are included on-line. Typical horizontal resolutions of the GCMs used in the 3rd Assessment Report from IPCC were 250–300 km in the atmosphere [1] and 100–150 km in the oceans [2]. In the 4th Assessment Report (AR4) from IPCC, the resolutions were increased by a factor 1.5–2 by some of the GCMs [3]. This is still insufficient for characterizing most regional and local impacts of climate change, and the coarse resolution constitutes an important source of errors in the global climate simulations and predictions.

Regionalization of global climate predictions by applying statistical and dynamical methods is therefore common. Dynamical downscaling, which is the subject of the present paper, employs Regional Climate Models (RCMs) with higher spatial resolution than contemporary GCMs, but in general only for selected physical compartments of the climate system and over selected geographical regions. By applying nesting [4,5], information from outside the RCM-domains is provided by the GCMs (or ESMs) through the open lateral boundaries of the RCMs, which define their geographical scope. For atmospheric RCMs, information from the global models is also provided through the lower boundary. An atmospheric RCM normally includes a dynamical land-surface model for the upper soil layers, including vegetation and simplified surface hydrology, whilst sea surface temperatures (SST) and sea-ice cover (SIC) are prescribed from the global model [6]. Similarly, oceanic regional models can be applied for dynamical downscaling over limited ocean regions by providing atmospheric fluxes from the GCM as upper boundary conditions [7]. In recent years, RCMs which couple atmospheric and oceanic processes on-line have been developed [8,9], but they are still not widely applied.

In this paper we focus on the use of atmospheric RCMs for dynamical downscaling of global climate simulations. A basic pre-requisite for a successful dynamical downscaling is that the atmospheric RCM produces data which refine and add value to the driving input data provided by the GCM. Such refinements can be partly due to higher resolution and better description of the ground surface forcing, and partly to an improved description of the internal atmospheric dynamics and physics [10,11]. One possible way to evaluate the enhanced quality of atmospheric RCMs is to perform *Perfect Boundary Experiments* (PBEs) [12,13], while the nesting method itself can be assessed through *Big Brother Experiments* [14,15].

There are several issues that need to be addressed concerning the nesting strategy [16]. One is the importance of the quality of the imposed driving data for the RCMs. Several studies suggest that RCM results for large scale variables, e.g. mean sea level pressure, depend crucially on the lateral boundary data [4,17,18]. On the other hand, for variables predominantly influenced by local conditions, e.g., 2 m temperature, the quality of the lateral data is less important. Furthermore, the importance of the lateral forcing generally decreases with the size of the integration domain [15].

In an atmospheric RCM the driving data provided by a coarse resolution GCMs can be divided into a part provided through the lower boundary conditions (in particular sea surface variables) and another part governing the lateral boundaries. In re-constructions of the present-day climate by atmospheric GCMs, sea ice surface variables are prescribed. In an experiment with four different data-sets for the

sea ice climatology which all were considered to represent the true situation equally well, high local sensitivities to the differences in sea ice properties were found, considerably smaller impacts were found remotely [19]. One reason for the small remote impact was linked to the fact that the same prescribed sea surface temperature (SST) was used in all simulations.

Significant effects of extra tropical SST anomalies at middle and high latitudes on atmospheric circulation patterns have been reported in existing literature [20,21]. Both of these studies showed a response in the North Atlantic circulation due to SST anomalies in the Labrador Sea. Furthermore, extra-tropical SST anomalies do indeed influence the atmosphere outside of the boundary layer, but this influence may be masked by the internal atmospheric variability [22]. The highest sensitivity to surface forcing is diagnosed during winter due to the relatively strong fluxes of latent and sensible heat in this period. Differences in sea-ice cover (SIC) will in particular enhance the sensitivities with respect to these fluxes along the Arctic boundaries. This is due to the very large temperature difference between the cold Arctic air and the underlying sea surface often observed during incidents of Arctic air outflow.

In a study, an evaluation of 14 GCMs from IPCC AR4 in the Arctic was performed and the penetration of the North Atlantic storm tracks into the Barents Sea was consistently missing or seriously underestimated [23]. In particular this shortcoming was seen in combination with too much sea-ice in the same area. It was not possible to conclude on the causes of this deficiency, but the combination of errors suggested that there is a connection between the state of the sea surface and the atmospheric dynamics. Such connections may limit the possibilities for dynamic downscaling with atmospheric RCMs in the Arctic.

There are relatively few published studies that focus the role of SST and SIC in atmospheric RCM simulations [24,25], even though the sea surface state shows impacts on the atmospheric dynamics in regional models. In addition, the sea surface temperatures have a profound impact on the precipitation in RCM simulations for the Baltic Sea area and the Anatolian Peninsula, respectively [26,27]. Another interesting issue in this connection is to what extent the importance of the surface forcing depends on the size of the integration domain. Several studies have concluded that the size of the integration domain is of importance and that the proper size may differ for different variables [28]. Closely linked to this is the relative importance of data imposed at the lateral boundaries *versus* at the ground surface as a function of the integration domain size. There are several reasons why this is an important issue. First, the relative importance of ground surface *versus* lateral boundary forcing in RCM's is not firmly established. Second, if the surface forcing is important, this will constitute an additional source of uncertainty in downscaled climate scenarios. Whilst the importance of the quality of the atmospheric lateral boundary data is recognised and widely studied, the quality of the ground-surface data, including the ocean surface, should be considered more carefully in connection with dynamical downscaling. Thus, a significant sensitivity to surface forcing would imply that a coupled RCM with an improved description of the sea surface forcing should further improve the atmospheric flows and physics compared to pure atmospheric downscaling with fixed coarse resolution surface forcing.

The aim of this study is to explore the importance of data for ground surface forcing (e.g., sea surface temperature (SST) and sea ice concentration (SIC)) relative to data for lateral boundary forcing in atmospheric RCMs. The importance of the forcing is of course closely connected to the employed models, but also closely coupled to the more universal issue with limited area models, what is the

proper size and location of the RCM domain. In this context we therefore also discuss the relevance of the size of the integration domain for dynamical downscaling

In Section 2 a description of the employed RCM is given, before the experiments are described in Section 3. Results are presented and discussed in Section 4 before the investigation is summarized and conclusions are drawn in Section 5.

2. Model Description

The regional climate model HIRHAM consists of the HIRLAM Eulerian grid-point model [29] and the ECHAM4 physical parameterization routine [30]. A description, with some minor modifications, is also available [31]. The model was used for dynamical downscaling of global climate scenarios over Northern Europe and parts of the adjacent North-Atlantic and Arctic oceans [32]. In this study the model makes use of a rotated spherical grid with mesh width 0.5 degree (~55 km) in the horizontal direction and 19 levels in the vertical. Two different integration domains are used, see Figure 1.

Figure 1. The applied HIRHAM Regional Climate Model (RCM) integration domains (including the lateral boundary zone).

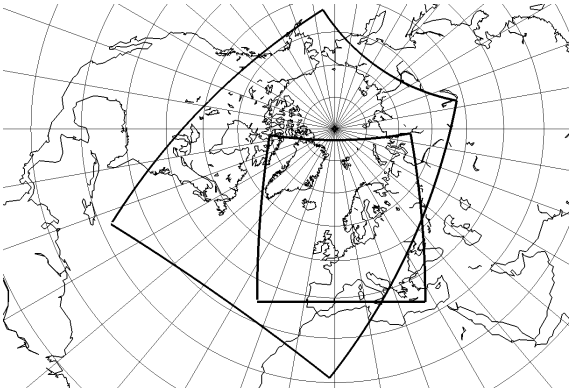

The model dynamics are quasi-hydrostatic, and include prognostic equations for specific humidity and the cloud water. Physical processes are only partly resolved, and therefore include parameterizations. The turbulent vertical fluxes from the sea surface to the atmospheric boundary layer, which are particularly important in connection with the studies in this paper, are calculated using bulk transfer relations in the atmospheric surface layer [30]. The roughness parameter for turbulent momentum over open ocean is computed from the Charnock formula whilst assigned a constant value over the ice-covered ocean. The roughness parameter for heat and moisture are approximated by an empirical relation to the momentum roughness parameter [30].

The lateral boundary conditions employs a relaxation scheme [33] over 7 grid points (also used in 6 out of 8 RCMs in the Arctic Model Intercomparison [24]). At the lateral boundaries the prognostic variables are relaxed towards the imposed data by a nudging coefficient which puts full weight on model-calculated values in the inner parts of the domain and gradually increase the weight towards a full weight on the externally imposed values across a relaxation zone along the lateral boundary. SST

and SIC are entirely specified from the externally global data; *i.e.*, these variables are not calculated by the RCM.

3. Description of Experiments

In this study a set of dynamical downscaling experiments is done with the HIRHAM model. All experiments are valid for the climate during the period 1960–1990. The first year is omitted in the analysis to avoid spin-up effects in the model results. The driving data are from the ECHAM4 GCM (The Max Planck Institute for Meteorology in Hamburg, Germany) and from the Hadley GCM (The Hadley Centre at the UK MetOffice). Hereafter we use the following naming conventions: HL for lateral boundary data from the Hadley GCM, HS for ground surface forcing data from the Hadley GCM, ML for lateral boundary data from the ECHAM4 GCM, and finally MS for ground surface forcing data from the ECHAM4 GCM.

The experiments are performed using a small and a large integration domain (Figure 1). The large domain consists of 150 × 165 grid points, while the small domain consists of 96 × 96 grid points. For the experiments in which HS replaces MS, this is only done for parts of the domain (30° W to 40° E). The differences in SST and SIC between MS and HS are seen throughout the whole year but are most pronounced during the winter seasons. In winter (December, January and February, DJF) the HS surface temperatures are considerable lower than for MS south of Greenland, while it is opposite near the sea ice edge along the eastern Greenland coast and in the Barents Sea (Figure 2). While the former differences are associated with the location of the warm North-Atlantic current (the "Gulf stream"), the latter are mainly due to the different location of the sea ice edge, and thereby the surface temperature. In addition there are differences along the coasts.

Figure 2. The average December, January and February (DJF), differences in surface forcing between HS and MS. Differences in sea surface temperature (1 °C intervals) is shown together with the sea ice concentration from the HS (dashed lines) and the MS solid lines.

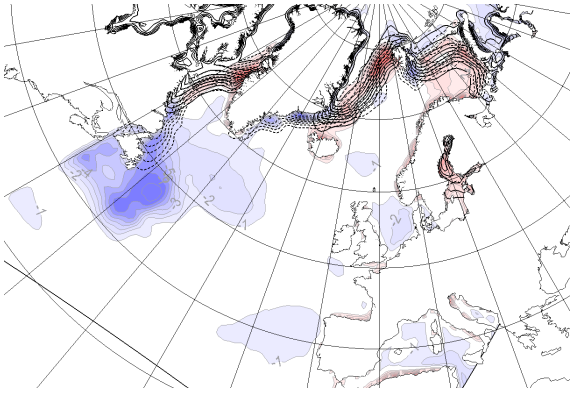

Five experiments are performed: (1) MLMS on the small domain; (2) MLHS on the small domain; (3) MLMS on the large domain; (4) MLHS on the large domain; and finally (5) HLHS on the small domain. The experiments are summed up in Table 1. For a straightforward interpretation of the results,

we mainly focus the comparison between combinations involving only one difference in the external variables (*i.e.*, different surface forcing only, different lateral boundary forcing only, or different domains only, see Table 1). Each experiment is run for 30 years and designed to be representative of the 1960–1990 climate.

Table 1. Overview of the experiments performed with the HIRHAM Regional Climate Model (RCM). The table lists which of the external specifications that are studied when a comparison of different experiments is done. Different surface forcing is named SFC, and different lateral forcing is named LBC. Combinations of experiments for which only one specification is different are written in italic bold.

	MLMS small domain	MLHS small domain	MLMS large domain	MLHS large domain	HLHS small domain
MLMS small domain		***SFC on small domain***	***Domain size***	Domain size & SF	***Driving data (SFC and LBC)***
MLHS small domain	***SFC on small domain***		Domain size & SFC	***Domain size***	***LBC on small domain***
MLMS large domain	***Domain size***	Domain size & SFC		***SFC on a large domain***	Driving data (SFC & LBC) and domain size
MLHS large domain	Domain size & SFC	***Domain size***	***SFC on a large domain***		LBC and domain size
HLHS small domain	***Driving data (SFC & LBC) on small domain.***	***LBC on small domain***	Driving data (SFC & lateral) and domain size	LBC and domain size	

4. Results

In this section a comparison of the 30 year long averages of mean sea level pressure (MSLP), 2 m air temperature (T2m) and daily amounts of precipitation from the different RCM simulations is presented. The attention will be on how the differences in the size of the integration domain and in the lateral- and surface forcing (referred to as external forcing of the RCM) alter the simulation results. The external forcing and RCM response is present throughout the entire year, but with a pronounced annual cycle. The results are presented for the winter season (DJF) when the differences in surface forcing and in the response are largest. These winter maxima are also found in other studies [19,24], and can be explained by larger latent and sensible heat fluxes from open water compared to the radiative forcing during the winter.

A general overview of the differences in the simulated climate from the different experiments is given below, before the impacts on selected Norwegian regions are discussed in more detail.

4.1. Differences in Simulated Climate due to Different Surface Forcing

The responses in T2m due to changed surface forcing are concentrated close to the areas of large forcing differences in both integration domains (Figure 3a and 4a shows the difference in response due to MLHS instead of MLMS forcing, small and large domain, respectively). The differences in surface forcings are shown in Figure 2. There is a local and apparent one-to-one relationship between the

differences in SST and the differences in T2m. The strong local response is expected because the T2m is estimated applying a stability dependent interpolation between the surface temperature (here SST) and the temperature in the lowest model level. The latter is between 50–150 m above ground in climate models. Effects of the lateral forcing are also seen as the response to the SST difference in the small domain is slightly weaker than in the large domain. Similar behaviour is found in the T2m response for other seasons; the local response dominates with similar patterns in both domains, but with larger amplitude in the large (not shown). However, the differences in T2m are more modest downstream in the prevailing westerly winds of the areas with large SST differences. This is in agreement with earlier findings which reported a modest non-local response to surface forcing [6]. This finding is explained by the fact that the prescription of more similar SSTs downstream effectively constrains the effect of the changes. However, other studies report larger remote responses, both in coupled models [34] and pure atmospheric models [20]. Also the shape and scale of the surface forcing can be important for the nature of the response [21].

Figure 3. Differences in simulated DJF climate, MLHS small domain minus MLMS small domain, of (**a**) 2 m air temperature (1 °C intervals); (**b**) mean sea level pressure (0.5 hPa intervals) and (**c**) daily precipitation (0.25 mm/day intervals).

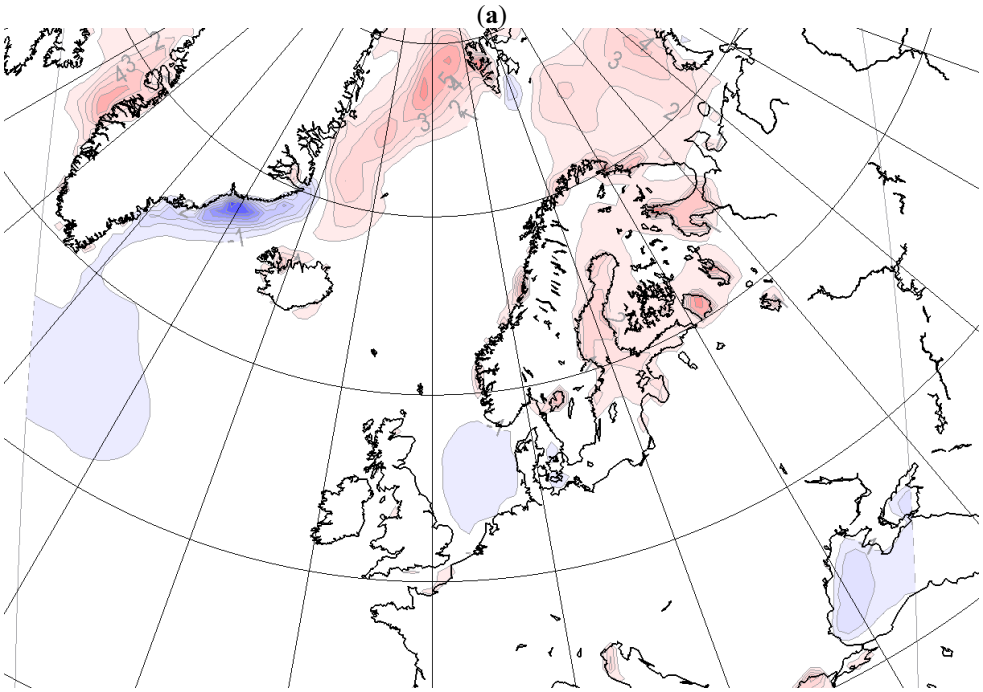

Figure 3. *Cont.*

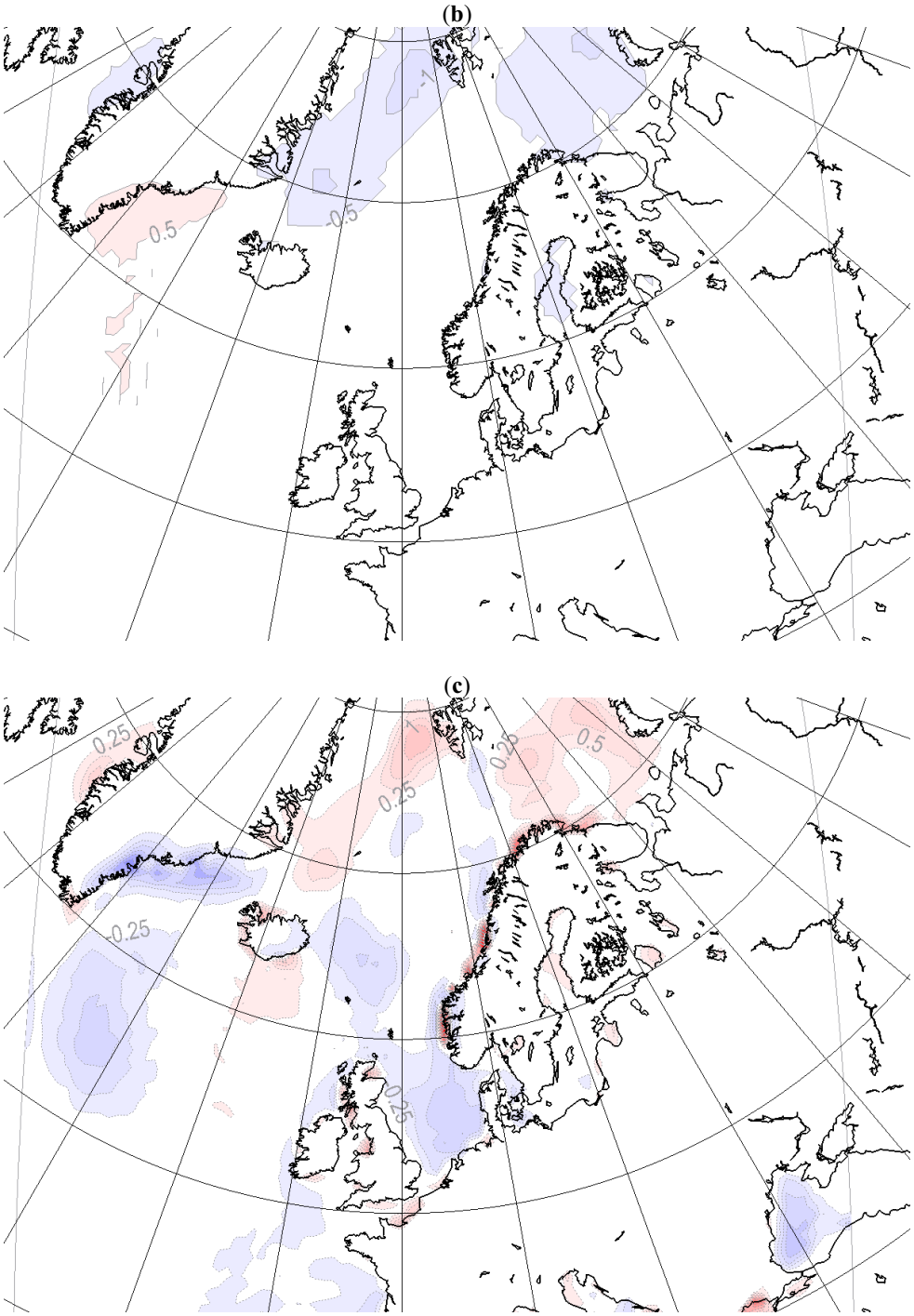

Figure 4. Differences in simulated DJF climate, MLHS large domain minus MLMS large domain, of (**a**) 2 m air temperature (1 °C intervals); (**b**) mean sea level pressure (0.5 hPa intervals) and (**c**) daily precipitation (0.25 mm/day intervals).

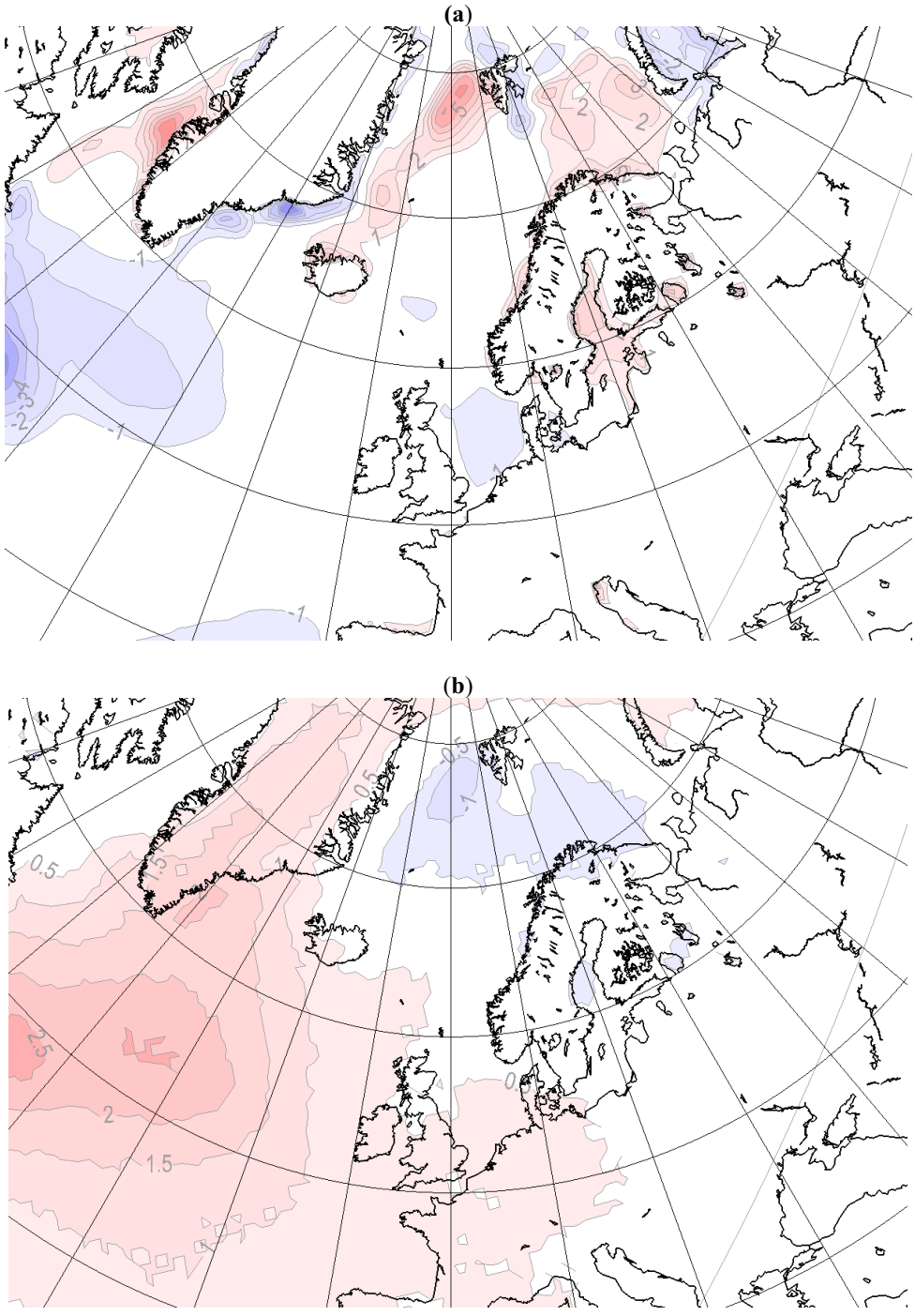

Figure 4. *Cont.*

(c)

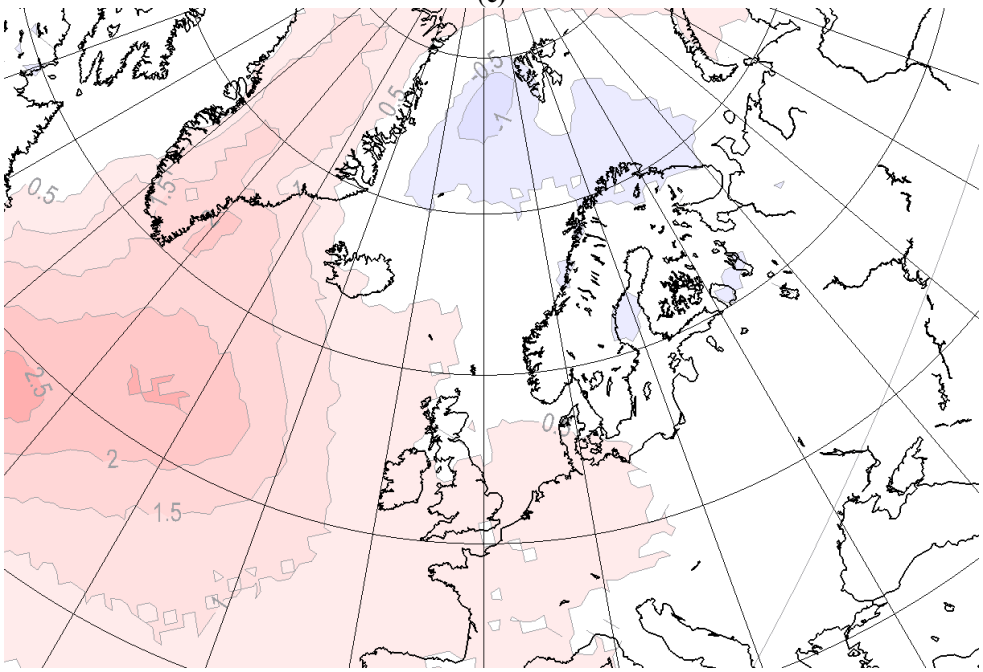

A response to surface forcing in Mean Sea Level Pressure is mainly seen in autumn and winter, and the response is clearly most pronounced in the large domain (Figure 3b and 4b, small and large domain, respectively). The MSLP response in the large domain is high locally, but is also seen in remote areas (e.g., over central Europe). The surface pressure increase (up to 2 hPa) over colder water and a reduction of about 1hPa is found in areas with warmer water. This implies a change in the north-south gradient of the MSLP for the Atlantic and changes in flow patterns when replacing MS with HS. Smaller response is calculated close to the lateral boundaries. In the Barents Sea the response is not sensitive to the size of the integration domain.

As for mslp, the response in precipitation is mainly seen in autumn and winter (Figure 3c and 4c, small and large domain, respectively). The patterns appear independent of the size of the integration domain, but the amplitudes are larger with the large domain. During winter, an increased surface temperature and reduced surface pressure is correlated with increased precipitation. The increased precipitation amounts to 1mm/day in regions with 2–4° increased SST (south of Greenland). The precipitation response is predominantly local to the surface forcing, but there are also changes in precipitation remotely at the Norwegian coast. The latter is likely to be connected with the changes found in the pressure gradients. In the large integration domain even more remote response in precipitation is seen over locations not included in the small domain, such as areas near the Alps. A possible explanation for this response might be a change in humidity in air flowing across the Mediterranean due to changed SST. However, this area is also situated close to the lateral boundary and might be influenced by the lateral boundary treatment.

So far, only the response in surface fields is studied, and figures for free tropospheric responses are not included. However, investigation of the thickness of the 1,000 hpa to 850 hPa layer and 850 hPa to 500 hPa layer reveals differences up to 10 m. Mainly, a reduction is seen in thickness south and east of the south tip of Greenland due to the colder surface in HS. Locally, the main difference is found in the lower part of the troposphere, whilst downstream of the forcing the main difference is found in the mid-troposphere. Close to the sea ice edge, an increase in thickness is found. In the lower parts of the atmosphere the response is closely linked to the surface forcing, whilst the response in mid-troposphere is more homogenous.

4.2. Differences in Climatology due to Different Size of the Integration Domain

The MLMS and MLHS data sets are downscaled with the HIRHAM RCM both in a "small" and a "large" integration domain. Differences in mean values valid for DJF between the large and the small integration domain are shown in Figure 5 (MLMS driven) and 6 (MLHS driven). The differences between the large and the small integration domain are almost independent on the surface forcing, since there are similar patterns in Figure 5 as in Figure 6. In the small domain, the Icelandic low is deeper and associated with a stronger westerly flow over Northern Europe than for the solution in the large domain. The increased low level advection of relatively warm air from the North Atlantic Ocean over Northern Europe, contributes to the 0.5–1.5 °K increase of the T2m in Scandinavia in the small domain. There are also temperature differences in the Arctic (not shown), which can be a consequence of changed circulation patterns and the proximity to the lateral boundary in the small domain. Similar explanations are plausible for the differences in precipitation in southern Europe and close to the Alps. At the Norwegian coast, the response in the small domain produces approximately 0.5–1.0 mm/day more precipitation than in the large domain. The maximum precipitation differences are around 10% of the daily precipitation in the downscaled MLMS in the small domain.

Although the results presented here can be specific to the employed RCM and the geographical area, they suggest that RCM results are highly sensitive to the choice of integration domain size. The optimal choice of integration domain depends on one's perspective on the purposes of dynamical downscaling. One perspective is that downscaling should mainly introduce small-scale features that are not resolved in GCMs, whilst the large scale features resolved in the driving GCM are kept unaltered. This is a linear perspective on the role of downscaling which can be achieved by choosing sufficiently small integration domains [5] so that the large scale circulation is restricted by the lateral boundaries, but still large enough for small scale features to develop by the RCM. Alternatively, so-called spectral nudging can be applied in the RCM to control the larger scales [35,36]. Another perspective on the role of regional climate modelling is more non-linear, in that the increased resolution in the RCM may introduce fine-scale features which may develop and upscale and thus contribute to improve the description of features on the larger scales that are resolved by the GCM providing the driving data. In this perspective, large integration domains are preferred in order to allow the upscale development in the RCM, and thus to potentially improve the large scale as well as the small scale features [15,37]. These different perspectives are discussed in more detail in existing literature [16].

Figure 5. Differences in simulated DJF climate, MLMS large domain minus MLMS small domain, of (**a**) 2 m air temperature (1 °C intervals), (**b**) mean sea level pressure (0.5 hPa intervals) and (**c**) daily precipitation (0.25 mm/day intervals).

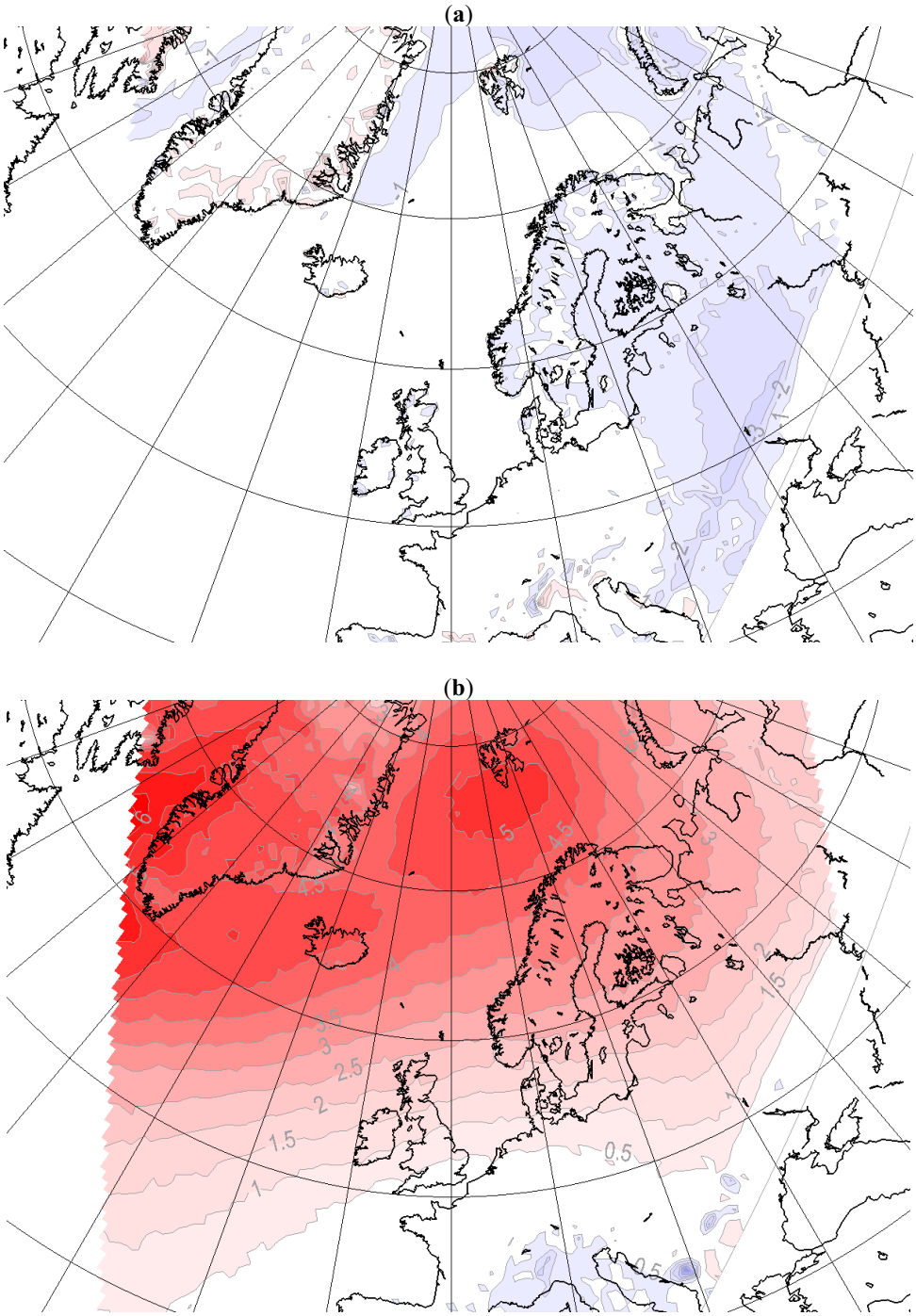

Figure 5. *Cont.*

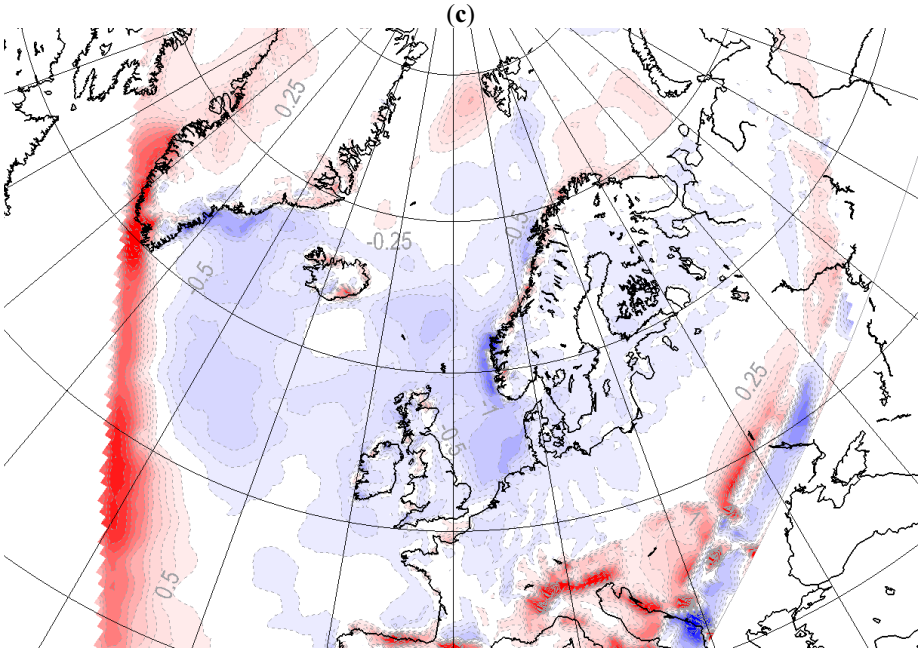

Figure 6. Differences in simulated DJF climate, MLHS large domain minus MLHS small domain, of (**a**) 2 m air temperature (1 °C intervals), (b) mean sea level pressure (0.5 hPa intervals) and (**c**) daily precipitation (0.25 mm/day intervals).

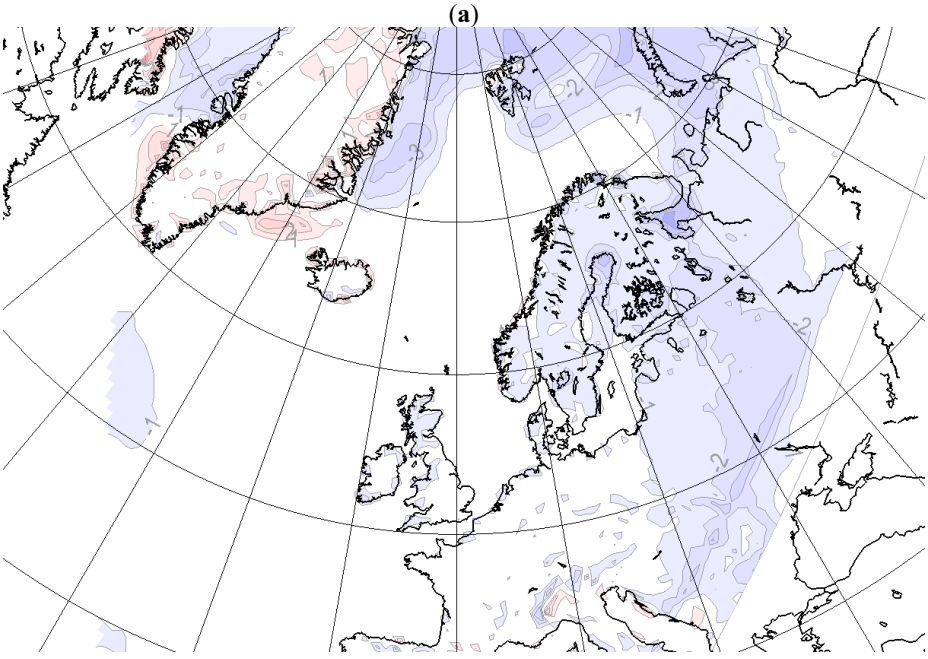

Figure 6. *Cont.*

(b)

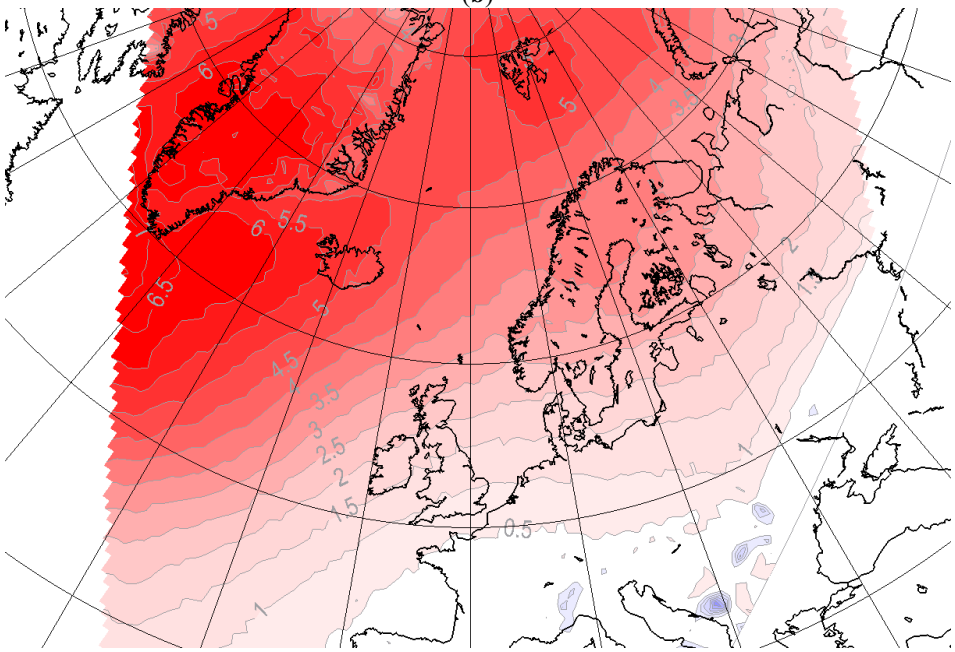

(c)

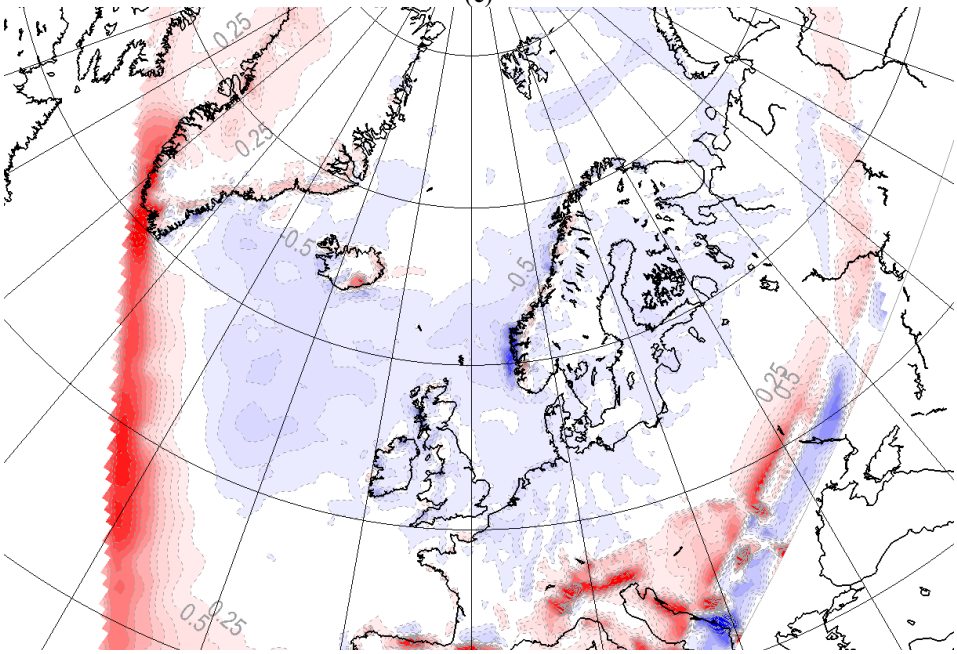

4.3. Differences in Climatology due to Different GCM Driving Data

In Figure 7, the differences in simulated winter climate (DJF) due to different lateral driving data but similar surface forcing (MLHS *versus* HLHS) are shown. This can be compared to another experiment (MLMS *versus* HLHS) shown in Figure 8. All simulations are done in the small integration domain. The differences are very similar and independent on the employed surface forcing (except locally over the ocean), implying that with this integration domain the lateral boundary forcing strongly constrains the flow and is of higher importance than the surface boundary conditions.

The ML driven RCM shows a considerable lower surface pressure in the Arctic and Northern Europe, while higher pressure are obtained south west of Iceland compared to the HL driven simulation. The differences mean that the Icelandic low is moved north-eastward in the ML driven simulation. This gives an increased on-shore wind component in southern Norway and an off-shore component in the more northerly parts of Norway. In conjunction with the Norwegian orography, this results in ~2mm/day more precipitation at the Norwegian west coast in the ML driven simulation. Temperature differences are smaller and mainly seen locally over the sea and sea ice where the surface forcing differs, as well as close to the lateral boundaries.

In these experiments there is little doubt that the large-scale parts of the RCM solutions strongly depend on the driving data. However, for more locally forced variables, such as near surface temperatures and parts of the precipitation, the solutions are less dependent on the lateral forcing data. An interesting question is whether the results of the RCM would converge with increasing integration domain, but this is left for further investigation.

Figure 7. Differences in simulated DJF climate, MLHS small domain minus HLHS small domain, of (**a**) 2 m air temperature (1 °C intervals); (**b**) mean sea level pressure (0.5 hPa intervals) and (**c**) daily precipitation (0.25 mm/day intervals).

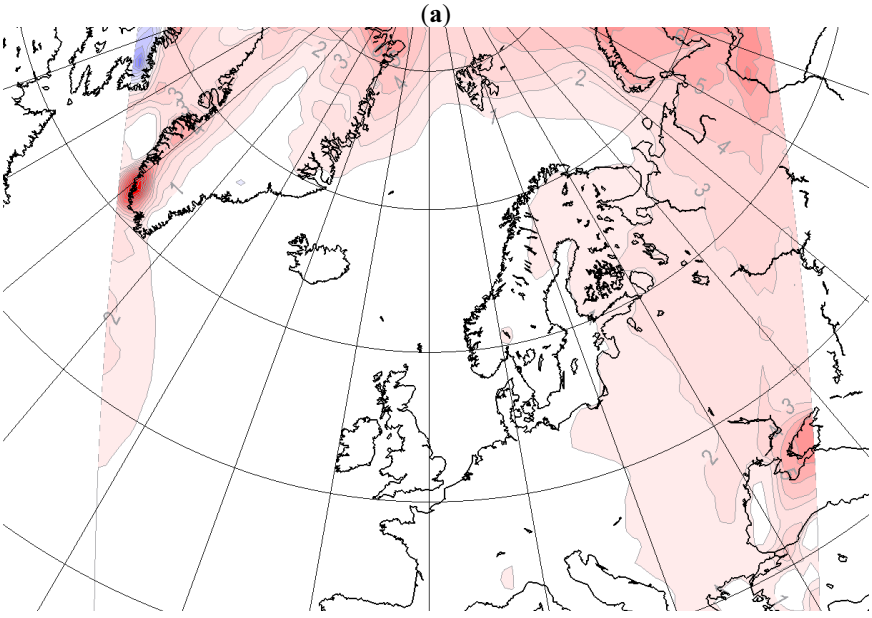

Figure 7. *Cont.*

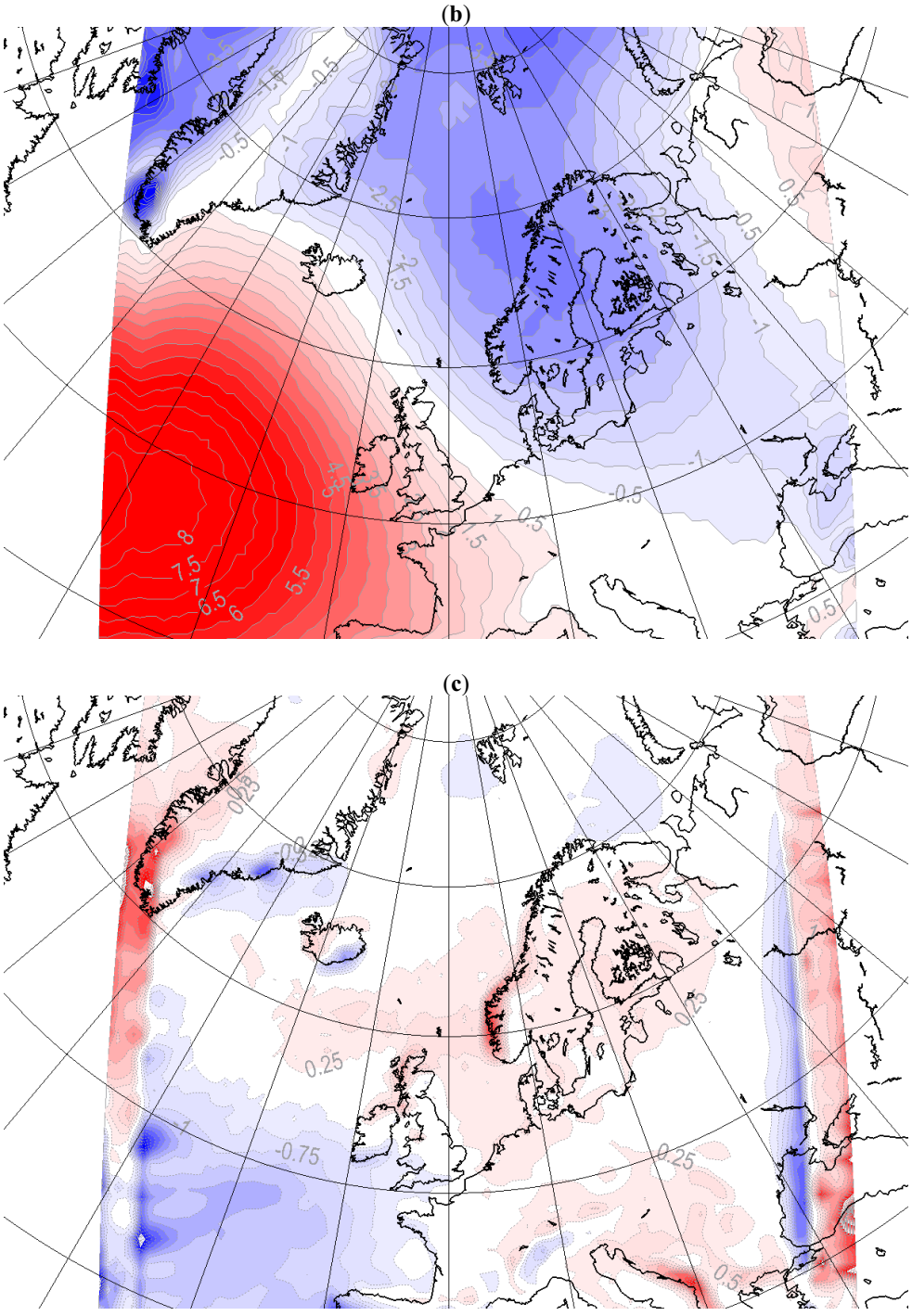

Figure 8. Differences in simulated DJF climate, MLMS small domain minus HLHS small domain, of (**a**) 2 m air temperature (1 °C intervals); (**b**) mean sea level pressure (0.5 hPa intervals) and (**c**) daily precipitation (0.25 mm/day intervals).

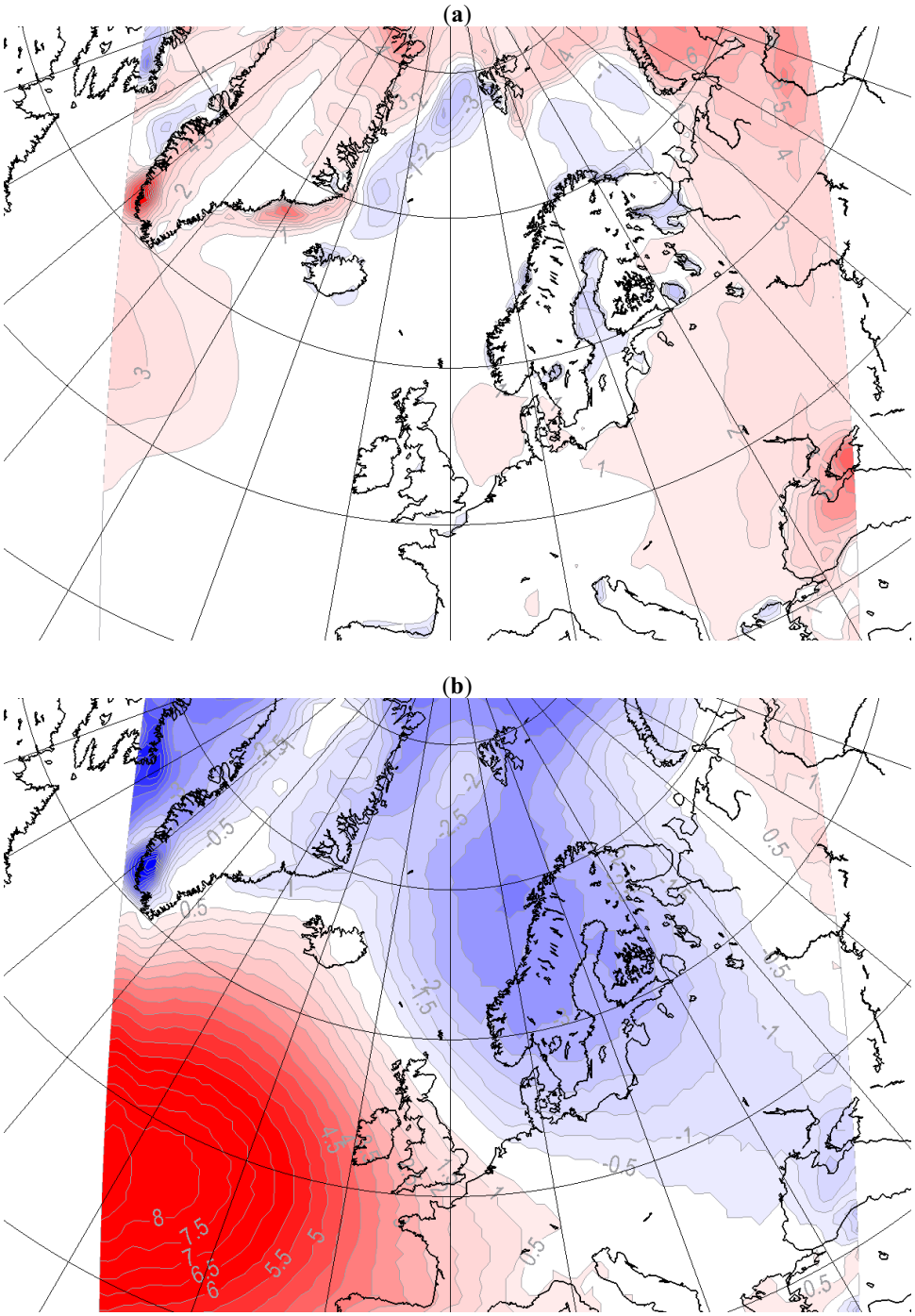

Figure 8. *Cont.*

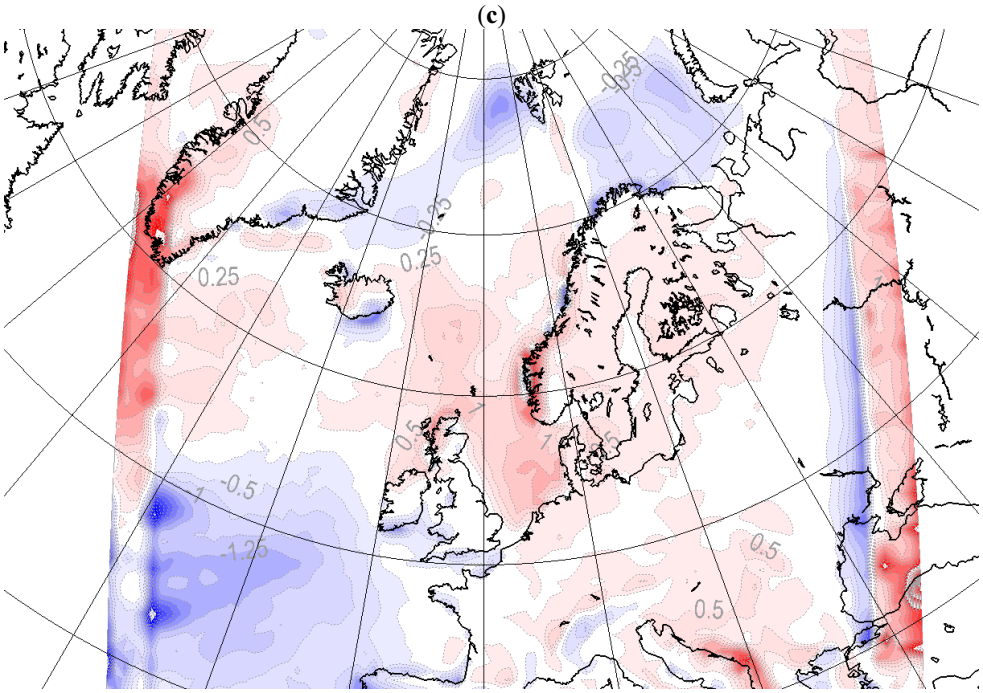

4.4. The Impacts of RCM Set-up on the Simulated Climate in Norwegian Regions

In this section, the RCM results for different regions in Norway are examined. We will investigate how the external forcing alters the RCM results with respect to mean value and month-to-month variability. The analysis is done for the three regions shown in Figure 9. The three regions have considerably different climates as illustrated with the MLMS driven RCM-climate for MSLP, T2m, and daily precipitation in winter (Figure 9). Eastern Norway has a pronounced continental climate with warm summers, cold winters and moderate annual precipitation amounts. Both Western and Northern parts of Norway are dominated by a coast line that is exposed to the westerly winds from the North Atlantic Ocean. Annual precipitation amounts are large while the difference between summer and winter temperatures is moderate. In addition, Northern Norway is strongly influenced by the proximity to the Arctic, even though the surrounding ocean is open all year. The three regions are hereafter denoted north, west and east Norway.

Figure 9. The three analysed regions, north, (south) west and (south) east Norway, marked with red. In addition, the MLMS small domain DJF climate, T2m (°C) in red/blue colors, mslp (hPa) in solid black lines and daily precipitation (mm/day) in dashed black lines.

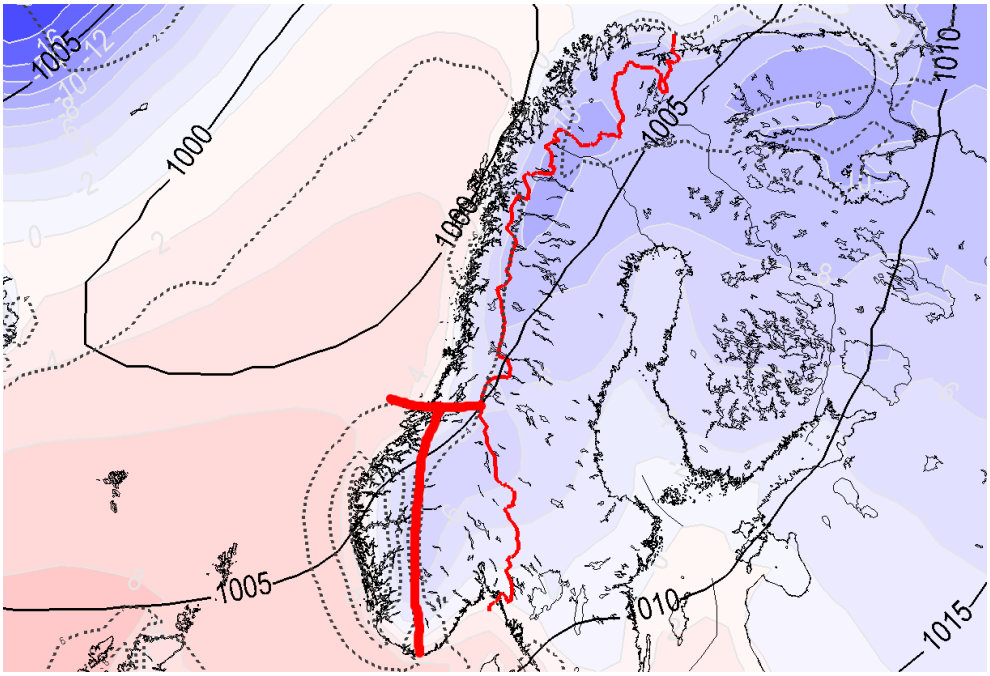

The results are presented as the mean differences between the different simulations and the ratio of month-to-month variance between different experiments for north Norway (Table 2), west Norway (Table 3) and east Norway (Table 4).

Table 2. The DJF mean difference and ratios of the month-to-month variance of MSLP (hPa), T2m (°C) and daily precipitation (mm/day) between the different experiments for the north Norway region. The numbers are the differences/ratios between the experiments in the column heading minus the experiment in the rows to the left.

	MLMS Small domain	MLHS Small domain	MLMS Large domain	MLHS Large domain	HLHS Small domain
MLMS Small domain		*Mean difference:* MSLP = 0.33 T2m = −0.47 Prec = −0.21 *Variance ratio:* MSLP = 0.96 T2m = 1.35 Prec = 1.07	*Mean difference:* MSLP = −2.84 T2m = 0.14 Prec = 0.08 *Variance ratio:* MSLP = 2.11 T2m = 0.93 Precip = 6.08	*Mean difference:* MSLP = −2.71 T2m = −0.22 Precip = 0.03 *Variance ratio:* MSLP = 1.89 T2m = 1.11 Precip = 5.27	*Mean difference:* MSLP = −3.86 T2m = 0.25 Precip = 0.20 *Variance ratio:* MSLP = 1.10 T2m = 1.13 Precip = 1.16

Table 2. *Cont.*

	MLMS Small domain	MLHS Small domain	MLMS Large domain	MLHS Large domain	HLHS Small domain
MLHS Small domain	*Mean difference:* MSLP = −0.33 T2m = 0.47 Precip = 0.21 *Variance ratio:* MSLP = 1.04 T2m = 0.74 Precip = 0.94		*Mean difference:* MSLP = −3.17 T2m = 0.61 Precip = 0.29 *Variance ratio:* MSLP = 2.19 T2m = 0.69 Precip = 5.67	*Mean difference:* MSLP = −3.04 T2m = 0.25 Precip = 0.24 *Variance ratio:* MSLP = 1.96 T2m = 0.82 Precip = 4.91	*Mean difference:* MSLP = −4.19 T2m = 0.72 Precip = 0.42 *Variance ratio:* MSLP = 1.14 T2m = 0.83 Precip = 1.09
MLMS Large domain	*Mean difference:* MSLP = 2.84 T2m = −0.14 Precip = −0.08 *Variance ratio:* MSLP = 0.47 T2m = 1.08 Precip = 0.16	*Mean difference:* MSLP = 3.17 T2m = −0.61 Precip = −0.29 *Variance ratio:* MSLP = 0.46 T2m = 1.45 Precip = 0.18		*Mean difference:* MSLP = 0.13 T2m = −0.36 Precip = −0.05 *Variance ratio:* MSLP = 0.9 T2m = 1.2 Precip = 0.87	*Mean difference:* MSLP = −1.02 T2m = 0.11 Precip = −0.12 *Variance ratio:* MSLP = 0.52 T2m = 1.21 Precip = 0.19
MLHS Large domain	*Mean difference:* MSLP = 2.71 T2m = 0.22 Precip = −0.03 *Variance ratio:* MSLP = 0.53 T2m = 0.90 Precip = 0.19	*Mean difference:* MSLP = 3.04 T2m = −0.25 Precip = −0.24 *Variance ratio:* MSLP = 0.51 T2m = 1.22 Precip = 0.20	*Mean difference:* MSLP = −0.13 T2m = 0.36 Precip = 0.05 *Variance ratio:* MSLP = 1.11 T2m = 0.83 Precip = 1.15		*Mean difference:* MSLP = −1.15 T2m = 0.47 Precip = 0.17 *Variance ratio:* MSLP = 0.58 T2m = 1.01 Precip = 0.22
HLHS Small domain	*Mean difference:* MSLP = 3.86 T2m = −0.25 Precip = −0.20 *Variance ratio:* MSLP = 0.91 T2m = 0.88 Precip = 0.86	*Mean difference:* MSLP = 4.19 T2m = −0.72 Precip = −0.42 *Variance ratio:* MSLP = 0.88 T2m = 1.20 Precip = 0.92	*Mean difference:* MSLP = 1.02 T2m = −0.11 Precip = 0.12 *Variance ratio:* MSLP = 1.92 T2m = 0.83 Precip = 5.26	*Mean difference:* MSLP = 1.15 T2m = −0.47 Precip = −0.17 *Variance ratio:* MSLP = 1.72 T2m = 0.99 Precip = 4.54	

Table 3. The DJF mean difference and ratios of the month-to-month variance of MSLP (hPa), T2m (°C) and daily precipitation (mm/day) between the different experiments for the west Norway region. The numbers are the differences/ratios between the experiments in the column heading minus the experiment in the rows to the left.

	MLMS Small domain	MLHS Small domain	MLMS Large domain	MLHS Large domain	HLHS Small domain
MLMS Small domain		*Mean difference:* MSLP = 0.10 T2m = −0.04 Precip =−0.09 *Variance ratio:* MSLP = 0.98 T2m=1.17 Precip= 0.90	*Mean difference:* MSLP = −2.1 T2m = 0.12 Precip = 0.38 *Variance ratio:* MSLP = 2.55 T2m = 0.98 Precip = 4.98	*Mean difference:* MSLP = −1.97 T2m = 0.18 Precip = 0.38 *Variance ratio:* MSLP = 2.67 T2m = 1.01 Precip = 1.03	*Mean difference:* MSLP = −2.4 T2m = 0.22 Precip = 0.70 *Variance ratio:* MSLP = 1.05 T2m = 1.06 Precip = 1.03
MLHS Small domain	*Mean difference:* MSLP = −0.10 T2m = 0.04 Precip = 0.09 *Variance ratio:* MSLP = 1.02 T2m = 0.85 Precip = 1.11		*Mean difference:* MSLP = −2.21 T2m = 0.17 Precip = 0.47 *Variance ratio:* MSLP = 2.61 T2m = 0.83 Precip = 5.52	*Mean difference:* MSLP = −2.07 T2m = 0.23 Precip = 0.47 *Variance ratio:* MSLP = 2.73 T2m = 0.86 Precip = 5.02	*Mean difference:* MSLP = −2.51 T2m = 0.27 Precip = 0.79 *Variance ratio:* MSLP = 1.08 T2m = 0.90 Precip = 1.14
MLMS Large domain	*Mean difference:* MSLP = 2.1 T2m = −0.12 Precip = −0.38 *Variance ratio:* MSLP = 0.39 T2m = 1.02 Precip = 0.20	*Mean difference:* MSLP = 2.21 T2m = −0.17 Precip = −0.47 *Variance ratio:* MSLP = 0.38 T2m = 1.20 Precip = 0.18		*Mean difference:* MSLP = 0.14 T2m = 0.06 Precip = 0.0 *Variance ratio:* MSLP = 1.05 T2m = 1.04 Precip = 0.91	*Mean difference:* MSLP = −0.30 T2m = 0.10 Precip = 0.32 *Variance ratio:* MSLP = 0.41 T2m = 1.08 Precip = 0.21
MLHS Large domain	*Mean difference:* MSLP = 1.97 T2m = −0.18 Precip = −0.38 *Variance ratio:* MSLP = 0.37 T2m = 0.99 Precip = 0.97	*Mean difference:* MSLP = 2.07 T2m = −0.23 Precip = −0.47 *Variance ratio:* MSLP = 0.37 T2m = 1.16 Precip = 0.20	*Mean difference:* MSLP = −0.14 T2m = −0.06 Precip = 0.0 *Variance ratio:* MSLP = 0.95 T2m = 0.96 Precip = 1.10		*Mean difference:* MSLP = −0.44 T2m = 0.04 Precip = 0.32 *Variance ratio:* MSLP = 0.39 T2m = 1.04 Precip = 0.23
HLHS Small domain	*Mean difference:* MSLP = 2.4 T2m = −0.22 Precip = −0.70 *Variance ratio:* MSLP = 0.67 T2m = 0.94 Precip = 0.97	*Mean difference:* MSLP = 2.51 T2m = −0.27 Precip = −0.79 *Variance ratio:* MSLP = 0.93 T2m = 1.11 Precip = 0.88	*Mean difference:* MSLP = 0.30 T2m = −0.10 Precip = −0.32 *Variance ratio:* MSLP = 0.49 T2m = 0.93 Precip = 4.76	*Mean difference:* MSLP = 0.44 T2m = −0.04 Precip = −0.32 *Variance ratio:* MSLP = 2.56 T2m = 0.96 Precip = 4.35	

Table 4. The DJF mean difference and ratios of the month-to-month variance of MSLP (hPa), T2m (°C) and daily precipitation (mm/day) between the different experiments for the east Norway region. The numbers are the differences/ratios between the experiments in the column heading minus the experiment in the rows to the left.

	MLMS small domain	MLHS Small domain	MLMS Large domain	MLHS Large domain	HLHS Small domain
MLMS Small domain		*Mean difference:* MSLP = 0.19 T2m = −0.04 Precip = −0.28 *Variance ratio:* MSLP = 0.99 T2m = 1.09 Precip = 0.73	*Mean difference:* MSLP = −1.77 T2m = −0.05 Precip = −0.06 *Variance ratio:* MSLP = 2.75 T2m = 0.95 Precip = 8.41	*Mean difference:* MSLP = −1.65 T2m = −0.15 Precip = −0.01 *Variance ratio:* MSLP = 3.02 T2m = 0.97 Precip = 9.66	*Mean difference:* MSLP = −2.12 T2m = 0.85 Precip = −0.03 *Variance ratio:* MSLP = 0.90 T2m = 0.99 Precip = 1.10
MLHS Small domain	*Mean difference:* MSLP = −0.19 T2m = 0.04 Precip = 0.28 *Variance ratio:* MSLP = 1.01 T2m = 0.92 Precip = 1.37		*Mean difference:* MSLP = −1.97 T2m = −0.02 Precip = 0.22 *Variance ratio:* MSLP = 2.78 T2m = 0.87 Precip = 11.50	*Mean difference:* MSLP = −1.84 T2m = −0.12 Precip = 0.26 *Variance ratio:* MSLP = 3.06 T2m = 0.89 Precip = 13.21	*Mean difference:* MSLP = −2.32 T2m = 0.89 Precip = 0.24 *Variance ratio:* MSLP = 0.92 T2m = 0.91 Precip = 1.50
MLMS Large domain	*Mean difference:* MSLP = 1.77 T2m = 0.05 Precip = 0.06 *Variance ratio:* MSLP = 0.36 T2m = 1.05 Precip = 0.12	*Mean difference:* MSLP = 1.97 T2m = 0.02 Precip = −0.22 *Variance ratio:* MSLP = 0.36 T2m = 1.15 Precip = 0.09		*Mean difference:* MSLP = 0.13 T2m = −0.10 Precip = 0.05 *Variance ratio:* MSLP = 1.10 T2m = 1.02 Precip = 1.15	*Mean difference:* MSLP = −0.35 T2m = 0.90 Precip = 0.02 *Variance ratio:* MSLP = 0.33 T2m = 1.04 Precip = 0.13
MLHS Large domain	*Mean difference:* MSLP = 1.65 T2m = 0.15 Precip = 0.01 *Variance ratio:* MSLP = 0.33 T2m = 1.03 Precip = 0.10	*Mean difference:* MSLP = 1.84 T2m = 0.12 Precip = −0.26 *Variance ratio:* MSLP = 0.33 T2m = 1.12 Precip = 0.08	*Mean difference:* MSLP = −0.13 T2m = 0.10 Precip = −0.05 *Variance ratio:* MSLP = 0.91 T2m = 0.98 Precip = 0.67		*Mean difference:* MSLP = −0.48 T2m = 1.01 Precip = −0.02 *Variance ratio:* MSLP = 0.3 T2m = 1.02 Precip = 0.11
HLHS Small domain	*Mean difference:* MSLP = 2.12 T2m = −0.85 Precip = 0.03 *Variance ratio:* MSLP = 1.11 T2m = 1.01 Precip = 0.91	*Mean difference:* MSLP = 2.32 T2m = −0.89 Precip = −0.24 *Variance ratio:* MSLP = 1.09 T2m = 1.10 Precip = 0.67	*Mean difference:* MSLP = 0.35 T2m = −0.90 Precip = −0.02 *Variance ratio:* MSLP = 3.03 T2m = 0.96 Precip = 7.69	*Mean difference:* MSLP = 0.48 T2m = −1.01 Precip = 0.02 *Variance ratio:* MSLP = 3.33 T2m = 0.98 Precip = 9.1	

For north Norway (Table 2), large differences in the surface pressure are found in the comparison of results from different integration domains and with different lateral boundary conditions. The latter reflect the difference in the driving data since the small domain is employed. The higher surface pressure with the large domain (but similar lateral data set) is also noticed in an earlier study [15]. The reason for this behaviour of the RCM is not known. We believe that the increased surface pressure is RCM dependent, but illustrate that with larger integration domain the RCM becomes less constrained by the lateral driving data. The differences between the small and the large integration domain are less than the differences with completely (lateral and surface) different driving data for the small domain. For the daily precipitation there are relatively large differences between the different simulations (maximum of 0.42 mm/day between MLHS and HLHS on the small domain, the MLMS climate give approximately 4 mm/day). The T2m show minor differences (maximum 0.72 °C between MLHS and HLHS on the small domain).

The month-to-month variability of the mslp is smaller in the large domain than in the small, a result also seen for precipitation. This is a result that contradicts an earlier study which states that in general the internal variability increases with domain size [38]. However, the ground surface boundary conditions are important in generating large scale variability in RCMs, and the importance increases as the integration domain increases [39]. Thus, large scale atmospheric variability tends to be increasingly underestimated as the domain size increases when the lower boundary conditions are prescribed. The month-to-month variability for T2m is less sensitive to the external forcing than the surface pressure and precipitation.

The differences in mean MSLP, T2m, and daily precipitation for west Norway are less than in north Norway (Table 3). However, there are still large differences in the mean sea level pressure when the integration domain is changed and when the lateral boundary conditions are changed. Associated with these differences we also see differences in precipitation with a maximum of 0.79 mm/day (MLHS *versus* HLHS on the small domain), which is between 5 and 10% of the total precipitation amount in the region. The T2m is remarkably similar in all simulations and seems almost independent of the external forcing of the RCM. This is in agreement with earlier findings that local forced variables, like T2m, are partly controlled by internal processes in the RCM [15].

The external forcing has little impact on the month-to-month variability when comparing results from similar integration domain (Table 3). However, for west Norway we find a substantial reduction in the variability for MSLP and precipitation when a different integration domain is employed.

The differences of mean MSLP, T2m and daily precipitation for east Norway (Table 4) are similar to the other regions with a pronounced difference in the MSLP between large and small integration domains. In this connection, the precipitation is slightly higher in the small domain, *i.e.*, approximately 0.25 mm/day whilst the MLMS winter mean is approximately 3.5 mm/day. For T2m, there is one major difference compared to the other regions. RCM simulations with ML lateral forcing are up to 1 °C warmer than simulations with HL lateral boundaries.

As for the other regions, the month-to-month variability is substantially lower for MSLP and daily precipitation when employing the large integration domain (Table 4), whilst the variability of the T2m shows little sensitivity to external forcing of the RCM. In general, the sensitivity in month-to-month variability depending on variable and geographical region is in agreement with earlier findings [38].

A statistical t-test for significance has been performed to evaluate if the probability that the mean values of the data sets differ by chance are smaller than 5%, *i.e.*, if the differences are significant at the 5% level and not due to noise (*i.e.*, high month-to-month variability of the mean value). There is a significant difference between ML and HL forced RCM results in the small domain for MSLP in all three regions. The differences between RCM-results in the large and small domains are also significant. Simulated precipitation in north and west Norway are significantly different with respect to different domain size and different surface forcing. For T2m the HL forced RCM simulation is statistically different from the ML forced simulation for north and east Norway. Summarizing the statistical tests we find that at least one combination of the investigated variables and change in the external forcing creates statistical significant differences for one or more Norwegian regions.

5. Summary and Conclusions

The aim of this study was to explore (i) the importance of the surface forcing (e.g., sea surface temperature and sea ice), (ii) the importance of the lateral boundary forcing, and (iii) the importance of the size of the integration domain for dynamical downscaling with the HIRHAM RCM. This has been done through a set of experiments where the three sources of differences have been systematically varied. The lateral boundary and surface forcings are taken either from simulations with the Hadley Centre GCM or the Max-Planck-Institute GCM, while the two integration domains are shown in Figure 1. The main purpose for all simulations was to simulate the Norwegian climate for the period 1961–1990. In principle, there should only be insignificant differences between the results since they are supposed to simulate the same climate. The highest sensitivity of the RCM results to the external forcing is found during winter, and the results for December-January-February were the subject of the analysis.

The analysis shows that the RCM climate is sensitive to both the lateral boundary and surface forcing, as well as to the size of the integration domain. For different Norwegian regions, several of the differences in response are significant. Changing the surface forcing shows a very strong local response, 2 m air temperature is immediately affected, but response is also seen in mean sea level pressure and precipitation. More remote response is also seen, although with considerably smaller amplitude.

For changes in the lateral boundary forcing there is a clear response in RCM simulated MSLP. The response is most pronounced in connection with the main storm tracks. A Change in the circulation pattern has in turn an effect on the geographical distribution of precipitation. The difference in daily precipitation amounts is around 10% at the Norwegian coast during winter. Elsewhere only minor precipitation impacts are found. Only minor differences (up to 0.5–1.0 °K in some regions) are found for the typically more local variable T2m.

Changing the size of the integration domain also alters the MSLP and the large scale circulation pattern. Also in this case an up to 10% change in daily RCM-estimated precipitation is found in coastal regions in Norway, whilst the local variable T2m is less sensitive. Results over Norway also indicate that the month-to-month variability decreases with increasing integration domain in a RCM. The surface forcing is important for generating variability [39], and a carefully designed coupled atmosphere-ocean RCM should be considered for a better simulation of the variability. Another

approach for controlling the variability with integration domains of different sizes might be to apply the spectral nudging approach [35-36] in addition to lateral boundary forcing.

In many aspects the results generated in this work support earlier findings. For example, in a large integration domain the RCM-results are less constrained by the lateral forcing than in a smaller domain [5,15]. This study also demonstrates that changes in surface forcing create local and remote responses, where the former is most pronounced. Similar results are reported for GCMs earlier in the literature [34].

Concerning remote responses in RCMs, considerably fewer studies are published. A plausible reason for this is that RCMS often employs integration domains that are too small to truly produce remote responses. In addition, the effect of differences in local forcing is damped downstream of areas with large differences. The smaller differences in surface forcing downstream act to relax the differences between the lower-level variables in the atmosphere.

In this paper, we have emphasized investigating the response in fields directly associated with weather and climate (2 m temperature, precipitation), since these variables are the main targets for dynamical downscaling of global data. The tropospheric response in the geopotential height of isobaric surfaces as well as the thickness fields are interesting in view of classical theory for extratropical, planetary-scale response to surface temperature anomalies, e.g., [40,41]. The difference between the experiments MLHS and MLMS can be viewed as study of the response of a negative temperature anomaly south and east of the south tip of Greenland, and a positive anomaly along the sea-ice edge of the northern rim of the Nordic and Barents Seas. However, the calculated response is clearly influenced by the constant lateral boundary conditions.

The cold anomaly is situated in the westerly wind-system over the North-Atlantic Ocean, whilst the latter is in a region with less pronounced background flow. There is a clear response in the 1,000 hPa geopotential height with a ridge-pattern slightly downstream of the cold anomaly increasing the warm air advection over it. A similar pattern with increased cold air advection is seen at 1,000 hPa over the warm anomalies. Higher up, the response is better characterized in terms of thickness in geopotential heights. Thus the thickness fields between 1,000 hpa and 850 hPa and between 850 hPa and 500 hPa (not shown) reveal mainly a reduction south and east of the south tip of Greenland. Close to the anomalies the main response is developed in the lower part of the troposphere, whilst downstream the main difference is found in the mid-troposphere. In connection with the warm anomalies close to the sea-ice edge where the background flow is weak, the thickness increases throughout the lower troposphere.

It is worth noting that different variables show different sensitivity to changed external forcing. Large scale variables like MSLP are sensitive to lateral forcing and size of integration domain, but less sensitive to surface forcing. However, more local forced variables like T2m are less sensitive outside regions of changed surface forcing. This is in agreement with earlier studies [15].

This study employs only a few different sets of forcing (e.g., only lateral- and surface forcing from two different GCM, and only two different integration domains). However, the results suggest that the choice of lateral driving data and size of integration might be of equal importance, while the RCM is less sensitive to changed surface forcing, although the latter also play a role. In agreement with an earlier study [38] there are indications that surface forcing is especially important for the simulated variability. Due to this, a coupled RCM would probably give higher variability compared to only an atmosphere RCM.

In this study the simulation of the Norwegian climate is more sensitive to external forcing than other regions. From a methodology perspective this can be explained since Norway is situated well inside the integration domains and thereby experiences less restriction by the lateral boundaries than other regions closer to the lateral boundaries. However, from a physical perspective, Norway is situated in the North-Atlantic Storm track and might be more sensitive to small perturbations of the mean flow. Several of the different simulations give a statistical different climate for different variables for Norwegian regions. The Norwegian regions also show different sensitivities to changes in the external forcing with north Norway experience the highest sensitivity.

This study, together with previous studies suggests that the set up of a RCM should be done with care. This might even be of higher importance for some regions than for other regions. The choices made concerning size of integration domain and lateral- and surface forcing in dynamical downscaling may contribute to uncertainties in future climate scenarios.

Acknowledgements

The work reported here is funded in part by the Norwegian Research Council, through grant no. 120656/720 to the Norwegian Meteorological Institute/RegClim. Computational costs are covered by a grant from the Research Council's Programme for Supercomputing.

References

1. *IPCC*, *Climate Change 2001: The Scientific Basis*; Houghton, J.T., Ding, Y., Griggs, D.J., Noguer, M., van der Linden, P.J., Dai, X., Maskell, K., Johnson, C.A., Eds.; Cambridge University Press: Cambridge, UK, 2001; p. 881.
2. Lambert, S.J.; Boer, G.J. CMIP1 evaluation and intercomparison of coupled climate models. *Clim. Dynam*. **2001**, *17*, 83-106.
3. Contribution of Working Group I to the Fourth Assessment Report of the Intergovernmental Panel on Climate Change. In *IPCC*, *Climate Change* 2007*: The Physical Science Basis*; Solomon, S., Qin, D., Manning, M., Chen, Z., Marquis, M., Averyt, K.B., Tignor, M., Miller, H.L., Eds.; Cambridge University Press: Cambridge, UK and New York, NY, USA, 2007; p. 996.
4. Noguer, M.; Jones, R.; Murphy, J. Sources of systematic errors in the climatology of a regional climate model over Europe. *Clim. Dynam*. **1998**, *14*, 691-712.
5. Jones, R.G.; Murphy, J.M.; Noguer, M. Simulation of climate change over Europe using a nested regional-climate model. I: Assessment of control climate, including sensitivity to location of lateral boundaries. *Quart. J. Roy. Meteorol. Soc*. **1995**, *121*, 1413-1449.
6. Christensen, J.H.; Hewitson, B.; Busuioc, A.; Chen, A.; Gao, X.; Held, R.; Jones, R.; Kolli, R.K.; Kwon, W.K.; Laprise, R.; *et al.* Contribution of working group I to the fourth assessment report of the intergovernmental panel on climate change. In *Regional Climate Projections, Climate Change, 2007: The Physical Science Basis*; Cambridge University Press: Cambridge, UK and New York, NY, USA, 2007; Chapter 11, pp. 847-940.
7. Ådlandsvik, B. Marine downscaling of a future climate scenario for the North Sea. *Tellus* **2008**, *60A*, 451-458.

8. Rinke, A.; Gerdes, R.; Dethloff, K.; Kandlbinder, T.; Karcher, M.; Kauker, F.; Frickenhaus, S; Köberle, C.; Hiller, W. A case study of the anomalous Arctic sea ice conditions during 1990: Insights from coupled and uncoupled regional climate model simulations. *J. Geophys. Res.* **2003**, *108 (D9)*, 4275.
9. Döscher, R.; Willen, U.; Jones, C.; Rutgersson, A.; Meier, H.E.M.; Hansson, U.; Graham, L.P. The development of the coupled regional ocean-atmosphere model RCAO. *Boreal Environ. Res.* **2002**, *7*, 1221-1234.
10. Anthes, R.A. The General Question of Predictability. *Chapter 27 in Mesoscale Meteorology and Forecasting*; Ray, P.S., Ed.; The American Meteorological Society: Boston, MA, USA, 1986; pp. 636-656.
11. Boer, G.J. Predictability regimes in atmospheric flow. *Mon. Weather Rev*. **1994**, *122*, 2285-2295.
12. Christensen, J.H.; Machenhauer, B.; Jones, R.G.; Schar, C.; Ruti, P.M.; Castro, M.; Visconti, G. Validation of present-day regional climate simulations over Europe: LAM simulations with observed boundary conditions. *Clim. Dynam.* **1997**, *13*, 489-506.
13. Rinke, A.; Dethloff, K.; Spekat, A.; Enke, W.; Christensen, J.H. High resolution climate simulations over the Arctic. *Polar Res.* **1999**, *18*, 1-9.
14. Denis, B.; Laprise, R; Caya, D.; Cote, J. Downscaling ability of one-way nested regional climate models: The big-brother experiment. *Clim. Dynam.* **2002**, *18*, 627-646.
15. Køltzow, M.; Iversen, T.; Haugen, J.E. On abilities and limitations of atmospheric dynamical downscaling of global climate scenarios. *Tellus* **2008**, *60A*, 398-410.
16. Laprise, R.; de Elía, R.; Caya, D.; Biner, S.; Lucas-Picher, P.H.; Diaconescu, E.P.; Leduc, M.; Alexandru, A.; Separovic, L. Challenging some tenets of regional climate modelling. *Meteorol. Atmos. Phys.* **2008**, *100*, 3-22.
17. Leduc, M.; Laprise, R. Regional climate model sensitivity to domain size. *Clim. Dynam.* **2009**, *32*, 833-854.
18. Diaconescu, E.P.; Laprise, R.; Sushama, L. The impact of lateral boundary data errors on the simulated climate of a nested regional climate model. *Clim. Dynam*. **2007**, *28*, 333-350.
19. Singarayer, J.S.; Valdes, P.J.; Bamber, J.L. The atmospheric impact of uncertainties in recent Arctic sea ice reconstructions. *J. Clim*. **2005**, *18*, 3996-4012.
20. Lopez, P.; Schmith, T.; Kaas, E. Sensitivity of the Northern Hemisphere circulation to North Atlantic SSTs in the ARPEGE Climate AGCM. *Clim. Dynam.* **2000**, *16*, 535-547.
21. Kvamstø, N.G.; Skeie, P.; Stephenson, D.B. Impact of labrador sea-ice extent on the North Atlantic Oscillation. *Int. J. Climatol*. **2004**, *24*, 603-612.
22. Kushnir, Y.W.; Robinson, A.; Blade, I.; Hall, N.M.J.; Peng, S.; Sutton, R. Atmospheric GCM response to extratropical SST Anomalies: Synthesis and evaluation. *J. Climate* **2002**, *15*, 2233-2256.
23. Chapman, W.L.; Walsh, J.E. Simulations of arctic temperature and pressure by global coupled models. *J. Climate* **2007**, *20*, 609-632.
24. Rinke, A.; Maslowski, W.; Dethloff, K.; Clement, J. Influence of sea ice on the atmosphere: A study with an Arctic atmospheric regional climate model. *J. Geophys. Res*. **2006**, *111*, D16103.
25. Semmler, T.; Jacob, D.; Heinke Schlunzen, K.; Podzun, R. Influence of sea ice treatment in a regional climate model on boundary layer values in the fraim strait region. *Mon. Weather Rev.* **2004**, *132*, 985-999.

26. Kjellstrøm, E.; Ruosteenoja, K. Present-day and future precipitation in the Baltic Sea region as simulated in a suite of regional climate models. *Clim. Change* **2007**, *81*, 281-291.
27. Bozkurt, D.; Sen, O.L. Precipitation in the Anatolian peninsula: Sensitivity to increased SSTs in the surrounding seas. *Clim. Dynam.* **2009**, *36*, 711-726.
28. Vannitsem, S.; Chome, F. One-way nested regional climate simulations and domain size. *J. Clim.* **2005**, *18*, 229-233
29. Gustafsson, N. *The HIRLAM2 Final Report*; HIRLAM Technical Report No. 9; Swedish Meteorological and Hydrological Institute: Norrkoping, Sweden, 1993.
30. Roeckner, E.; Arpe, K.; Bengtsson, L.; Christoph, M.; Claussen, M.; Dümenil, L.; Esch, M.; Giorgetta, M.; Schlese, U.; Schulzweida, U. *The Atmospheric General Circulation Model ECHAM4: Model Description and Simulation of Present-Day Climate*; MPI Report No. 218; MPI für Meteorologie: Hamburg, Germany, 1996.
31. Christensen, J.H.; Christensen, O.B.; Lopez, P.; van Meijgaard, E.; Botzet, M. *The HIRHAM4, Regional Atmospheric Climate Model*; Scientific Report No. 96-4; Danish Meteorological Institute: Copenhagen, Denmark, 1996.
32. Bjørge, D.; Haugen, J.E.; Nordeng, T.E. *Future climate in Norway*; DNMI Research Rep. No. 103; Norwegian Meteorological Institute: Oslo, Norway, 2000; p.41.
33. Davies, H.C. A lateral boundary formulation for multi-level prediction models. *Quart. J. Roy. Meteorol. Soc.* **1976**, *102*, 405-418.
34. Dethloff, K.; Rinke, A.; Benkel, A.; Køltzow, M.; Sokolova, E.; Kumar Saha, S.; Handorf, D.; Dorn, W.; Rockel, B.; von Storch, H.; *et al*. A dynamical link between the Arctic and the global climate system, Geophys. *Res. Lett*. **2006**, *33*, L03703.
35. Kida, H.; Koide, T.; Sasaki, H.; Chiba, M. A new approach to coupling a limited area model with a GCM for regional climate simulation. *J. Meteor. Soc. Japan* **1991**, *69*, 723-728.
36. von Storch, H.; Langenberg, H.; Feser, F. A spectral nudging technique for dynamical downscaling purposes. *Mon. Weather Rev.* **2000**, *128*, 3664-3673
37. Mesinger, F.; Brill, K.; Chuang, H.; DiMego, G.; Rogers, E. Limited Area Predictability: Can "Upscaling'" Also Take Place? *Research Activities in Atmospheric and Oceanic Modelling*; Ritchie, H., Ed.; World Meteorological Organization: Geneva, Switzerland, 2002.
38. Alexandru, A.; de Elía, R.; Laprise, R. Internal variability in regional climate downscaling at the seasonal time scale. *Mon. Weather Rev*. **2007**, *135*, 3221-3238.
39. Castro, C.L.; Pielke, R.A., Sr.; Leoncini, G. Dynamical downscaling: Assessment of value retained and added using the regional atmospheric modeling system (RAMS). *J. Geophys. Res.*, **2005**, *110*, D05108.
40. Held, I.M. Stationary and Quasi-stationary Eddies in the Extratropical Atmosphere: Theory. In *Large Scale Dynamical Processes in the Atmosphere*; Hoskins, B.J., Pearce, R.P., Eds.; Academic Press: Burlington, MA, USA, 1983; pp. 127-168.

41. Hoskins, B.J.; Karoly, D.J. The steady linear response of a spherical atmosphere to thermal and orographic forcing. *J. Atmos. Sci*. **1981**, *38*, 1179-1196.